A Molecular Mechanism for GBF1 Recruitment to *cis*-Golgi Membranes

by

Douglas Quilty

A thesis submitted in partial fulfillment of the requirements for the degree of

Doctor of Philosophy

Department of Cell Biology

University of Alberta

Abstract

ADP-ribosylation factors (Arfs) play a central role in the regulation of vesicular trafficking through the Golgi. Arfs are activated on *cis*-Golgi membranes exclusively by the guanine nucleotide exchange factor (GEF) Golgi-specific BFA resistance factor 1 (GBF1), upon recruitment from cytosol. Membrane association of Arf is essential for its activation; therefore the recruitment of GBF1 to *cis*-Golgi membranes is a crucial step in Arf activation and Golgi maintenance. Here, we describe a novel mechanism for the regulation of GBF1 recruitment to *cis*-Golgi membranes. *In vivo* pharmacological treatments with 2-(4- Fluorobenzoylamino)-benzoic acid methyl ester (Exo1), brefeldin A (BFA), or golgicide A (GCA), as well as transient expression assays including expression of wild-type or mutant Arf and ArfGAP1 constructs, result in selective GBF1 recruitment to *cis*-Golgi membranes. Specifically, Arf•GDP stimulates further recruitment of GBF1 to Golgi membranes, likely through the activation of a putative GBF1 receptor. The recruitment of GBF1 to Golgi membranes was reconstituted *in vitro*, which allowed for confirmation of Arf•GDP regulation. Importantly, GBF1 recruited to Golgi membranes by Arf•GDP remains active. Specifically, we demonstrate that GBF1 supports Golgi maintenance, COPI recruitment, and increases Arf activation under Arf•GDP-dependent recruitment conditions. Here we present data suggesting that ArfGAP1 is a critical producer of regulatory Arf•GDP, likely a specialized function at the Golgi. We also determined that Arf•GDP regulates GBF1 recruitment through a mechanism that is dependent on both the N-terminal myristate moiety of Arf•GDP and localisation to

the *cis*-Golgi compartment. Together, these requirements for association of GBF1 with Golgi-membranes suggest regulation of a *cis*-Golgi membrane bound factor, potentially a protein receptor. Further evidence for the requirement of a Golgi-localised protein was obtained from *in vitro* experiments in which heat denaturation or protease treatment of Golgi membranes abrogated GBF1 recruitment. We propose that this protein is likely a GBF1 receptor, which would explain the specificity of GBF1 recruitment. Our expectation is that Arf•GDP will positively regulate the GBF1 receptor. A GBF1 truncation library was used to determine that the HDS1 and HDS2 domains of GBF1 are required for association with Golgi membranes and potentially a GBF1 receptor. To identify a putative GBF1 receptor, a far western blot was performed and the results suggest a 32 kDa GBF1 binding partner found on Golgi membranes. In summary, the work described here identified a novel Arf•GDP-stimulated mechanism for GBF1 recruitment and for the first time attributed a role for Arf•GDP in the cell. This mechanism is proposed to support steady-state levels of Arf•GTP at the *cis*-Golgi during cycles of Arf-dependent trafficking events to maintain Golgi morphology and function. In addition, this work has also yielded novel insight into how BFA potentially acts *in vivo*. Our increasing understanding of GBF1 recruitment to Golgi membranes provides important insights into how the ERGIC and Golgi compartments are established and maintained.

Preface

A version of Chapter 3 has been published as "Arf activation at the Golgi is modulated by feed-forward stimulation of the exchange factor GBF1." (Quilty et al., 2014). Permission for reproduction was obtained through the Copyright Clearance Center, confirmation number 11593613.

I was responsible for experimental design, performing experiments, data analysis, preparation of figures, and writing of the manuscript. Fraser Gray participated in the experiments and quantitation that resulted in Figure 3.12 as part of an undergraduate research project. Nathan Summerfeldt performed preliminary experiments. Dr. Dan Cassel provided reagents and technical assistance. Dr. Paul Melançon played a role in planning experiments, data analysis, and writing the manuscript.

The work contained in chapter 4 has not been published. I was responsible for experimental design, performing experiments, data analysis, and preparation of figures. Katie Yurkiw assisted in performing replicate experiments that resulted in Figures 4.1, 4.2, and 4.3 as part of an undergraduate research project under my supervision. Calvin Chan assisted in performing replicate experiments and experimental planning that resulted in Figures 4.11 and 4.12 as part of an undergraduate research project under my supervision. Dr. Paul Melançon played a role in planning experiments, and data analysis.

All other components of this thesis are my original work completed under the supervision of Dr. Paul Melançon.

Dedication

I would like to dedicate this thesis to my family.

To my wonderful and supportive wife Melanie, I could not imagine completing this journey without you. Countless times you were there for me when I was ready to quit. You have been supportive in every way possible, all while showing incredible patience. You have become a fantastic mother; juggling both babies when I need to focus on writing. You deserve more recognition than I can possibly give you. I will always love you more. It is time for a new chapter in my life, but I know the characters will all remain the same.

To my children, Conner and Kayleigh, your arrival during the writing of this thesis was a significant challenge. However, it turns out you were the perfect motivation to finish my degree. From the moment I first held you my perspectives and priorities were immediately changed. You are, and will always be, my greatest achievement. Your Dad loves you very much.

Last, but not least, thank you to my father, Michael. You have always supported my pursuit of education, even if the end goal was sometimes unclear. You have always been there when challenges have presented themselves, making sure I was always going to persevere. I am incredibly lucky to have such a supportive parent. You have played a significant role in the completion of this degree.

Acknowledgments

I would first like to acknowledge my supervisor, Dr. Paul Melançon for providing me with a fantastic opportunity to learn in a supportive environment. Working in a small lab where I was given considerable freedom led to significant growth as a scientist. Thank you for allowing me to pursue my interests in teaching science. You have served as an excellent mentor in science, teaching, and life in general. Our oft-differing views and interpretations resulted in excellent scientific discussions, which resulted in a stronger body of work. I hope we have another significant discovery on the horizon. Despite some challenging times, I hope you are happy with your decision to take on "the cracked golden pot". I am very happy with how it worked out.

I would also like to thank Dr. Richard Rachubinski for his strong mentorship throughout my time in the Department of Cell Biology. As a strong advocate for the students, you provided me with excellent advice during times of conflict and during times of scientific discovery. Your impact on this thesis is significant and your suggestions played a large role in the experiments that make up Chapter 4. I have always enjoyed our conversations and look forward to additional fruitful discussions in the near future.

Thank you to my supervisory committee members, Dr. Rick Wozniak and Dr. Paul LaPointe, for their willingness to be a significant part of my graduate studies. Your opinions, suggestions, and constructive criticisms have shaped and strengthened my project. I would also like to thank Dr. Richard Lehner for serving on both my candidacy exam and Ph.D. defense committees. Discussions we had on GBF1 recruitment led directly to our testing of ArfGAP1, and therefore played an important role in advancing this project. I would also like to thank Drs. Tom Hobman, Paul LaPointe, Gary Eitzen, Andrew Simmonds, Ben Montpetit, and Luc Berthiaume for their generosity with equipment, reagents, and their time throughout the course of my graduate work.

Lastly, I would like to thank Dr. Victor Hsu for serving as my external examiner. I look forward to our discussion regarding this body of work and hope it generates new and exciting directions to pursue.

Table of Contents

List of Tables

List of Figures

List of symbols and abbreviations

ADP	adenosine diphosphate
AP	adaptor protein
Arf	ADP-ribosylation factor
Arl	ADP-ribosylation factor-like
ATCC	American type culture collection
ATP	adenosine triphosphate
BIGs	brefeldin A-inhibited guanine nucleotide exchange factor
BFA	brefeldin A
COP	coatomer protein
ddH_2O	double distilled water
DMSO	dimethyl sulfoxide
EGFP	enhanced green fluorescent protein
EM	electron microscopy
ER	endoplasmic reticulum
ERES	ER exit sites
ERGIC	ER-Golgi intermediate compartment
Exo1	2-(4-fluorobenzoylamino)-benzoic acid methyl ester
FBS	fetal bovine serum
g	gram
GAP	GTPase activating protein
GBF1	Golgi-specific BFA resistance factor 1
GCA	Golgicide A
GDP	guanosine diphosphate
GEECs	GPI-Aps enriched early endosomal compartments
GEF	guanine nucleotide exchange factor
GFP	green fluorescent protein
GGA	Golgi-localising, Gamma-adaptin ear domain homology, Arf-binding proteins
GPI	glycosylphosphatidyl inositol
GTP	guanosine triphosphate
IF	immunofluorescence
IP	immunoprecipitation
kDa	kilodalton
LPAT	lysophospholipid acyltransferase
LPL	lysophospholipid
ManII	mannosidase II
mCherry	monomeric Cherry (red fluorescent protein)
min	minute
NRK	normal rat kidney
PBS	phosphate buffered saline
PCR	polymerase chain reaction

PH	plekstrin homology
PtdIns4*P*	phosphatidylinositol 4-phosphate
PL	phospholipases
SNARE	soluble N-ethylmaleimide sensitive factor attachment receptor
VSV	vesicular stomatitis virus

Chapter 1: Introduction

1.1 The early secretory pathway: The ERGIC and Golgi compartments

The highly organized endomembranes of the secretory pathway, found in eukaryotic cells, are comprised of the endoplasmic reticulum (ER), the ER-Golgi intermediate compartment (ERGIC), the individual cisternae of the Golgi complex (*cis*-, *medial*-, *trans*-), and the *trans*-Golgi network (TGN) (Figure 1.1) (Bonifacino and Glick, 2004). Individual compartments function in a sequential manner in which only correctly synthesized, folded, modified, and sorted proteins will enter a bidirectional pathway and ultimately reach their final destination. Roughly 1400 individual proteins, or seven percent of proteins encoded by the human genome, have been implicated in the biogenesis and maintenance of the secretory pathway through quantitative proteomic studies (Gilchrist et al., 2006). This thesis focuses on the enzymatic activation of small GTPases in the early pathway, and for this reason, this chapter will focus on the ERGIC and Golgi compartments and their components. It will not discuss the ER and TGN and associated components such as coatomer protein complex II (COPII) and clathrin. Importantly, it will focus on ADP-ribosylation factors (Arfs) that control the trafficking of proteins and maintenance of these compartments dependent on the coatomer protein complex I (COPI).

1.1.1 COPI molecular machinery

Protein trafficking vesicles, which are required for ERGIC and Golgi maintenance and function, are generated and surrounded by protein coats that are specific to the small GTPases that recruit them and the target membrane (Jackson, 2014). The proteins that make up these coats initiate, promote, and/or stabilize

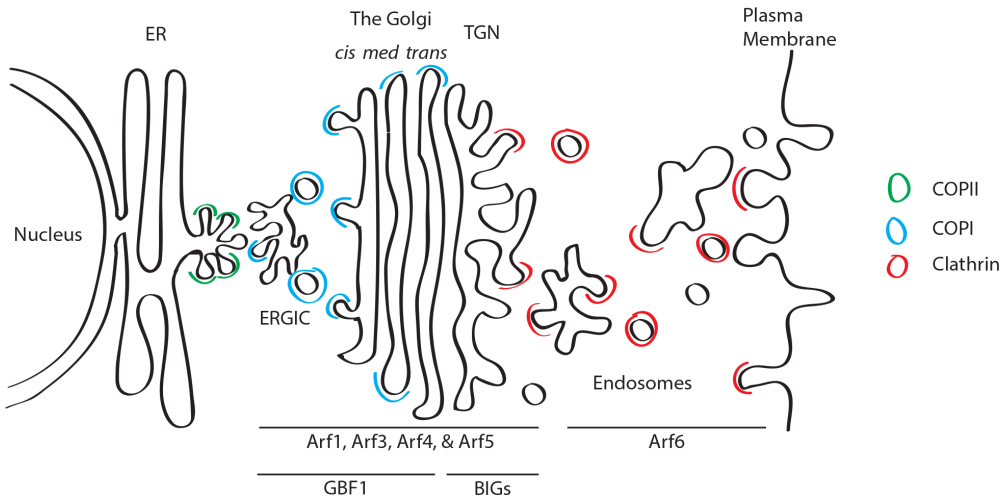

Figure 1.1 Schematic depiction of the human secretory pathway. The secretory pathway is comprised of many membrane bound compartments that exchange cargo through membrane carriers that are dependent of coat proteins. Newly sythesized secretory cargos are produced at the ER and must trafficked anterograde through the ERGIC, Golgi, TGN, and endosomal compartments to be secreted from the plasma membrane. Conversely, endocytosed cargo can be trafficked retrograde from the plasma membrane. These trafficking steps are mediated by specific coats. Specifically, COPII (green) mediates export form the ER at ERES, COPI (blue) mediates trafficking at the ERGIC and Golgi, and clathrin (red) functions at the TGN, endosomes, and plasma membrane. At the Golgi, COPI is recruited by Arf proteins 1, 3, 4, and 5 as indicated. Activation of these small GTPases is dependent on ArfGEFs. At the Golgi, the only identified ArfGEF is GBF1.

membrane deformation and curvature through protein-interaction driven assembly, which promotes vesicle formation (Gallop et al., 2006; Zimmerberg and Kozlov, 2006). Moreover, these coats selectively anchor specific cargoes into newly forming vesicles (Duden, 2003). Because of its significance in the establishment and maintenance of compartment of the early secretory pathway, the COP1 molecular machinery will be discussed first.

The COPI coat, or coatomer, is a heptameric complex consisting of α, β, β', ε, γ, δ, and ζ subunits. This large, roughly 700 kDa protein complex is essential in metazoan cells and it is recruited *en bloc* to Golgi membranes (Hara-Kuge et al., 1994). However, the COPI complex is often considered to be two subcomplexes, namely the B-subcomplex (α, β', and ε) and F-subcomplex (β, γ, δ, and ζ). In a simplified model of COPI-dependent vesicle formation, the small GTPase Arf1 is activated, cargo is acquired, COPI is polymerized at the Golgi membrane, and vesicle formation occurs as a consequence (Bremser et al., 1999; Serafini et al., 1991).

Structural analysis of the COPI coat has provided additional insights into the mechanisms of COPI recruitment to Golgi membranes (Jackson, 2014). The *en bloc* nature of COPI recruitment can be further explained by specific protein-protein interactions. It has been shown that two components of the F-subcomplex, namely β- and γ-COP, interact with Golgi-bound Arf1•GTP to promote membrane recruitment (Ren et al., 2013; Yu et al., 2012). To ensure simultaneous recruitment of the B-subcomplex, many protein-protein interactions are formed between the two subcomplexes (Eugster et al., 2000; Watson et al., 2004). Moreover, the B-

subcomplex itself can recognize and bind di-lysine recognition motifs on specific cargoes via WD-repeat domains found in the α-COP and β'-COP subunits (Jackson et al., 2012; Ma and Goldberg, 2013). Recently, the δ-COP subunit domain structure was further studied resulting in the identification of a helix proximal to the N-terminal longin domain that is essential for COPI function in the early secretory pathway (Arakel et al., 2016). It is postulated that this helix probes membranes for lipid packing states and potentially interacts with cargo, due to its analogous structure and location to a helix characterized in the clathrin adapter protein (AP) 2 (AP2). The multivalent nature of COPI recruitment is required to generate sufficient affinity for COPI to be recruited to sites of vesicle formation (Jackson, 2014).

The role of COPI in protein trafficking at the Golgi has proved to be a complicated biological process to define. In mammalian cells, COPI specifically localises to the stacked *cis*-Golgi and ERGIC compartments (Duden, 2003; Scales et al., 1997). The role of COPI in dilysine retrieval signal-mediated retrograde trafficking from the Golgi to ER for the purpose of recycling the COPII machinery used for vesicle formation from ER exit sites (ERES) is well established (Letourneur et al., 1994). This mechanism requires *en bloc* recruitment of COPI where the α, β' subunits directly bind to the dilysine motifs found at the carboxy terminus of cargo proteins that must be returned to the ER (Cosson and Letourneur, 1994; Elsner et al., 2003; Hara-Kuge et al., 1994; Letourneur et al., 1994). COPI can also efficiently bind and traffic transmembrane proteins of the p24 family following dimerization, although in this case binding is mediated by the γ-COP subunit (Bethune et al.,

2006a). These data indicate that different COPI subunits can bind different cargoes and therefore have distinct roles in mediating protein trafficking.

1.1.2 The ERGIC compartment

In animal cells, newly synthesized secretory cargoes, once properly folded and modified, are targeted to specialized regions of the ER called ERES. These proteins are then packaged into vesicles in a COPII-dependent manner to allow for delivery to the ERGIC. The ERGIC, also referred to as vesicular tubular clusters (VTCs), was characterized as a complex membrane system consisting of a convoluted network of vesicles and tubules (Bannykh et al., 1998; Hauri and Schweizer, 1992; Saraste and Kuismanen, 1992). While the ERGIC is in very close proximity to the ERES, these structures remain distinct from each other and can be resolved by electron microscopy (Appenzeller-Herzog and Hauri, 2006; Schweizer et al., 1988; Schweizer et al., 1990). ERGIC structures are often identified by the presence of the lectin marker protein ERGIC-53/p58, despite it localising promiscuously across the ER, Golgi, along with the ERGIC. The ERGIC structures are additionally immunoreactive for the marker proteins β-COP, p115, GM130, p23, and Surf4 (Mitrovic et al., 2008; Orci et al., 1998; Rojo et al., 1997; Schindler et al., 1993). The structure of the ERGIC, consisting of both vesicles and highly dynamic tubules, is best visualized by expression and imaging of green fluorescent protein (GFP)-tagged p58 (Ben-Tekaya et al., 2005). The structure of the ERGIC appears to require both Surf4 and ERGIC-53 as the membrane architecture collapses in cells in which either protein has been depleted (Mitrovic et al., 2008).

Early work on the ERGIC compartment suggested these membranes structures were either highly specialized subdomains of the ER (Sitia and Meldolesi, 1992) or Golgi (Mellman and Simons, 1992). However, further studies suggest that the membranes of the ERGIC comprise a unique and independent compartment within the secretory pathway (Appenzeller-Herzog and Hauri, 2006). Currently, there are two hypotheses regarding the manner in which the ERGIC compartment is generated and maintained. The ERGIC could result from the homotypic fusion of many COPII vesicles released from ERES or alternatively, the ERGIC may represent a stable, long lived compartment that receives cargo from ERES through heterotypic fusion events (Bethune et al., 2006b). In support of the latter, live cell imaging experiments provide strong support for ERGIC being a collection of stable, long-lived sorting structures that may also play a role in quality control (Appenzeller-Herzog and Hauri, 2006; Ben-Tekaya et al., 2005; Fan et al., 2003).

1.1.3 Trafficking of proteins to and through the ERGIC

Closely mirroring the debate regarding the generation of the ERGIC, two discrepant models for anterograde trafficking from the ER to the Golgi exist. The first model, called the transport complex model, posits that anterograde transport vesicles generated at ERES fuse to form larger pleiomorphic carriers that can traffic cargo to the Golgi in a microtubule-dependent manner (Bannykh et al., 1998; Stephens and Pepperkok, 2001). Primary support for this model was obtained by live cell imaging of over-expressed fluorescent GFP-labeled vesicular stomatitis virus (VSV) glycoprotein (VSV-G), which showed that VSV-G exits ERES and traffics to the

Golgi along microtubules by minus-end directed motor protein dynein (Presley et al., 1997; Scales et al., 1997). Moreover, utilization of a 15 degree Celsius temperature block that is known to cause accumulation of secretory cargo in ERGIC did not increase the number of ERGIC structures, but instead resulted in VSV-G accumulation in ERGIC structures that were already present (Klumperman et al., 1998). Interpretation of these experiments is limited due to the assumption that VSV-G was trafficked efficiently through ERGIC as there was no way to determine if the carriers imaged were in fact ERGIC. Additionally, there may also be consequences such as alterations to the normal protein trafficking pathways due to the over-expression of a viral glycoprotein. Interestingly, imaging experiments may also hint that ERGIC structures are not transport carriers due to the observed consistent close proximity to ERES, as opposed to an even distribution between the ERES and Golgi that would be expected for a transport carrier.

The alternate hypothesis for the role of ERGIC in anterograde transport of proteins to the Golgi complex proposes that the ERGIC is a stable, long-lived compartment that likely plays a role in protein sorting and quality control (Ben-Tekaya et al., 2005). Using two-colour live-cell imaging experiments with fluorescently labeled ERGIC marker and cargo, the authors demonstrated that many ERGIC structures remained stationary while cargo was trafficked to the Golgi. These results support a stable compartment model while also being consistent with previous studies that suggested the ERGIC was an early sorting station that allowed for differential packaging of anterograde and retrograde cargoes (Martinez-Menarguez et al., 1999). While it remains possible that either model for anterograde

traffic may be accurate, current data support the theory that anterograde carriers derived from ERGIC traffic cargo to the Golgi following sorting at the ERGIC.

Either model of ERGIC trafficking intimately involves the COPI complex for maintenance of ERGIC structure and sorting of anterograde and retrograde cargo. The sorting function is linked to COPI by experiments reporting that retrograde cargoes within the ERGIC co-localised with COPI, while anterograde cargoes were found in ERGIC domains lacking COPI proteins (Martinez-Menarguez et al., 1999).

1.1.4 The Golgi compartment

Following sorting and anterograde trafficking from the ERGIC, cargo proteins are delivered to the Golgi. The Golgi is a critical site for post-translational protein modification, lipid modification, and protein sorting. Within the secretory pathway, the Golgi serves as a central hub for bi-directional protein trafficking (Bankaitis et al., 2012; Emr et al., 2009). The Golgi consists of a series of stacked membranes, or cisternae, that were observed in electron microscopy (EM) experiments (Bethune et al., 2006b; Mogelsvang et al., 2004). A more advanced 3-dimensional visualization technique, called EM tomography has provided further structural information of the Golgi. Specifically, it was discovered that the Golgi is a complex, continuous ribbon of membrane cisternae, with many associated fenestrations and vesicles, which weaves and rotates through the cellular cytoplasm (Donohoe et al., 2006; Mogelsvang et al., 2004). Within the Golgi ribbon, individual cisternae can be classified as *cis*, *medial*, and *trans* based on both proximity to ER and on biochemical properties. Newly synthesized proteins are trafficked from the ER in COPII-coated vesicles of

approximately 50 nm diameter that mobilize to the highly fenestrated *cis*-face of the *cis*-cisternae of the Golgi (Marsh et al., 2001). Once cargo has arrived at the *cis*-Golgi, it is then trafficked through the *medial* and *trans* cisternae where cargo is then packaged into vesicles and delivered to the trans Golgi network (TGN) where additional sorting occurs to ensure delivery of cargo to the plasma membrane or target endomembrane (Glick and Nakano, 2009).

The sub-compartmentalization of the Golgi allows for the Golgi to perform multiple enzymatic modifications of proteins as they are trafficked towards the cell surface. Individual cisternae house a variety of Golgi proteins including glycosyltransferases, Golgi matrix proteins, and GTPases (Pfeffer, 2003). Specific marker proteins can be imaged to resolve the individual Golgi cisternae from each other. Specifically, EM and confocal microscopy can resolve p115, mannosidase II (ManII), and TGN46 as they localise to the *cis*, *medial,* and *trans*-cisternae, respectively (Nelson et al., 1998; Velasco et al., 1993; Zhao et al., 2002).

The Golgi also plays a critical role as a platform for cellular signaling pathways. For instance, many kinases act on proteins while they are localised at the Golgi (Acharya et al., 1998; Lowe and Kreis, 1998; Sutterlin et al., 2002). In addition, several kinases involved in mitosis have important roles in Golgi structure disassembly and reassembly during the cell cycle. A growing body of work has linked the Rab small GTPases with the maintenance of function of the Golgi, specifically during Golgi fragmentation and reassembly during mitosis in a microtubule dependent manner (Pfeffer, 2012). Golgi reassembly has been further linked to the p97 ATPase in conjunction with the adaptor subunit protein p47. Interestingly, p97

also facilitates Golgi membrane fusion events during interphase through the p37 adaptor protein (Uchiyama et al., 2006).

1.1.5 Trafficking of proteins to and through the Golgi

A large number of proteins have been implicated in trafficking of protein cargoes to and through the Golgi (Bonifacino and Glick, 2004; Glick and Nakano, 2009). Traffic through the Golgi is bidirectional (anterograde or retrograde) and transport in either direction likely requires a similar series of events. All together, proteins to be trafficked must be recruited to cisternal sub-domains where vesicle budding is initiated by cargo carrier proteins and coat complex proteins. Once vesicle formation has occurred, motors travel along microtubules to move vesicles directionally until they reach the target acceptor membrane (McNew et al., 2000). When the vesicle meets the target membrane, soluble N-ethylmaleimide sensitive factor attachment receptor (SNARE) proteins mediate docking and fusion events that ultimately deliver their contents to the acceptor compartment. In addition to the SNARE, coat, and motor proteins involved in Golgi vesicle trafficking, tethering factors such as regulatory Rab1 and p115 tether have important roles in regulating vesicle trafficking. Rabs are global regulators of trafficking events and have been implicated in the associations with motor proteins and the recruitment of critical trafficking factors such as tethering factors and SNAREs (Balch, 2004). All these regulatory proteins must work together to ensure correct and efficient delivery of cargo to target compartments.

Retrograde and anterograde trafficking at the Golgi is required for maintenance of Golgi structure and function. While it is known that COPI is required for Golgi structure and function, the exact mechanisms of COPI function at the Golgi remain debatable. Initially, there were two prevailing models for COPI mediated anterograde trafficking at the Golgi. The cisternal maturation model postulates that anterograde cargo is transported in bulk in the lumen of the Golgi cisternae (Glick et al., 1997; Glick and Nakano, 2009). The model predicts that the fusion of pre-Golgi carriers results in the generation of a new *cis* cisternal compartment that can then mature through COPI-dependent acquisition and loss of different sets of Golgi enzymes into *medial* and *trans* cisternae, sequentially. Cargoes would progress through the Golgi in the lumen of the maturing cisternae while the requisite sorting and modification machinery is delivered and removed by COPI-mediated vesicles. However, the cisternal maturation model fails to account for the presence of anterograde cargo packaged in COPI vesicles (Nickel et al., 1998; Pepperkok et al., 2000) or the reports of differential rates of anterograde trafficking of different cargo proteins (Bonfanti et al., 1998). While a growing body of recent work suggests that cisternal maturation is not sufficient to explain all protein transport across the Golgi (Dancourt et al., 2016; Lavieu et al., 2013; Pfeffer, 2013), recent studies suggest that cisternal maturation is important for transport of specific protein cargoes (Ishii et al., 2016).

The second major model for COPI-dependent anterograde trafficking of cargo through the Golgi is the vesicular transport model. This model postulates that Golgi cisternae are stable compartments that produce anterograde vesicles. Compartment

maintenance is dependent on retrograde COPI vesicles that retrieve and return any cisternal enzymes or machinery that are trafficked through the Golgi. In short, the vesicular transport model favors stable, long-lived Golgi compartments that remain stationary within the secretory pathway. Like the cisternal transport model, the vesicular transport model fails to explain all published data on anterograde trafficking data. Specifically, trafficking of very large cargo such as procollagen that is many times larger than a COPI vesicle. Moreover, observations that large procollagen cargoes are trafficked at almost identical rates as small cargoes such as VSV-G are not consistent with the vesicular transport model (Mironov et al., 2003).

As is often the case when two well-supported models are proposed within an area of research, newer models arise that combine aspects of the previous competing models. In the case of trafficking through the Golgi, the percolating vesicle model marries aspects of the cisternal and vesicular transport models (Orci et al., 2000; Pelham and Rothman, 2000). This model proposes that COPI mediates the production of two populations of cargo carriers, one that traffics anterograde cargo rapidly between Golgi sub-compartments while the second population functions to retrieve cargoes destined for retrograde trafficking back to the ER. Another model for intra-Golgi transport is unrelated to previous proposals, and instead aim to account for observations that cargo arriving at the Golgi exits with exponential kinetics rather than with a lag or transit time (Patterson et al., 2008). In this model, transmembrane cargo and enzymes to be recycled are partitioned into two distinct lipid phases that allow for different rates of trafficking.

A Rab-dependent model for intra-Golgi trafficking has also been proposed called the cisternal progenitor model. In this model, homotypic fusion and fission of membranes marked by a specific Rab would result in the sequential formation of stable compartments that retain a stacked organization (Pfeffer, 2012). An initial organizing Rab would initiate the recruitment of additional Rabs, SNAREs, tethering factors, and even the glycosyltransferases that are characteristic for that specific cisterna. Once established, this newly generated cisterna would then provide the activated Rab required for the production of the subsequent cisternae in the stack. In this model, the homotypic fusion events would be responsible for the majority of cargo trafficking through the Golgi. These fusion events would likely appear as tubules forming connections between neighboring cisternae, which has been reported by many independent research groups (Pfeffer, 2010). This model does not constitute the only model that is fundamentally based on the requirement for Golgi tubule formation for trafficking of cargo.

Work done by Rothman and Lavieu attempts to reconcile competing Golgi trafficking models and has centered around imaging of cargo under different conditions that would impair protein trafficking (Pfeffer, 2013). The first experiments involved utilizing cargo that could be aggregated in particular compartments to determine if trafficking could still proceed, as predicted by the cisternal maturation model. The authors used imaging and biochemical techniques to demonstrate that aggregated cargoes in the Golgi failed to be trafficked, suggesting that Golgi cisternae are static (Lavieu et al., 2013). Additionally, the authors demonstrated that soluble large cargo aggregates could be efficiently

trafficked via vesicles generated at the edges, or rims, of the Golgi cisternae. These findings were consistent with additional studies that have demonstrated trafficking of large cargoes in large vesicles (Volchuk et al., 2000). However, efficient trafficking of large cargoes in mammalian cells requires an intact Golgi ribbon, suggesting trafficking of large cargoes via large vesicles is an inefficient process (Lavieu et al., 2014). Interestingly, however, the Rothman and Lavieu research groups demonstrated that small cargoes were trafficked in small vesicles that were generated at the edges of the Golgi cisternae (Pellett et al., 2013). These results have led to the 'rim to rim' model of protein trafficking through the Golgi. However, there are some concerns that these aggregated cargoes could impair normal Golgi function (Pfeffer, 2013). Further, Rothman and Lavieu recently published additional work that supports cisternal maturation-independent protein trafficking at the Golgi. In this publication, biochemical stabilization of inter-cisternal tethering interactions tested the validity of the cisternal maturation model. Specifically, the authors proposed that stabilization of Golgi tethering interactions would prevent cisternal maturation by "gluing" the compartments in place and could therefore impair protein trafficking (Dancourt et al., 2016). The authors conclude that trafficking through the "glued" Golgi is maintained and that the presence of numerous COPI vesicles provides additional support for this novel "rim to rim" mechanism of protein trafficking in the Golgi. While the involvement of peripherally produced COPI vesicles in Golgi trafficking is well supported, it does not preclude other mechanisms of transport that could occur simultaneously.

A more recent model for Golgi trafficking is the continuity model, which is predominantly based on the discovery of tubular intra-cisternal connections in the Golgi by electron tomography (Trucco et al., 2004). This model includes the use of polymorphic tubular carriers that can connect to adjacent cisternae to mediate delivery of protein cargo. COPI vesicles would serve a role in controlling cisternal fusion events and maintaining Golgi morphology (Bethune et al., 2006b). More recent studies have established a role for COPI in the formation of Golgi tubules that serve as anterograde cargo carriers (Yang et al., 2011a). These tubules preferentially traffic anterograde cargo proteins while retrograde cargoes are preferentially packaged into classical COPI vesicles. Further, these tubules were shown to traffic cargo *in vivo* and are regulated by the small GTPase CDC42 (Park et al., 2015). While these findings appear to support the continuity model, it remains possible if not likely, that the complexity of Golgi trafficking is best described by a currently undefined model that combines different aspects of many of the proposed hypotheses.

1.1.6 Lipid modifying enzymes in trafficking at the Golgi and ERGIC

Lipid modifying enzymes play a critical role in many Golgi-related processes, including protein trafficking. For example, phospholipases (PL) are a diverse group of enzymes that are responsible for a variety of biological processes including metabolic signaling, lipid homeostasis, and membrane biogenesis (Brown et al., 2003). The phospholipases can be broadly classified into four groups depending on the bond in the phospholipid that is hydrolyzed: PLA (PLA_1 and PLA_2), PLB, PLC, and

PLD. PLA_2 enzymes are themselves a large and diverse super family that primarily hydrolyzes phospholipids at the sn-2 position to generate lysophospholipid (LPL) species and a free fatty acid (FA) (Balsinde et al., 2002; Murakami and Kudo, 2002). PLA_2 enzymes are assigned to one of 14 groups (Groups I-XIV). Interestingly, only members of Groups IV, VI, VII, and VIII localise to the cytoplasm and have been linked to membrane trafficking (Balsinde et al., 2002; Murakami and Kudo, 2002). These PLA_2 enzymes are unified in that they contain a serine esterase motif (GXSXG, GXSGS, or GXSXV) (Brown et al., 2003). PLA_2 enzymes are primarily associated with the production of signaling molecules, such as arachidonic acid (AA), that have roles in inflammation, cell growth and smooth muscle contraction (Bechler et al., 2011). However, it has been elucidated that these enzymes play a critical role in the regulation of Golgi structure and trafficking by mediating membrane tubulation by a poorly understood mechanism.

There are currently only three known PLA_2 enzymes that regulate membrane tubulation including $cPLA_2\alpha$, PAFAH1B, and $iPLA_2\beta$ (Bechler et al., 2011). The best studied in this group is the cytoplasmic Group IV PLA_2 enzyme ($cPLA_2\alpha$). $cPLA_2\alpha$ translocates to Golgi membranes in a calcium-dependent manner where it initiates tubule formation from COPI buds (Burke and Dennis, 2009; Leslie et al., 2010; Yang et al., 2011b). The recruitment of $cPLA_2\alpha$ to Golgi membranes is regulated by moderate increases in cytoplasmic calcium, released from the Golgi due to increase secretory load (San Pietro et al., 2009). Once active at Golgi membranes, $cPLA_2\alpha$ enzymatic activity is required to produce lysophosphatidic acid (LPA) that promotes tubule formation, by providing membrane curvature-inducing lysophospholipids

(LPL) in the outer leaflet of the Golgi membrane (San Pietro et al., 2009). cPLA$_2$α-dependent tubules are required for both anterograde and retrograde transport of cargoes (Yang et al., 2011b). These tubules provide an inducible continuity through the Golgi that can mediate rapid trafficking in response to increased secretory load providing the first clear explanation of how COPI mediates anterograde trafficking (Emr et al., 2009). Like cPLA$_2$α, PAFAH1B partially localises to Golgi elements but is thought to play a redundant role in tubule formation of ERGIC, Golgi, and TGN membranes (Bechler et al., 2010). Importantly, work on PAFAH1B has clearly demonstrated a direct relationship between the PLA$_2$ enzyme and microtubules as the Lis1 subunit interacts with dynein (Judson and Brown, 2009). These data strongly implicate PLA$_2$ enzymes in generating membrane tubules, but fail to explain negative regulatory mechanisms that maintain lipid homeostasis.

Lysophospholipid acyltransferases (LPAT), specifically the Golgi localised lysophosphatidic acid acyltransferase (LPAAT) 3 enzyme, inhibits tubule formation by converting PLA$_2$ generated LPL species back to phospholipids (Yang et al., 2011b). LPATs are transmembrane proteins that localise to discrete compartments (Schmidt and Brown, 2009; Schmidt et al., 2010). Currently, LPAAT enzymes are the best-characterized LPATs with respect to trafficking. Currently, the lysophosphatidyl choline acyltransferase enzymes remain poorly characterized but are potential candidates in regulating protein traffic and tubulation of membranes (Jackson et al., 2008).

Interestingly, a similar PLA-dependent mechanism of membrane tubulation has been proposed at the ERGIC. Tubulation of ERGIC membranes has been

demonstrated to occur in response to BFA treatment (Lippincott-Schwartz et al., 1990), accumulation of ERGIC cargo by temperature shift (Ben-Tekaya et al., 2010), GBF1 knockdown (Szul et al., 2007), and co-knockdown of both Arfs 1 and 4 (Ben-Tekaya et al., 2010). Tubules generated by co-knockdown of Arfs 1 and 4 or accumulation of ERGIC cargoes is dependent on iPLA$_2$β activity (Ben-Tekaya et al., 2010). iPLA$_2$β is a member of the Group VI family of Ca^{2+}-independent PLA$_2$ enzymes that reside predominantly in the cytoplasm (also named iPLA$_2$B, GVIA-2 iPLA$_2$, and PNPLA9; gene name PLA2G6) (Bechler et al., 2011; Burke and Dennis, 2009). iPLA$_2$β activity has been linked to a variety of important biological processes including neurodegenerative disease (Gregory et al., 2008; Morgan et al., 2006), glucose-mediated insulin secretion (Ramanadham et al., 1999) and adipocyte differentiation (Su et al., 2004). While the classification of this enzyme suggests it localises to the cytoplasm, it also localises to the ERGIC (Ben-Tekaya et al., 2010). Further linking tubulation to iPLA$_2$β, it was observed that inhibition of iPLA$_2$β activity by the suicide substrate inhibitor Bromoenol Lactone (BEL) resulted in significant fragmentation and dispersion of ERGIC structures (Ben-Tekaya et al., 2010). Additionally, supplementing cells with lysophosphatidylcholine (LPC) during iPLA$_2$β inhibition recovered the ability to generate tubules suggesting that iPLA$_2$β production of LPC is a potential mechanism inducing tubule formation (Ben-Tekaya et al., 2010). Interestingly, iPLA$_2$β was recruited to ERGIC membranes in response to co-knockdown of Arf1 and 4, suggesting a regulatory role for Arf in inhibiting iPLA$_2$β activity by impeding ERGIC localisation through interaction (Ben-Tekaya et al., 2010).

1.2 ADP-ribosylation factors (Arfs)

The ADP-ribosylation factor (Arf) family of proteins is a subset of the large RAS superfamily of GTPases. Members of the Arf family, including Arf, Arf-like, and Sar1 play a critical role in the maintenance of, and trafficking through, the secretory pathway (Gillingham and Munro, 2007). The first of these proteins, Arf1, was identified due its critical role in bacterial toxin entry into eukaryotic cells (Kahn and Gilman, 1986). Members of the Arf family are small GTP-binding proteins that are classically considered active in their GTP-bound form and inactive in their GDP-bound form (Pevzner et al., 2012). This on/off manner of regulation has led to these proteins being referred to as "rheostat regulators" of trafficking. Arf activation requires exchange of GDP for GTP that is facilitated by guanine nucleotide exchange factors (GEFs). Inactivation, on the other hand, requires hydrolysis of GTP to GDP catalyzed by a GTPase activating protein (GAP). The processes of Arf activation and inactivation, and required protein factors, will be discussed at length in sections 1.3 and 1.4 of this introduction.

1.2.1 Arf classification

Arf proteins have been sub-divided into three classes based predominantly on sequence homology. In mammalian cells these classes include: Class I (Arfs 1-3), Class II (Arfs 4-5), and Class III (Arf6) (Donaldson and Jackson, 2011). Class I Arfs are the most widely conserved across eukaryotic diversity and share approximately 96% sequence identity. Class II Arfs arose from divergent evolution from Class I Arfs in the animal lineage and retained approximately 90% sequence identity (Manolea

et al., 2010; Schlacht et al., 2013). As is the case for Class I Arfs, Class III Arfs are ancient and conserved across eukaryotes. Mammals express a single Class III Arf, which bears only 60% sequence identity to Arfs of other classes (Kahn et al., 1991).

1.2.2 Arf domain architecture and functional mutants

The protein structure of Arf proteins is dependent on the nucleotide that is bound. Specifically, GTP binding promotes conformational changes that result in the stable exposure of the N-terminal amphipathic helix (Antonny et al., 1997). Importantly, there is a large excess of GTP relative to GDP in the cytoplasm that ensures that GTP will quickly occupy an empty nucleotide-binding domain, a critical aspect of Arf activation (Traut, 1994).This conformational change occurs predominantly in two regions termed switch I and switch II, present in all regulatory small G proteins (Pasqualato et al., 2002). The N-terminal amphipathic helix can facilitate strong membrane binding, in large part due to the myristate moiety that is covalently added co-translationally on a glycine residue (G2) (Kahn et al., 1988; Kahn et al., 1992). This N-terminal myristoylation is essential for Arf activation and subsequent and downstream effects, due to the requirement for membrane association of Arf prior to activation.

1.2.3 Sub-cellular localisation and function of Arfs

In mammalian cells, most of the Arf isoforms expressed localise throughout the secretory pathway, although some isoforms can be further localised to specific structures. In addition, specific functions for Arf proteins at various compartments

within the secretory pathway have been proposed. Class I and Class II Arfs (Arfs 1, 3, 4, and 5 in human cells) localise promiscuously throughout the secretory pathway, specifically localising to the ERGIC, Golgi, TGN, and endosomal compartments (Donaldson and Jackson, 2011). The TGN, which serves as an intermediate between the Golgi and endosomal compartments, is also a target membrane for Class I and Class II Arfs. Further, a specific relationship between Arf3 activation and the TGN has been established (Manolea et al., 2010). Interestingly, none of the Golgi-localised Arfs are independently required for Golgi maintenance and function (Volpicelli-Daley et al., 2005). Instead, it appears they work in pairs to perform specific trafficking functions. Arf3, the sole class III Arf, on the other hand, localises to the plasma membrane, where it has an essential role in endocytosis, and endosomes (D'Souza-Schorey and Chavrier, 2006).

Despite the functional redundancy within the Golgi-localised Arf proteins, unique functions for specific Arf isoforms have been postulated. It has been suggested that Arf3 is selectively localised to the TGN where it is activated by brefeldin A-inhibited GEFs (BIGs), despite differing from Arf1 in only seven amino acid residues (Manolea et al., 2010). This targeting to the TGN was distilled down to two conserved Arf3 specific residues in the C-terminal amphipathic helix that may play a role in insertion into the cytosolic side of a compartments lipid bilayer. Further studies of specific Arf localisation resulted in the identification of a Golgi-targeting sequence in the third α-helix that destines proteins to a specific membrane compartment (Honda et al., 2005).

A growing body of work suggests a role for Arf in lipid droplet homeostasis. The class I Arf was identified as having a role in lipid droplet homeostasis through an RNAi screen performed in *Drosophila* (Guo et al., 2008). In addition, Arf1 was identified in proteomic analyses of mammalian lipid droplets (Bartz et al., 2007b). This machinery was further linked to the delivery of the lipid modifying enzymes adipose triglyceride lipase (ATGL) and adipophilin to the surface of lipid droplets (Soni et al., 2009). In addition, there have been direct links to COPI having a role at the surface of lipid droplets, presumably recruited by activated Arf (Beller et al., 2008). Specifically, both Arf1 and coatomer have been co-localised with lipid droplet resident enzymes (Guo et al., 2008; Wilfling et al., 2014). This Arf1 activation at lipid droplets has been linked to GBF1 (Bartz et al., 2007a). The proposed localisation of GBF1 to lipid droplets has been linked to a domain downstream of the catalytic Sec7d (Bouvet et al., 2013). Completing the COPI machinery, ArfGAP1 has been shown to dynamically associate with lipid droplets in hepatocytes (Gannon et al., 2014; Suzuki et al., 2015; Takashima et al., 2011). Currently, this COPI machinery is linked to the budding of small, 60 nm lipid droplets from larger lipid droplets causing increases in surface tension that promotes lipid droplet fusion with the ER (Thiam et al., 2013; Wilfling et al., 2014). These fusion events are required for trafficking of proteins and lipids to and from lipid droplets. While there appears to be growing evidence for GBF1-dependent COPI machinery at lipid droplets, full-length GBF1 has not been localised to these structures to date.

Lastly, Arf1 has also been postulated to have a role at the plasma membrane in the glycosylphosphatidyl inositol (GPI) anchored protein targeted endocytosis

(Kumari and Mayor, 2008). These specialized functions, along with the primary trafficking roles, further highlight the importance of Arf proteins for cellular function and viability.

1.2.4 Arf receptors and effectors

Arf proteins have a significant number of interacting partners that are intimately linked to Arf function. Activated, GTP-bound, Arf proteins recruit coat proteins, lipid modifying enzymes, tethering factors, and other miscellaneous effectors that are critical for trafficking events and maintenance of various compartments in the secretory pathway (D'Souza-Schorey and Chavrier, 2006; Donaldson and Jackson, 2011; Gillingham and Munro, 2007). A primary function of activated Arf proteins is coat recruitment, (Beck et al., 2009). Likewise, Arf proteins at the TGN recruit AP and Golgi-localising, Gamma-adaptin ear domain homology, Arf-binding protein (GGA) adaptor proteins that serve as recruiters of clathrin coat proteins (Bonifacino and Lippincott-Schwartz, 2003). Without these processes lipid trafficking fails to take place resulting in compartment collapse and ultimately cell death.

Arf recruitment of lipid modifying enzymes results in alteration of the lipid environment and composition. The first of these Arf-recruited enzymes identified was phospholipase D (PLD), which functions to produce phosphatidic acid from substrate phophatidylcholine (Brown et al., 1993; Hong et al., 1998). Active, GTP-bound, Arf can also recruit phosphatidylinositol 4-phosphate, 5-kinase (PIP5K), an enzyme that generates phosphatidylinositol 4,5-bisphosphate ($PI4,5P_2$) through

phosphorylation at the 5th carbon of phosphatidylinositol 4-phosphate (PI4P) (D'Souza-Schorey and Chavrier, 2006). The production of critical lipids at the Golgi also requires Arf activation. Specifically, PI4P production is dependent on phosphatidylinositol 4-kinase that is recruited to Golgi membranes by activated Arf1 (De Matteis and Godi, 2004). Arf1 has also been implicated in recruitment of members of the oxysterol-binding proteins through interaction with the PI4P-specific plekstrin homology domains, which has been postulated to be required for lipid homeostasis at the Golgi (D'Angelo et al., 2008; De Matteis and Godi, 2004).

Interestingly, there has not been a role or function attributed to the inactive, GDP-bound, Arf proteins to date. Arf•GDP association with membranes, which is required for Arf activation, was primarily thought to be due to membrane sampling by the myristoylated N-terminal amphipathic helix. Since the recruitment of Arf to membranes is required for activation, many groups have studied the mechanism of Arf recruitment. These studies have resulted into the identification of the putative Arf receptor p23, which is thought to recruit Arf1•GDP to sites of activation (Gommel et al., 2001). More recently, Arf1•GDP has been shown to interact with a Golgi-localised SNARE protein, membrin, a proposed transmembrane receptor that promotes Arf activation by recruited Arf•GDP to the Golgi membrane (Honda et al., 2005).

1.3 Guanine nucleotide exchange factor (GEF) activation of Arfs

The activation of Arf proteins requires catalysis by diverse Arf guanine nucleotide exchange factors (GEF) (ArfGEF) enzyme family, referred to as the Sec7

family (Figure 1.2) (Casanova, 2007; Cox et al., 2004; Donaldson and Jackson, 2011).The Sec7 family is defined by the presence of a central Sec7 catalytic domain (Sec7d), as the name suggests, that facilitates the nucleotide exchange on Arf. The ArfGEF family can be subdivided into three subfamilies based on enzyme size. The small ArfGEFs including cytohesin, ARNO, and EFA6 range from 40-80 kDa. The intermediate ArfGEFs including BRAG and SYT1 range in size from 100-150 kDa. Lastly, the large ArfGEFs including GBF1/GEAs and BIGs/SEC7 fall between 160 and 230 kDa in size (Cox et al., 2004; Mouratou et al., 2005). Interestingly, members of the small and intermediate ArfGEFs contain additional classical domains such as plekstrin homology (PH) and coiled-coil (CC) domains that facilitate membrane and protein interactions. Interestingly, the large ArfGEFs GBF1 and BIGs do not contain these domains and therefore must be recruited to membranes by a different mechanism.

1.3.1 The large Arf-GEF sub-family

The large ArfGEFs are not only similar in size, but also share significant functional and sequence similarities (Mouratou et al., 2005). Interestingly, the large ArfGEFs have orthologues in all eukaryotic organisms sequenced to date. The large ArfGEFs can be further subdivided into two distinct, but related classes. The first class includes the mammalian Golgi-specific brefeldin A (BFA) resistance factor 1 (GBF1), along with *Arabidopsis thaliana* GNOM, *S. cerevisiae* Gea1p and Gea2p, and *Drosophila melanogaster* Garz; the second class is comprised of Sec7 characterized in

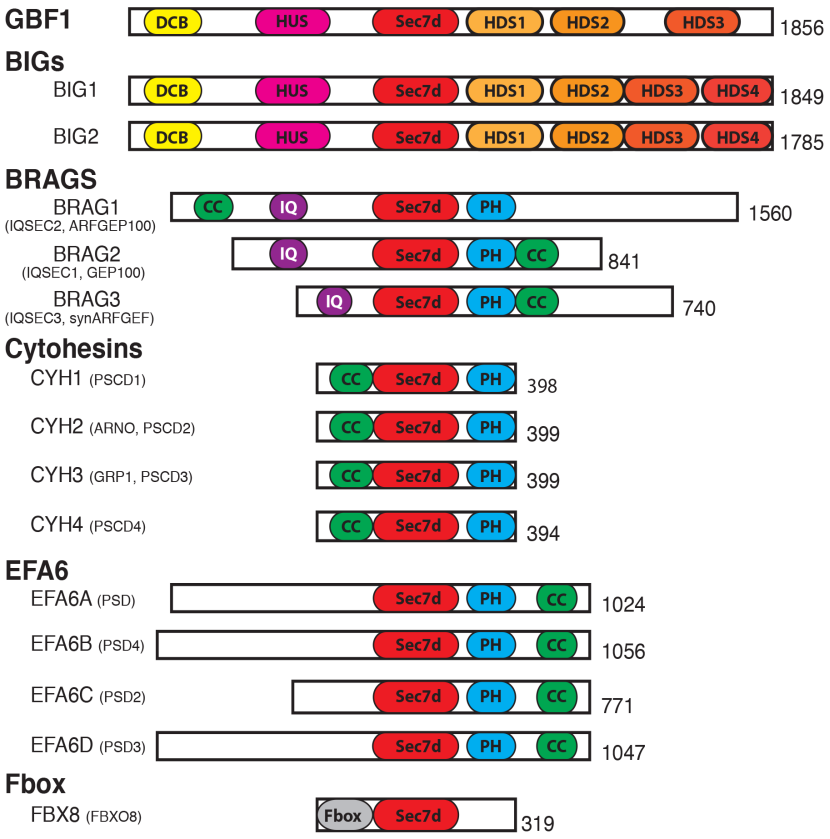

Figure 1.2 Domain organization of the Sec7 family of ArfGEFs in human cells. *Homo sapiens* express six different subfamilies of ArfGEFs, which are represented above. Each ArfGEF is organized into the individual subfamily and labeled with name, domain organization, and protein size in amino acid residues. Alternate names are given in parantheses. Domains are colour coded and labeled including Sec7d (red), which is common to all members of the Sec7 family. Additional domain include the DCB: dimerization and cyclophilin binding domain, HUS: homology upstream of Sec7 domain, HDS1-4: homology downstream of Sec7 domain, PH: plekstrin homology domain, CC: coiled-coil domain, IQ: IQ motif, and Fbox: Fbox motif. Adapted from (Casanova, 2007).

yeast and the mammalian BIG1 and BIG2 (Jackson and Casanova, 2000). In addition to protein size, the large ArfGEFs are unified by sensitivity to the fungal metabolite BFA, as the names given to the proteins suggest (Casanova, 2007). This drug has proved to be a critical pharmacological tool for the study ArfGEF function and the early secretory pathway. While mammalian cells only express GBF1, yeast cells express two enzymes, Gea1p and Gea2p which appear redundant as suggested by only double deletion strains displaying significant defects in viability and protein secretion (Peyroche et al., 1996). Interestingly, this redundancy arises despite only 50% sequence identity. GBF1 was originally identified as a BFA resistance factor expressed in a mutated Chinese hamster ovary (CHO) cell line (Yan and Melancon, 1994). Interestingly, further characterization of GBF1 confirmed that GFB1 is, in fact, sensitive to BFA and only provides BFA resistance when over-expressed (Claude et al., 1999). Resistance was assayed by the disassembly of the Golgi complex and normal distribution of Golgi markers. Specifically, it was shown that the Golgi-localisation of the β-COP subunit of the COPI was resistant to BFA treatment in GBF1 over-expression conditions.

1.3.2 GBF1 localisation and function

The large ArfGEFs have specific functions that are intimately linked to their sub-cellular localisation. Although primarily cytosolic, GBF1 localises to the ERGIC and the *cis*-Golgi compartments (Kawamoto et al., 2002; Manolea et al., 2008; Zhao et al., 2006; Zhao et al., 2002). GBF1 association with target membranes is transient with the enzyme continuously cycling on and off membranes rapidly, despite lacking

classical membrane binding domains (Niu et al., 2005; Szul et al., 2007). At the ERGIC and *cis*-Golgi, GBF1 regulates COPI-dependent vesicle trafficking and Golgi maintenance through the activation of Arf proteins (Garcia-Mata et al., 2003; Manolea et al., 2008). GBF1 is not only essential for protein secretion, but also cell viability since pharmacological inhibition or knockdown of protein level result in Golgi collapse followed by cell death through induction of the unfolded protein response (Citterio et al., 2008; Sciaky et al., 1997). This is partially due to the fact that GBF1 is the only known ArfGEF that localises to the ERGIC and *cis*-Golgi (Claude et al., 1999; Garcia-Mata et al., 2003; Kawamoto et al., 2002; Zhao et al., 2002). Knockdown of GBF1 demonstrates that it is solely responsible for activation of class I and class II Arf proteins at these compartments (Manolea et al., 2008).

In addition to primary localisation to the ERGIC and *cis*-Golgi, multiple secondary localisations and associated functions have been described for GBF1. The first example involves the recruitment of the *Drosophila* encoded GBF1 homologue *garz* to the plasma membrane where it is implicated in the endocytosis of glycosylphosphatidylinositol-anchored proteins (GPI-APs) into GPI-APs enriched early endosomal compartments (GEECs) (Gupta et al., 2009). Imaging data suggest that GBF1 can be localised to the plasma membrane, although it is clear that only a small proportion of the total pool of GBF1 is found there at any given time. The proposed role of GBF1/*garz* at the plasma membrane is to activate Arf1, which was previously suggested to be critical in the GEEC-type endocytic pathway (Kumari and Mayor, 2008). Beyond the proposed involvement of Arf1 and *garz* in this specialized endocytic pathway, the exact mechanism for this process remains unclear.

An additional secondary localisation for GBF1 has been proposed to be lipid droplets. The link between GBF1 and lipid droplets has been suggested to be both physical and functional. It was first suggested that GBF1 activity is required for the delivery of critical lipid modifying enzymes to lipid droplets from the ERES and/or ERGIC compartments (Soni et al., 2009). This requirement for the COPI-Arf-GBF1 machinery in lipid droplet homeostasis was independently confirmed for the delivery of lipid modifying enzymes (Beller et al., 2008). Perhaps most interestingly, the mechanism by which GBF1, and specifically COPI, could play a role in the delivery of cargo to a lipid monolayer remains intriguing. COPI has not been previously implicated in deformation of lipid monolayers or the production of micelles, and therefore the mechanism of this proposed function remains unclear.

1.3.3 The Sec7 domain (Sec7d)

The central Sec7d that defines the divergent Sec7 family consists of approximately 200 amino acid residues (Casanova, 2007). Sec7 domains are characterized based on sequence homology. The structure of Sec7d consists of 10 transverse α-helices that are partitioned into two subdomains by a deep hydrophobic groove (Cherfils et al., 1998; Goldberg, 1998). Within the Sec7d, a highly conserved catalytic glutamate residue, referred to as the 'glutamic finger', is located at the tip of a hydrophobic loop between helices 6 and 7. Structural studies indicates that the catalytic glutamate functions by insertion into the nucleotide-binding fold of the Arf protein where it forces the GDP nucleotide out of the binding domain (Traut, 1994) through electrostatic competition with the β-phosphate

(Beraud-Dufour et al., 1998). In order for this to occur, the Sec7d essentially forces a significant change in the core structure of the Arf, by opening the switch 1 and switch 2 domains, and thereby releasing the previously bound GDP (Renault et al., 2003). As a result, the nucleotide-binding domain is made available for binding of the more abundant high affinity GTP nucleotide and thereby activating the Arf as described previously (Traut, 1994) (Figure 1.3). Interestingly, BFA acts as an uncompetitive inhibitor of the catalytic Sec7 domain (Mansour et al., 1999; Peyroche et al., 1999). It forms a non-productive complex between the Sec7 domain and the substrate Arf1•GDP by intercalating into a small cavity that forms at the interface (Renault et al., 2003).

1.3.4 The other domains of GBF1

In animal cells, GBF1 is a protein comprised of six evolutionarily conserved domains (see Figure 1.2) (Mouratou et al., 2005). As described in detail in section 1.3.3, Sec7d remains the best characterized of these domains. Upstream of the centrally located Sec7d are two highly conserved domains, namely the dimerization/cyclophilin binding (DCB) domain and the homology upstream of Sec7d (HUS) domain. Work performed in the model organism *Arabidopsis thaliana* suggested the DCB domain is potentially involved in dimerization as well as binding of cyclophilin 5 (Grebe et al., 2000), however cyclophilin 5 binding has not been further supported (Anders et al., 2008). The role of the DCB in dimerization has been further supported using a yeast two-hybrid system, which indicated interactions

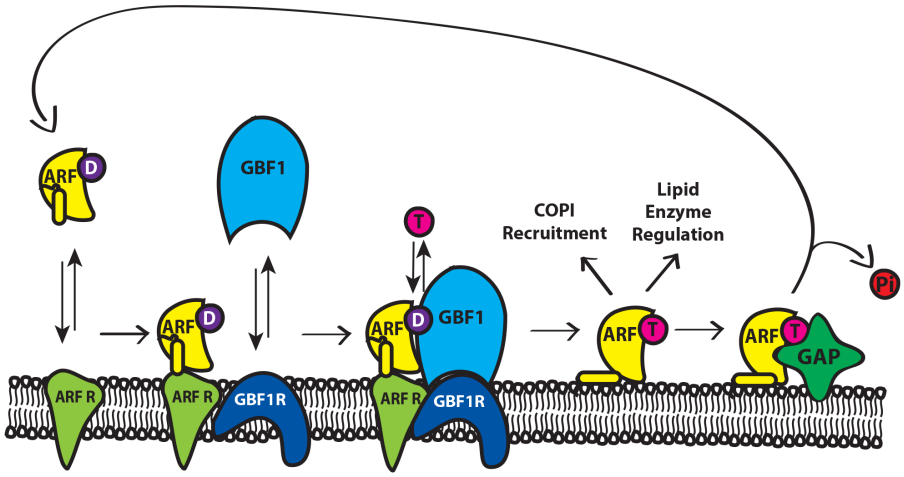

Figure 1.3 Diagram depicting the activation of Arf by GBF1 at *cis*-Golgi membranes. The activation of Arf proteins at the *cis*-Golgi and ERGIC is dependent on the activity of the sole *cis*-Golgi-localized ArfGEF GBF1. The activation process requires membrane association of the Arf, and therefore requires co-recruitment of both the Arf and GBF1. This critical recruitment of Arf is mediated by an N-terminal myristate moiety and/or interaction with receptors. GBF1 recruitment is poorly understood, but we postulate that a currently unidentified GBF1 receptor is required. Once both Arf and GBF1 are found at the membrane and in close proximity, GBF1 can catalyze nucleotide exchange by displacing the GDP nucleotide and thus allowing the more abundant GTP nucleotide to bind, activating the Arf. Once active, Arf proteins can then modulate the activity of effector proteins including COPI and lipid modifying enzymes. GTP-bound Arf can subsequently be inactivated by GTP hydrolysis, which is dependent on the acitivty of an ArfGAP. These processes are required to maintain Golgi morphology and function.

between DCB-DCB and DCB-HUS mammalian GBF1 domains (Ramaen et al., 2007). While dimerization studies of the GBF1 paralogs BIG1/BIG2 have provided significant support for dimerization, dimerization of GBF1 *in vivo* remains poorly supported (Mansour et al., 1999; Ramaen et al., 2007).

Downstream of the Sec7d are three additional homology domains, although poorly conserved relative to HUS and DCB. The homology downstream of Sec7 (HDS) domains 1, 2, and 3 are defined by sequence similarity but their functions remain unclear. Recent studies have proposed roles in intracellular localisation of large ArfGEFs through direct interactions with target membranes, such as the ERGIC/Golgi (Bouvet et al., 2013). Specifically, GBF1 may be capable of localising directly to lipid droplets because a GBF1 truncation consisting of the HDS1 domain alone displayed colocalisation with lipid droplet markers. However, this localisation was not confirmed for larger fragments of GBF1. Further, the HDS1 domain has also been implicated in the trafficking of adipose triglyceride lipase (ATGL) to lipid droplets through protein interaction (Ellong et al., 2011). However, it remains unclear how this domain would perform both functions or if these observations made using the HDS1 domain alone are in fact relevant to the intact GBF1 protein.

1.3.5 GBF1 interacting partners

Despite the large size of GBF1 and considerable potential for protein-protein interactions, very few interacting partners have been identified. Further, of these interacting partners, there have been very few follow-up studies to confirm initial interaction reports. To highlight the difficulties in characterizing authentic GBF1

binding partners, identification of a complex between wild-type GBF1 and Arf from cell lysates has remained elusive despite knowing they must interact. Reported interacting partners include the Golgi-associated p115, GGAs, and Rab1b.

The first published interacting partner for GBF1 was the essential membrane transport factor p115 (Alvarez et al., 1999). Previous studies of p115 function suggest a significant role in trafficking to and through the Golgi. The interaction profile for p115 is quite extensive and includes many canonical Golgi-localised proteins, suggesting a role as a molecular scaffold. Interacting partners include GM130 (Linstedt et al., 2000), giantin (Nelson et al., 1998), Rab1 (Allan et al., 2000), and many members of the SNARE family (Shorter et al., 2002). The interaction of p115 with GBF1 was identified by yeast two-hybrid and then confirmed by co-immunoprecipitation both *in vivo* and *in vitro*. The critical interacting domains were mapped to a poorly conserved proline-rich domain of GBF1 in the extreme C-terminus and to the head region of p115. The proposed function of the p115-GBF1 complex is intra-Golgi trafficking and Golgi maintenance, likely through the formation of a large multi-protein complex at Golgi membranes. Interestingly, the proposed p115-GBF1 interaction is not required for GBF1 association with Golgi membranes (Garcia-Mata and Sztul, 2003).

Another published GBF1 interacting partner, GGAs, (Lefrancois and McCormick, 2007) is one that that cannot be readily reconciled with the predominant localisation of GBF1. LeFrancois reports co-localisation of both BIGs and GBF1 with GGA at the TGN. However, others and we have clearly demonstrated that GBF1 localises specifically to the *cis*-Golgi (see 1.3.2). These author's data do not

support the interpretation as there is an obvious difference in the fluorescence pattern of GBF1 and GGAs. The GBF1-GGA protein-protein interaction was identified by co-immunoprecipitation from HeLa cell lysates (Lefrancois and McCormick, 2007). The authors also presented data suggesting that the interaction could be mapped to the N-terminal half of GBF1 and the VHS-GAT domains of GGA proteins. The proposed function of this protein-protein interaction is the recruitment of GGAs to the TGN and correct protein trafficking.

The last of the published GBF1 binding partners, and perhaps the most interesting, is Rab1b. Rab1b was shown to interact with GBF1 in a GTP-dependent manner by GST-pulldown (Monetta et al., 2007). Specifically, the authors indicate that Rab1b binds directly to the N-terminal half of GBF1 (lacking the Sec7d). In addition, depletion of cellular Rab1b, or expression of a dominant-negative Rab1b mutant, causes a significant redistribution of GBF1 to the cytosol. This redistribution is consistent with Rab1b being required for GBF1 recruitment to membranes. Interestingly, expression of a dominant-active mutant of Rab1b recruited GBF1 specifically to the ERGIC and not the Golgi while Arf•GTP levels remain unchanged. Moreover, Rab1b was previously shown to interact with p115 (Garcia-Mata and Sztul, 2003) and GM130 (Moyer et al., 2001), suggesting that Rab1b plays a role in the formation of a large protein complex at Golgi membranes that may be involved in membrane tethering. However, the role of Rab1b remains unclear as manipulations of Rab1b were shown to have no effect on p115 localisation to Golgi membranes (Monetta et al., 2007), which could be explained by redundancy between Rab1b and the closely related Rab1a. In conclusion, Monetta *et al.* postulate that Rab1b may be a

master regulator of COPI coat recruitment and therefore trafficking. The authors postulate this occurs specifically at ERGIC structures, although considerable additional experimentation would be required to strengthen this claim. The potential role for Rab1a in GBF1 recruitment remains unclear and should be further assessed, including testing of the redundant Rab1b for a role in GBF1 recruitment.

1.3.6 GBF1 mutations and pharmacological inhibitors

Mutational studies of the GBF1 homologues expressed in *Arabidopsis* identified mutants that resulted in significant alterations is pattern formation in embryos (Jurgens, 1995). Characterization of these mutations revealed a specific point mutation, E658K, which abrogated guanine nucleotide exchange on Arf proteins (Shevell et al., 1994). Subsequently, this mutation was replicated in several other ArfGEFs and each mutant ArfGEF was found inactive. This mutant was mapped to amino acid residue 794 in human GBF1 protein (E794K) and shown to similarly abolish nucleotide exchange on Arf proteins (Garcia-Mata et al., 2003). Note that studies with ARNO Sec7d bearing the glutamate to lysine mutation established that even though the mutant does not support GDP nucleotide displacement and confer a phenotype similar to that of BFA treatment, it retains Arf•GDP binding capacity (Beraud-Dufour et al., 1998). Interestingly, the more conservative E794D substitution was also capable of rendering the GBF1 enzyme catalytically inactive (Lefrancois and McCormick, 2007).

In addition to mutational studies performed on GBF1, truncation studies have been performed in an attempt to characterize known domains and identify novel

functional domains (Bouvet et al., 2013). Fixed-cell imaging experiments using a GBF1 truncation library suggest that the N-terminal DCB domain is required for GBF1 association with Golgi membranes. In addition, the published results suggest that deletion of the HDS1 domain also impairs Golgi-localisation. While this study suggests domains that may be critical for Golgi association, further work is required to confirm these observations.

A great deal of our understanding of protein trafficking and more specifically GBF1 function originates from studies utilizing the large ArfGEF inhibitor BFA. More recently, additional GBF1 inhibitors have been described. One such inhibitor of particular interest is Golgicide A (GCA) that was identified in a large scale screen for chemicals that altered Shiga toxin trafficking in cells (Saenz et al., 2009). Further characterization of the inhibitor demonstrates the phenotypes observed closely mirror those observed for dominant-negative GBF1 mutants and BFA treatment, suggesting the inhibitor likely targets GBF1. Structural analysis suggests that GCA resembles BFA and binds the same Arf-Sec7 domain interface. However, because GCA is slightly larger than BFA it is highly specific to GBF1 and has no early effects on BIGs or TGN morphology. This discovery provides researchers with a valuable tool that allows for the study of GBF1 activity without confounding inhibition of BIGs and off target effects observed for BFA (Saenz et al., 2009).

1.3.7 A putative GBF1 receptor

The primary function of GBF1 is promoting nucleotide exchange on Arf proteins, a process that requires Arf recruitment to membranes in order for

nucleotide exchange to occur. Without GBF1 activity, the Golgi complex collapses into the ER and protein trafficking halts, ultimately resulting in cell death through the induction of the unfolded protein response (Citterio et al., 2008). Furthermore, it remains clear that GBF1 has a specific intra-cellular localisation within the secretory pathway. Together, these facts suggest the importance of specific recruitment of GBF1 to membranes of the ERGIC and *cis*-Golgi. The simplest explanation for accomplishing highly specific recruitment of GBF1 to ERGIC and *cis*-Golgi membranes is the presence of a putative GBF1 receptor (Niu et al., 2005; Zhao et al., 2006). Despite the identification of multiple GBF1 interacting partners, none of these have been convincingly presented as a GBF1 receptor governing compartment-specific recruitment.

1.4 Arf GTPase activating proteins (ArfGAPs)

The diverse members of the Arf GTPase activating proteins (ArfGAPs) protein family are partially defined by the presence of a highly conserved ArfGAP domain, consisting of a four-cysteine zinc-finger motif and an invariant catalytic arginine residue (Kahn et al., 2008). ArfGAPs can be subdivided into 10 subfamilies of which two subfamilies have been shown to associate with the Golgi, namely ArfGAP1 and ArfGAP2/3. Importantly, ArfGAP2 and ArfGAP3 are evolutionarily related and result from a gene duplication event resulting in approximately 58% sequence similarity (East and Kahn, 2011). ArfGAP1, however, shares little to no sequence similarity with the other Golgi-localised ArfGAPs outside the family defining ArfGAP domain. The presence of unique domains in different ArfGAP proteins suggests specific

functional and regulatory roles for individual ArfGAPs (Kahn et al., 2008). In addition, specific compartmental localisation of ArfGAPs within the Golgi likely also influence the physiological roles of these proteins (East and Kahn, 2011). It is likely that within the Golgi-localised ArfGAPs there are specialized functions that may be influenced by specific compartmental localisations.

1.4.1 Function of Golgi-localised ArfGAPs

ArfGAP1 has been shown to localise to the *cis*-Golgi (Cukierman et al., 1995) where it can interact with the KDEL receptor, a COPI cargo protein (Aoe et al., 1997; Aoe et al., 1999). In addition to the GAP domain, ArfGAP1 has two amphipathic ArfGAP lipid packing sensor (ALPS) motifs that promote binding to highly curved membranes (Ambroggio et al., 2010). This would further support a role for ArfGAP1 in COPI-mediated vesicle formation, as COPI facilitates membrane curvature and therefore creates a regions of Golgi membranes that could be bound by ArfGAP1 via the ALPS domains. Recruitment to Golgi membranes may be, in part, due to interactions with components of the COPI complex (Liu et al., 2005). Specifically, the δ-COP subunit is suggested to bind tryptophan-based sequences found in cargo and ArfGAP proteins including ArfGAP1 (Suckling et al., 2015). ArfGAP1 interaction with another COPI cargo protein, p24, was suggested to have an inhibitory effect on ArfGAP activity (Goldberg, 2000; Lanoix et al., 2001). Together, these findings suggest a role for ArfGAP1 preventing the formation of empty COPI-mediated vesicles by quickly hydrolyzing Arf-bound GTP in the absence of cargo, while allowing vesicle formation in the presence of sufficient cargo. A role for ArfGAP1 in

COPI mediated vesicle formation has been further supported by *in vitro* vesicle formation assays in which ArfGAP1 and GTP hydrolysis were required (Hsu et al., 2009; Lee et al., 2005; Yang et al., 2002). However, this was disputed by another publication that failed to find ArfGAP1 in COPI vesicles or to observe an ArfGAP1 requirement for COPI vesicle formation (Beck et al., 2009). Interaction of truncated ArfGAP1 with coatomer was shown to potentially stimulate GAP activity (Goldberg, 2000), however a conflicting report concluded that COPI coat did not alter activity of full length ArfGAP1 in the context of purified Golgi preparations (Szafer et al., 2000). Moreover, work studying the roles for ArfGAPs on COPI coat assembly in living cells suggest that ArfGAP1 is not required (Kartberg et al., 2010). It remains difficult to generate a single model that takes into account the published work, as many of these findings are inconsistent with each other.

Like ArfGAP1, ArfGAP2/3 have also been reported to potentially bind to COPI. However, unlike ArfGAP1, there does not appear to be a controversy that this interaction stimulates ArfGAP activity (Beck et al., 2009; Weimer et al., 2008). ArfGAP2/3 have been shown to have GAP activity enhanced through interactions with COPI coat proteins (Kliouchnikov et al., 2009; Luo and Randazzo, 2008; Weimer et al., 2008). To further confuse the potential for ArfGAP1 and ArfGAP2/3 having different roles at the Golgi, *in vitro* studies using large unilamellar vesicles (LUVs) suggested that both ArfGAP1 and ArfGAP2 could facilitate vesiculation in the presence of cargo and soluble coatomer (Shiba et al., 2011), despite previous studies suggesting ArfGAPs was not essential (Bremser et al., 1999). Perhaps most importantly, work done in live cells suggest that ArfGAP2 and ArfGAP3 are essential

for COPI coat assembly as observed during double knockdown (Kartberg et al., 2010). To date, there is no consensus as to whether or not ArfGAP1 and ArfGAP2/3 have discrete functions within mammalian cells as may be expected based on differences in sequence and localisation.

1.4.2 ArfGAP localisation within the Golgi

Another potential explanation for ArfGAPs serving separate and unique roles in live cells is differential localisation within the Golgi and secretory pathway. Early localisation studies of ArfGAPs suggest that ArfGAP1 was evenly distributed throughout the Golgi complex, whereas ArfGAP2 and ArfGAP3 were thought to display a preference of the *cis*-Golgi stack portion (Weimer et al., 2008). However, more recent reports demonstrate that ArfGAP3 co-localises well with a TGN marker and is thus primarily found at the TGN and endosomes where it is required for trafficking of the mannose-6-phosphate receptor (Shiba et al., 2013). Together, linking ArfGAP3 localisation and function to the TGN provides strong evidence for specialized localisation and function at the TGN. There are no reports of ArfGAP1 or ArfGAP2 having a primary localisation to a structure other than the *cis*-Golgi stack, although secondary localisations have been proposed. The study of ArfGAPs in yeast has provided a useful paradigm for differential localisation and function of ArfGAPs through the Golgi. Specifically, it has been demonstrated that each of four ArfGAPs expressed in *Saccharomyces cerevisiae* have both unique and overlapping roles (Zhang et al., 2003). Moreover, it appears that the subcellular localisation of each ArfGAP differs slightly with some having more *cis* or *trans* localisations.

1.4.3 Possible redundancy of Golgi-localised ArfGAPs

Understanding how the Golgi-localised ArfGAPs function remains somewhat unclear due to conflicting reports. For example, no consensus has emerged on whether ArfGAP1 and ArfGAP2/3 are redundant and perform similar functions in the cell. Studies suggest that both ArfGAP1 and ArfGAP2 promote COPI vesicle formation (Shiba et al., 2011). This hypothesis is supported by multiple reports that both single and double knock-down of ArfGAP1/2/3 failed to produce a phenotype, while triple knockdown resulted in Golgi collapse and cell death (Frigerio et al., 2007; Saitoh et al., 2009). Interestingly, the Golgi collapse phenotype closely resembles that which was described for β-COP knockdown, supporting a significant role for ArfGAP1/2/3 in COPI function. Further, recovery experiments suggest that expression of any of ArfGAP1/2/3 could recover Golgi morphology phenotypes that resulted from the knockdown of all three (Saitoh et al., 2009). These data do not support the idea of specific localisations and functions for each of the Golgi-localised ArfGAPs. However, a more recent publication describes significant phenotypes resulting from the double knockdown of ArfGAP2 and ArfGAP3, which suggests that ArfGAP1 is not redundant with ArfGAP2/3 (Kartberg et al., 2010). However, the long duration of incubations required to achieve sufficient knock-down make these studies particularly prone to compensatory artifacts and therefore challenging to interpret. Clearly additional work is required to provide a consensus on whether Golgi-localised ArfGAPs have discrete functions at the Golgi, or if they preform redundant roles.

1.4.4 Molecular tools for the study of ArfGAPs

Study of ArfGAP function in living cells has resulted in the identification and characterization of catalytically inactive ArfGAP mutants. The catalytic ArfGAP domains of ArfGAP1 and ArfGAP2/3 are found at the N-terminus of the protein. Various catalytically inactive ArfGAP mutants have been constructed ranging from single point mutations, double point mutations, to truncations of the N-terminus. As mentioned previously, ArfGAP catalytic activity is dependent on the GAP domain and specifically the arginine finger. As predicted, deletion of the first 63 residues of ArfGAP1 (ArfGAP1Δ63) including part of the GAP domain eliminated catalytic activity (Huber et al., 1998). Interestingly, study of this mutant in live cells suggested there was no obvious Golgi morphology phenotype (Liu et al., 2005), likely the result of lack of interaction with its substrate Arf•GTP. Huber and colleagues also identified a point mutant in which one of the critical cysteine residues (C22A) that form the essential zinc-finger motif within the GAP domains also conferred a loss in ArfGAP catalytic activity (Huber et al., 1998). This point mutant was further characterized in ArfGAP3 indicating this mutation not only impairs catalytic activity, but also prevents binding of Arf•GTP altogether through the pairing of two cysteine mutations (CC25,28SS). Lastly, it has been demonstrated that mutation of the catalytic arginine residue to glutamine resulted in a loss of catalytic activity in ArfGAPs (Luo et al., 2007). For the Golgi-localised ArfGAPs, this mutation maps to R50 for ArfGAP1, R53 for ArfGAP2, and R53 for ArfGAP3 (Shiba et al., 2013). Interestingly, similar to the ArfGAPΔ63 truncations, the RQ mutant forms of ArfGAP1 did not cause a significant Golgi morphology phenotype relative to expression of

ArfGAP1 wild-type (Lee et al., 2005). Unlike the N-terminal deletion mutant, however, the RQ point mutants can still bind Arf•GTP, although non-productively. In addition, these inactive mutants have also led to the suggestion that ArfGAPs have functions independent of catalytic activity based on evidence that suggest RQ mutants may support specific ArfGAP functions (Shiba et al., 2011). These mutant ArfGAPs serve as valuable tools for studying ArfGAP functions.

Pharmacological inhibitors and activators of ArfGAPs have not been established, however one activating drug has been suggested. 2-(4-Fluorobenzoylamino)-benzoic acid methyl ester (Exo1) was identified in a large screen based on it causing rapid Golgi collapse into the ER, through the inhibition of membrane trafficking (Feng et al., 2003). While this compound caused a phenotype that closely resembled that seen for BFA, it was demonstrated that Exo1 had no inhibitory effect on GBF1 itself. This suggests that Exo1 has an alternate target, and although it is not conclusive, it has been postulated that Exo1 increases ArfGAP activity by a currently unknown mechanism.

1.5 Hypothesis and thesis plan

Golgi function is essential for protein secretion and maintenance of Golgi structure, and that of the secretory pathway as a whole. Ultimately, failure to efficiently traffic protein through the Golgi results in cell death through the unfolded protein response. Arf activation is essential for the recruitment of coat proteins or effectors such as lipid modifying enzymes. To date, GBF1 is the only ArfGEF that localises to the ERGIC and Golgi compartments and is thus solely responsible for the

activation of Arf proteins at these compartments within the secretory pathway, as confirmed by knockdown studies. It has been established that Arf activation can only occur at membrane surfaces due to required conformation changes that occur during membrane association. Since the activation of Arf is membrane-dependent, it becomes essential that the predominantly cytosolic GBF1 be efficiently recruited to Golgi membranes in order to activate Arf and maintain Golgi structure and function. We hypothesize that, due to the importance and specificity of GBF1 recruitment to Golgi membranes, this process is likely tightly regulated. To test our hypothesis, we utilized live cell and fixed cell imaging experiments to identify the mechanism by which GBF1 recruitment to Golgi membranes is regulated. Previously published work has demonstrated pharmacological agents that prevent Arf activation or alter Arf•GTP hydrolysis result in subsequent GBF1 accumulation on membranes of the ERGIC and Golgi. We hypothesize that GBF1 maintains homeostatic Arf activation in the cell by altering levels of GBF1 membrane association in response to changes in Arf•GTP:Arf•GDP ratio. Additionally, we established an *in vitro* GBF1 recruitment assay that allowed us to further test our hypothesis, providing confirmation that Arf•GDP stimulates GBF1 recruitment to Golgi membranes. By establishing the mechanisms that govern Golgi membrane recruitment, we hope to establish experiments that will allow us to confirm and identify a putative GBF1 receptor found at the membranes of the ERGIC and Golgi compartments.

Chapter 2: Materials and methods

2.1 Reagents

During this study, the various chemicals, reagents, enzymes, and commercial kits were used according to manufacturers instructions unless specifically stated otherwise. Workplace Hazardous Materials Information System (WHMIS) and the University of Alberta Environmental Health and Safety office recommendations and protocols were followed for all reagents and procedures.

Table 2.1 List of chemicals and reagents

Chemical/Reagent	Supplier
6x Loading Dye	Promega
Acetic acid, glacial	Fisher Scientific
30% acrylamide/bis (29:1)	Bio-rad
Agarose (Ultrapure)	Invitrogen
Ammonium persulfate	Bio-rad
Ammonium sulfate	Sigma
Ampicillin	Novopharm
Bactotryptone	BD Biosciences
Bacto-yeast	BD Biosciences
Brefeldin A	Sigma
Brilliant blue G-250	Sigma
Bromophenol blue	Sigma
Calcium chloride	Sigma
Calf intestinal alkaline phosphatase (CIAP)	Invitrogen
CO2-independent medium	Gibco (Invitrogen)
Complete, EDTA-free protease inhibitor cocktail	Roche
Difco LB (Luria-Bertani) broth, Miller	BD Biosciences
Difco LB (Luria-Bertani) agar, Miller	BD Biosciences
DTT (dithiothreitol)	Sigma
1 M DTT solution	Sigma
DMEM (Dulbecco's Modified Eagle Medium)	Gibco (Invitrogen)
DMSO (dimethyl sulfoxide)	Sigma
dNTPs (deoxyribosemucleotide triphosphate)	Invitrogen
EDTA (ethylenediamine-tetraacetic acide)	Sigma
95% Ethanol	Fisher Scientific
Exo1	Calbiochem

Fetal Bovine Serum (FBS)	Gemini Bio-Products
Gelatin	Fisher Scientific
GeneRuler 1 kb DNA Ladder	Fermentas
O'GeneRuler 1 kb DNA Ladder	Fermentas
Glycerol	Fisher Scientific
100 mM GTP Li salt	Fisher Scientific
HEPES	Sigma
Hydrochloric acid	Fisher Scientific
IGEPAL CA-630 (NP-40)	Sigma
Isopropanol	Fisher Scientific
Kanamycin sulfate	Gibco (Invitrogen)
L-glutamine	Gibco (Invitrogen)
Lipofectamine 2000	Invitrogen
Magnesium chloride	BDH
Magnesium sulphate	Fisher Scientific
Methanol	Fisher Scientific
Opti-MEM	Gibco (Invitrogen)
Paraformaldehyde	Sigma
Penicillin/streptomycin	Gibco (Invitrogen)
PBS (Dulbecco's phosphate buffered saline)	Gibco (Invitrogen)
10x DPBS pH 7.4 (Dulbecco's phosphate buffered saline)	Gibco (Invitrogen)
Phosphoric acid	Fisher Scientific
Platinum Pfx DNA polymerase	Invitrogen
Potassium chloride	BDH
Precision Plus Dual Colour Protein Standard	Bio-rad
Prolong Gold with DAPI antifade reagent	Molecular Probes (Invitrogen)
Prolong Gold antifade reagent	Molecular Probes (Invitrogen)
Protein G sepharose	GE Healthcare
Restriction Endonucleases	Invitrogen or NEB
Sodium bicarbonate	Caledon
Sodium chloride	Fisher Scientific
SDS (sodium dodecyl sulfate)	Bio-rad
Sodium hydroxide (5N and 10N)	Fisher Scientific
Sucrose	Sigma
SYBR Safe DNA gel stain	Molecular Probes (Invitrogen)
T4 DNA Ligase	Invitrogen
TEMED (tetramethylethylenediamine)	OmniPure
TransIT-LTI transfection reagent	Mirus
TransIT 20/20 transfection reagent	Mirus
Tris-base	Roche
Tris-HCl	Roche
Triton X-100	VWR
Trypsin (type IX-S) from porcine pancreas	Sigma
0.25% Trypsin-EDTA	Gibco (Invitrogen)

Trypsin inhibitor from Glycine Max (Soybean)	Sigma
Tween-20	Fisher Scientific
Water	Sigma

Table 2.2 Commercial kits

Commercial Kit	Supplier
Dynabeads Co-IP Kit	Life Technologies
Plasmid Maxi Kit	Qiagen
Plasmid Midi Kit	Qiagen
QIAprep Spin Mini Prep Kit	Qiagen
QIAquick Gel Extraction Kit	Qiagen
QIAquick PCR Purification Kit	Qiagen
QuickChange Kit	Stratagene

Table 2.3 Commonly used buffers and solutions

Solution	Composition
Colloidal Coomassie Stain	10% (v/v) phosphoric acid, 100 g ammonium sulfate, 1.2 g G250 Coomassie Blue, 20% (v/v) methanol
Colloidal Coomassie Fixation	50% (v/v) ethanol, 2% (v/v) phosphoric acid
Cell Freezing Medium	15% (v/v) DMSO in FBS
Homogenization Buffer	25% Sucrose, 5 mM $MgCl_2$, 2x Complete protease inhibitor
In vitro GBF1 Recruitment Assay Buffer	25 mM Hepes pH 7.4, 180 mM NaCl, 5 mM $MgCl_2$, 2x Complete protease inhibitor
Luria-Bertani (LB) Broth	1% (w/v) bactotryptone, 0.5% (w/v) bacto-yeast extract, 1% (w/v) NaCl, pH 7.0
3% Paraformaldehyde	3% (w/v) paraformaldehyde, 0.1 mM $CaCl_2$, 0.1 mM $MgCl_2$
Permeabilization Buffer	0.1% (v/v) Triton X-100, 0.05% (w/v) SDS in PBS
Quench Buffer	50 mM NH_4Cl in PBS
Running Buffer	25 mM Tris-HCl, 190 mM glycine, 0.1% (w/v) SDS

Modified SDS-PAGE Sample Buffer (6x)	30% (v/v) glycerol, 20% (w/v) SDS, 125 mM DTT, 0.025% (w/v) bromophenol blue, 125 mM Tris-HCl pH 8.0
4x Separating Gel pH 8.8	0.4% (w/v) SDS, 1.5 M Tris-HCl, pH 8.8
SOC Medium	2% (w/v) bactotryptone, 0.5% (w/v) bacto-yeast extract, 10 mM NaCl, 2.5 mM KCl, 10 mM $MgCl_2$, 20 mM glucose
4x Stacking Gel pH 6.8	0.4% (w/v) SDS, 0.5 M Tris-HCl, pH 6.8
50x TAE	2 M Tris base, 5.71% (v/v) glacial acetic acid, 50 mM EDTA, pH 8.0
TBS-T	50 mM NaCl, 0.5% (v/v) Tween-20, 20 mM Tris-HCl, pH 7.5
Transfer Buffer	25 mM Tris-HCl, 190 mM glycine, 20% (v/v) methanol, 2.5% (v/v) isopropanol

2.2 Cell culture

The cell lines used in the experiments that comprise this thesis include HeLa cells (ECACC; Sigma-Aldrich, 93031013), NRK-52E cells (ATCC CRL-1571), and NRK cells stably expressing GFP-tagged GBF1 (described in (Zhao et al., 2006)).

Growing tissue cultures were maintained in DMEM medium supplemented with 10% FBS, 100 µg/mL penicillin and 100 µg/mL streptomycin in a 5% CO_2 incubator set at 37° Celsius. During acquisition of live cell imaging experiments, cells were kept in CO_2-independent medium supplemented with 10% FBS.

2.3 Antibodies

Antibodies used in the experimentation done in this thesis, along with the dilutions, are listed in the following tables: primary antibodies for

immunofluorescence (IF) in Table 2.4, secondary antibodies for IF in Table 2.5, primary antibodies for immunoblots in Table 2.6, and secondary antibodies for immunoblots in Table 2.7.

Table 2.4 Primary antibodies used in immunofluorescence

Antibody	Dilution	Source
Mouse anti-β-coatomer protein I (COPI) (clone m3a5) monoclonal	1:400	Sigma
Mouse anti-GBF1 (clone 25) monoclonal	1:400	BD Biosciences
Rabbit anti-GBF1 (9D2) IgG polyclonal	1:400	In house. (Zhao et al., 2006)
Mouse anti-P115 (7D1) monoclonal	1:1000	Dr. Gerry Water; Princeton University, Princeton, USA
Sheep anti-TGN46 polyclonal	1:1000	AbD Serotec

Table 2.5 Secondary antibodies used in immunofluorescence

Antibody	Dilution	Source
Alexa Fluor 546 goat anti-rabbit	1:600	Molecular Probes (Invitrogen)
Alexa Fluor 555 donkey anti-sheep	1:600	Molecular Probes (Invitrogen)
Alexa Fluor 647 donkey anti-mouse	1:600	Molecular Probes (Invitrogen)

Table 2.6 Primary antibodies used in immunoblots

Antibody	Dilution	Source
Mouse anti-Arf (1D9) monoclonal	1:500	AbCam
Mouse anti-GBF1 monoclonal	1:2000	BD Biosciences
Rabbit anti-GBF1 (9D4) polyclonal final bleed	1:2500	In house. (Manolea et al., 2008)
Rabbit anti-GGBF (Arf1) 19966	1:500	In house. (Taylor et al., 1992)

polyclonal		
Goat anti-GFP polyclonal	1:5000	Eusera, University of Alberta, Edmonton, Canada
Rabbit anti-GFP polyclonal	1:50 000	Eusera, University of Alberta, Edmonton, Canada
Rabbit anti-ManII polyclonal	1:2000	Dr. Kelley Moremen; University of Georgia, Athens, USA
Mouse anti-tubulin monoclonal	1:1000	Sigma

Table 2.7 Secondary antibodies used in immunoblots

Antibody	Dilution	Source
Alexa Fluor 680 goat anti-rabbit	1:10 000	Molecular Probes (Invitrogen)
Alexa Fluor 750 goat anti-mouse	1:10 000	Molecular Probes (Invitrogen)
Alexa Fluor 790 donkey anti-goat	1:10 000	Molecular Probes (Invitrogen)

2.4 Construction of plasmids

2.4.1 Construction of fluorescently-tagged Arf proteins

Zoya Shapovalova constructed the plasmids used for Arf-GFP expression in this study by insertion of human Arf1, Arf3, Arf4, and Arf5 encoding fragments between the *XhoI* and *KpnI* sites of pEGFP-N1 (Clonetech, Mountain View, CA). The Arf encoding sequences used as template were described previously (Berger et al., 1988). The required fragments were obtained by PCR amplification from vectors containing human Arf sequences using forward primers that introduce a *XhoI* site upstream of the ATG start site, and reverse primers that replaced the TGA stop

codon with a CGC and introduced a *KpnI* site immediately downstream that allowed in-frame translation of EGFP following a 12-residue linker (AVPRARDPPVAT).
To study Arf1-6-1, the pXS-Arf1-6-1 HA-tagged construct was obtained from Dr. J. Donaldson (Honda et al., 2005). We then subcloned the Arf1-6-1 coding region into our Arf-GFP encoding pEGFP-N1 vector by PCR amplification, subsequent insertion via *XhoI* and *KpnI* digestion as described for Arf1, 3, 4, and 5 (sense oligo 5'-CCACTCGAGAGCATGGGGAATATCTTTGCAAAC-3', antisense oligo 5'-CACAGGTACCGCTTTCTGGTTCCGGAGCTG-3').

The Arf1(T31N) fragment was amplified using a plasmid encoding bovine HA-tagged Arf1(T31N) (Peters et al., 1995) obtained from Dr. V. Hsu (Harvard Medical School, Boston, MA). Additional T31N mutant Arf isoforms were generated by site-directed mutagenesis using the QuickChange kit (Stratagene, La Jolla, CA), as per manufacturers instructions. Arf1-6-1 T31N mutant was constructed as a part of this study by site-directed mutagenesis, as described above (sense oligo 5'-CTGGATGCTGCGGGAAAGAACATCCTGTACAAACTGAAG-3', antisense oligo 5'-CTTCAGTTTGTACAGGATGGTGTTCTTTCCCGCAGCATCTAG-3'). Assad Omar, an AHFMR summer student under the supervision of Mary Schneider, performed mutagenesis of Arf4.

The Arf1-mCherry encoding plasmid was derived from an Arf1-RFP plasmid that was constructed Dr. J. Donaldson (NIH, Bethesda, MA). Then, insertion of the complete bovine Arf1 cDNA between the *BglII* and *EcoRI* sites of the RFP-N1 (Clonetech, Mountain View, CA) was performed by restriction digestion (Cohen et al., 2007). To generate Arf1-mCherry, Zoya Shapovalova exchanged the *BamHI-NotI*

fragment containing the RFP tag with a similar one encoding mCherry as described (Chun et al., 2008). The described fluorescent tag replacement introduced a 13-residue linker (GILQSTVPRARDP) between Arf1 coding region and the mCherry tag.

2.4.2 Generation of pEGFP-*SbfI*-C1 vector

Previously, we utilized a p5TO-*NheI*-GFP-GBF1 expression vector for transient expression in various cell lines. This vector was generated using the original cDNA that resulted in large portions of the 5' and 3' untranslated regions (UTR) being included in the plasmid and transcript (Zhao et al., 2006). The 5' UTR makes up a considerable portion of the large linker encoded by this construct while the 3' UTR was found between the stop codon and the 3' restriction site *NotI*. To simplify the generation of our pEGFP-GBF1 truncation library, we generated a new GFP-tagged GBF1 vector which lacking the 5' and 3' UTR regions thereby simplify the polymerase chain reactions (PCR) that would be required. To achieve this, we first needed to modify the pEGFP-C1 vector (Clonetech, Mountain View, CA) to be compatible with subcloning of GBF1. For this purpose, we introduced an *SbfI* site in the multiple cloning site of pEGFP-C1 due to its unique sequence and compatibility with *SacII* that will be used at the 5' end of GBF1. The *SbfI* site was introduced by cutting the pEGFP-C1 vector at the *SmaI* site generating a linearized vector with blunt ends. The linearized vector was then treated with calf intestinal alkaline phosphatase (CIAP) (Invitrogen, Carlsbad, CA) to remove the 5' phosphate and prevent self-ligation. A DNA duplex of the *SbfI* site (5'-ATACCTGCAGGTAT-3') was ordered from Integrated DNA Technologies (San Diego, CA) and was ligated by T4

DNA ligase (Invitrogen, Carlsbad, CA) into the *SmaI* cut site. The new pEGFP-*SbfI*-C1 vector will subsequently be used as the target vector for various GBF1 inserts generated by PCR.

2.4.3 Generation of pEGFP-*SbfI*-GBF1 truncation library

We generated a GFB1 truncation library based on the published domain and interdomain boundaries (Mouratou et al., 2005). A cartoon representation of each of the truncated mutants is shown in Figure 4.15A. Construction of the GBF truncation was done by PCR amplification of the regions of interest with specific primers where the forward primer introduced a *SacII* restriction site and the reverse primer introduced an *SbfI* restriction site. Primers used to generate each truncation are listed in Table 2.8 below. These sites were used to directional insertion of GFB1 truncation PCR products into the pEGFP-*SbfI*-C1 vector described above, resulting in a GBF1 truncation bearing an N-terminal EGFP tag containing an 19 residue linker (SGLRSRAQASNSAVDGTAV).

Table 2.8 Primers used for generating the pEGFP-*SbfI*-GBF1 truncation library

Primer Name	Primer Sequence
GBF1 WT Forward	5'-*CCGCGG*GGATGGTGGATAAGAATTACATCATTAACGGAGAA-3'
GBF1 WT Reverse	5'-**CCTGCAGG**TTAGTTGACTTCAGAGGTGGGAATAGGG-3'
205-1856 Forward	5'-*CCGCGG*TGAGCTATGTGGGAACCAACATGAAGAAG-3'
390-1856 Forward	5'-*CCGCGG*TGGAAGGCACAGCTTTGGTTCCTTAT-3'
565-1856 Forward	5'-*CCGCGG*AGTCTGGTCAACTTTATACCACACACCTACTG-3'
696-1856 Forward	5'-*CCGCGG*TTAACAAAAAGAAGCTGCTGATCACTGGC-3'
885-1856 Forward	5'-*CCGCGG*AGCCCGAGGAACAGACAGG-3'
1065-1856 Forward	5'-*CCGCGG*AGATGCCATCAAACCGAGGAGAG-3'
1276-1856 Forward	5'-*CCGCGG*TGAAGCCTCCAGATGCTCTACAG-3'

1533-1856 Forward	5'-*CCGCGG*ATGACTCACGCACCCTCTGG-3'
1645-1856 Forward	5'-*CCGCGG*GGCTCACCATCCTGGACTTCATG-3'
1-204 Reverse	5'-**CCTGCAGG**TTACTTGGGTTCTTCTTTAAACTGAGGTAACCT-3'
1-389 Reverse	5'-**CCTGCAGG**TTACTTCTGGGAGGACTGTGTGAAGC-3'
1-564 Reverse	5'-**CCTGCAGG**TTACACAGGAAAGGCATTCTTGGACAGC-3'
1-695 Reverse	5'-**CCTGCAGG**TTACTTAATTTCAATTAGTTCCCGTGGATC-3'
1-884 Reverse	5'-**CCTGCAGG**TTACATCACGATTTCCTCATTCTTGATGGCATG-3'
1-1064 Reverse	5'-**CCTGCAGG**TTACTCCTCCCGCTGTAGAGAGATCTTACC-3'
1-1275 Reverse	5'-**CCTGCAGG**TTACACGCCTGAGCCAATACACTCC-3'
1-1532 Reverse	5'-**CCTGCAGG**TTAAGCTTCAATCTTTCGGCCACCTGA-3'
1-1644 Reverse	5'-**CCTGCAGG**TTACCACAGGGCAGCAAAGGT-3'

SacII site in *italics, SbfI* site in **bold**, and the stop codon is underlined.

2.5 Additional plasmids and recombinant proteins

pEGFP-ArfGAP1, 2 and 3 constructs expressing both the wild-type and catalytically dead RQ mutations were obtained from Dr. Dan Cassel (Technion – Israel Institute of Technology, Haifa, Israel) (Parnis et al., 2006). Plasmids encoding EYFP-PH^{FAPP} were acquired from Dr. Antonella De Matteis (Telethon Institute of Genetics and Medicine, Pozzuoli, Italy). Lastly, the myc-Membrin encoding plasmid was obtained from Dr. Julie Donaldson (NIH, Bethesda, MA).

Dr. Dan Cassel (Technion – Israel Institute of Technology, Haifa, Israel) generously supplied the recombinant ArfGAP1 used in *in vitro* GBF1 recruitment assays (Technion – Israel Institute of Technology, Haifa, Israel).

2.6 NRK cell line stably expressing EGFP-GBF1

The generation and isolation of the stably expressing EGFP-GBF1 normal rat kidney (NRK) cell line has been described previously (Zhao et al., 2006).

2.7 Plating of cells and transient transfection

Imaging experiments were performed with tissue culture cells that were grown on #1.5 glass coverslips in 6-well plates. Coverslips were sterilized by dipping in 70% ethanol and ignition by open flame. Transfection of plasmids for transient expression of protein was performed on cells grown to approximately 60-80% confluence using TransIT-LTI transfection reagent (Mirus, Madison, WI) or Lipofectamine 2000 (Invitrogen, Carlsbad, CA) according to manufacturer's instructions and cultured for approximately 18 hours to allow for protein expression.

2.8 Immunofluorescence

Typically, following required treatments, cells were washed in PBS warmed to 37° Celsius and fixed with 3% paraformaldehyde (with 100 μM calcium chloride and 100 μM magnesium chloride in PBS) at 37° Celsius for 20 minutes. Fixation was halted by incubation in quench buffer (50 mM ammonium chloride in PBS) for 10 minutes at room temperature. Subsequently, cells were incubated in permeabilization buffer (0.1% Triton X-100 in PBS) to allow antibodies access to intracellular structures. Prior to antibody incubations, cells were blocked in a 0.2% gelatin solution made in PBS. Cells were double-labeled with antibodies or differing species and processed as described previously (Zhao et al., 2002).

2.9 Fluorescence microscopy

2.9.1 Spinning-disc confocal microscopy

Cells for live cell microscopy experiments were grown on #1.5 25 mm round glass coverslips (Fisher Scientific, Ottawa, ONT) in 6 well dishes. When ready for imaging, coverslips were transferred to Attofluor cell chambers (Invitrogen, Carlsbad, CA) and media was changed to CO_2-independent DMEM (Gibco Laboratories, Grand Island, NY) supplemented with 10% FBS (Gemini Bio-Products, Sacramento, CA) before imaging commenced. Image acquisition took place on a Zeiss Axiovert 200M confocal microscope equipped with an UltraVIEW ERS 3E spinning disk confocal head (PerkinElmer, Waltham, MA), 63x objective lens (plan-Apocromat, NA=1.4), temperature-controlled stage set to 37° Celsius (BioOptics, Tulsa, OK), and objective heater set to 37° Celsius (BioOptics, Tulsa, OK). Live cell imaging experiments were performed in a room heated to roughly 30° Celsius; a thermocouple placed on the glass coverslip inside the chamber indicated a temperature in the 30-34° Celsius range during image acquisition. Images were captured with a 9100-50 electron multiplier CCD digital camera (Hamamatsu, Hamamatsu City, Japan) and processed with Volocity software (PerkinElmer, Waltham, MA). Experiments involving drug addition were performed by adding 250 μL of medium containing 6 times the desired drug concentration, which was then added to the cell chamber containing 1250 μL of medium. If required, small corrections to the focus could be performed immediately following drug addition.

Fixed cell imaging samples were prepared as stated in section 2.7 and imaged with the setup described above, without heating elements.

2.9.2 Live cell epifluorescence microscopy

Cells for live cell microscopy experiments were grown on #1.5 25 mm round glass coverslips (Fisher Scientific, Ottawa, ONT) in 6 well dishes. When ready for imaging, coverslips were transferred to Attofluor cell chambers (Invitrogen, Carlsbad, CA) and media was changed to CO_2-independent DMEM (Gibco Laboratories, Grand Island, NY) supplemented with FBS (Gemini Bio-Products, Sacramento, CA) to 10% before imaging commenced. Live cell epifluorescence experiments were performed on a DeltaVision Elite (GE Healthcare, Buckinghamshire, UK) microscope equipped with a front-illuminated sCMOS camera driven by softWoRx 6 (GE Healthcare, Buckinghamshire, UK) at 37° Celsius (Applied Precision, Mississauga, ONT) using a 60× 1.4 NA oil objective (Olympus, Richmond Hill, CAN). Multiple fields of view were acquired simultaneously by programming the automated stage. Focus was maintained by use of the UltimateFocus feature. Before analysis, images were deconvolved in softWoRx 6 and processed in FIJI (National Institutes of Health, Bethesda, MD).

2.10 Cell fractionation and preparation of cytosol

Wild-type or GFP-GBF1 stably expressing NRK cells were used for the production of cytosol and/or microsomes. Cells were grown on 15 cm tissue culture dishes to confluence and harvested by trypsin treatment. Trypsin was inactivated by

two volumes on complete DMEM supplemented with 10% FBS and then cells were pelleted and supernatant was aspirated. The weight of the cell pellet was measured. Cells were then washed in PBS to remove residual medium components and re-pelleted. Washed cells were then resuspended in four-volumes of ice-cold homogenization buffer and placed on ice. Cells were subsequently homogenized by 20 passages through a cell homogenizer (Isobiotech, Heidelberg, GER) with a 14 μm clearance. Homogenate was then centrifuged at 4° Celsius and 400 x g for 5 minutes to pellet nuclei and unbroken cells. The resulting supernatant was then centrifuged at 4° Celsius and 55 000 rpm for 15 minutes to pellet the microsomes (Thick wall polycarbonate, TLA-120.1 rotor, Optima TLX Benchtop Ultra) (Beckman Coulter, Brea, CA). The cytosol, resulting supernatant, was collected and immediately aliquoted and frozen at -80° Celsius for storage. Microsome fractions, resulting pellet, were resuspended in PBS and also frozen at -80° Celsius for storage.

2.11 *In vitro* GBF1 recruitment assay

Dr. Wei Lai (W) first uncovered that Golgi fractions (G) could be isolated from low-speed pellets traditionally referred to as the nuclear (N) pellet; hence the designation WNG fraction (Dominguez et al., 1999). These highly stacked Golgi membranes were used as the Golgi membrane in the recruitment assay. To perform *in vitro* GBF1 recruitment assays we mixed 5 μL WNG and 20 μL GFP-GBF1 NRK cytosol in recruitment assay buffer. The volume of the assay was brought up to 50 μL through the addition of water. Samples were then incubated at 37° Celsius for five minutes to allow for GBF1 recruitment. Following incubation the samples are

returned to ice. Complete assays were then centrifuged at 4° Celsius and 55 000 rpm for 15 minutes to pellet the membrane components (Thick wall polycarbonate, TLA-120.1 rotor, Optima TLX Benchtop Ultra) (Beckman Coulter, Brea, CA). Resulting supernatants are then resuspended in SDS-PAGE loading buffer and boiled. Pellets were washed gently with 50 µL of PBS to remove residual amounts of cytosol. Pellets were subsequently resuspended in 50 µL of PBS and mixed with 10 µL SDS-PAGE loading buffer and heated to 95° Celsius. Pellet samples were sonicated in a Bioruptor Pico (Diagenode, Denville, NJ) prior to SDS-PAGE electrophoresis.

2.12 Western blotting

Following protein separation by SDS-PAGE, proteins were transferred to nitrocellulose membrane (GE Healthcare, Buckinghamshire, UK) at 376 mA for two hours in transfer buffer (25 mM Tris-HCl, 190 mM glycine, 20% (v/v) methanol, 2.5% (v/v) isopropanol) Resulting membranes were then blocked in Licor Odyssey Blocking Reagent (Licor Biotechnology, Lincoln, NE) for at least an hour. Blocked membranes were then incubated with primary antibodies in 50% Licor Odyssey Blocking Reagent. Following 3 washes in PBS, membranes were then incubated in fluorescent secondary antibody for 1 hour in 25% Licor Odyssey Blocking Reagent followed by two 10 minute TBST washes and three 10 minute PBS washes. Membranes were then scanned on a Licor Odyssey scanner (Licor Biotechnology, Lincoln, NE).

2.13 Quantitation of immunoblots

Quantitation of immunoblots was performed in Licor Odyssey software version 3.1 (Licor Biotechnology, Lincoln, NE). Band intensities were quantified by manually drawing a rectangle around the region of interest, which was automatically corrected for background based on the dimmest pixels in a 3-pixel region along the edges of the drawn rectangle. For *in vitro* GFB1 recruitment assays, we corrected GFP-GBF1 band intensity to ManII band intensity to correct for the amount of membrane in each assay, a measure of loading error. Quantitated intensities were exported to Excel worksheets (Microsoft, Redmond, WA) where mean, standard deviation, t-test, and normalization calculations were performed.

2.14 Image quantitation and analysis

Quantification was carried out using Imaris software (Bitplane Scientific Software, South Windsor, CT). A minimum of ten cells from each condition was quantified and this was repeated for each of three independent replicates. Three-dimensional surfaces were created around areas of interest in selected cells using the surfaces feature in Imaris. Average pixel intensity values in the surveyed regions were exported into Excel spreadsheets (Microsoft, Redmond, WA). Average Golgi intensity values were corrected for the average value of the cytosolic intensity and the calculated values for whole cell intensity were further corrected for the intensity of the image background. Graphs were generated using Excel (Microsoft, Redmond, WA) with the percent of GBF1 signal at the Golgi for each condition representing the mean of three independent replicates and the error bars representing the standard

deviation across the selected cells for each condition. Unpaired, two-tailed t-tests were performed in Excel (Microsoft, Redmond, WA) and p-values reported.

The equation used for the correction of the GBF1 signal at the Golgi is:

$$\% \text{ Sig at Golgi} = \frac{\text{Golgi Vol (Golgi Int} - \text{Cytosol Int)}}{\text{Cell Vol (Cell Int} - \text{Background Int)}} \text{ X } 100\%$$

Line scan analysis was performed on extended focus images in which colours were corrected to be true and then imported from Volocity into the FIGI software (National Institute of Health, Bethesda, MA). Linescans were generated using the RGB plug-in.

Chapter 3: Arf activation at the Golgi is modulated by feed-forward stimulation of the exchange factor GBF1

A version of this chapter has been published as "Arf activation at the Golgi is modulated by feed-forward stimulation of the exchange factor GBF1." (Quilty et al., 2014). Permission for reproduction was obtained through the Copyright Clearance Center, confirmation number 11593613.

Fraser Gray participated in the experiments and quantitation that resulted in Figure 3.12 as part of an undergraduate research project. Nathan Summerfeldt performed preliminary experiments. Dr. Dan Cassel provided reagents and technical assistance. Dr. Paul Melançon played a role in planning experiments, data analysis, and writing the manuscript.

3.1 Abstract

ADP-ribosylation factors (Arfs) play central roles in the regulation of vesicular trafficking through the Golgi. Arfs are activated at the Golgi membrane by guanine nucleotide exchange factors (GEFs) that are recruited from cytosol. Here, we describe a novel mechanism for regulation of recruitment and activity of the ArfGEF Golgi-specific BFA resistance factor 1 (GBF1). Conditions that alter the cellular Arf•GDP/Arf•GTP ratio result in GBF1 recruitment. This recruitment of GBF1 occurs selectively on *cis*-Golgi membranes in direct response to increased Arf•GDP. GBF1 recruitment requires Arf•GDP myristoylation-dependent interactions suggesting regulation of a membrane bound factor. Once recruited, GBF1 causes increased Arf•GTP production at the Golgi, consistent with a feed-forward, self-limiting mechanism of Arf activation. This mechanism is proposed to maintain steady-state levels of Arf•GTP at the *cis*-Golgi during cycles of Arf-dependent trafficking events.

3.2 Background

The Golgi functions as a central organizing organelle in the secretory pathway (Emr et al., 2009; Farquhar and Palade, 1998). The central Golgi stack (consisting of *cis-, medial-, and trans*-cisternae) processes and facilitates the targeting of newly synthesized cargo proteins as they emerge from the ER-Golgi intermediate complex (ERGIC) and traffic through the *trans*-Golgi network (TGN). The exact mechanism through which individual compartments are created and maintained remains unknown, but it is generally assumed that the recruitment of protein factors to specific compartment is required to establish and define each compartment (Lippincott-Schwartz, 2011).

Members of the Arf family of small GTPases play central roles in vesicular trafficking at the Golgi. Primate cells express 5 Arf proteins (Arf1, 3, 4, 5, and 6) that are classified into three classes (Class I: Arf1 and 3, Class II: Arf4 and 5, and Class III: Arf6). Class I and II Arfs are found differentially distributed through the Golgi complex (Chun et al., 2008; Dejgaard et al., 2007; Manolea et al., 2010). Arf proteins exert their regulatory effect through cycles of GTP binding and hydrolysis, induced by Arf guanine nucleotide exchange factors (GEFs) and Arf GTPase-activating proteins (GAPs). Activation of Arf proteins occurs at the membrane and requires simultaneous membrane association of both substrate and activating GEF (Cherfils and Melançon, 2005). The initial association of Arfs with membranes depends on its N-terminal myristoyl moiety (Franco et al., 1996; Haun et al., 1993; Randazzo and Kahn, 1995; Tsai et al., 1996), while stable association is triggered upon GTP-induced stabilization of the exposed N-terminal amphipathic motif (Pasqualato et al.,

2002). Recent work suggests that initial Arf association with membranes further depends on Arf receptors that are present in the Golgi membrane (Gommel et al., 2001; Honda et al., 2005).

It is well established that the Golgi apparatus is sensitive to the drug brefeldin A (BFA) (Doms et al., 1989; Fujiwara et al., 1988; Lippincott-Schwartz et al., 1989). This drug acts as a uncompetitive inhibitor of a sub-family of large ArfGEFs that includes GBF1 (Golgi-specific Brefeldin A-resistance factor 1) and BIGs (BFA-inhibited GEFs) (Casanova, 2007). Whereas GBF1 localises and functions at the early Golgi, BIGs function at the TGN (Kawamoto et al., 2002; Manolea et al., 2008; Zhao et al., 2006; Zhao et al., 2002). Thus GBF1 appears to be the primary, if not only, GEF responsible for activation of Class I and Class II Arfs at the ERGIC and *cis*-Golgi membranes.

The model described above predicts co-accumulation of GBF1 and Arf on Golgi membranes following BFA treatment. Our laboratory tested this prediction using live cell imaging but failed to detect accumulation of the Arf at the Golgi (Chun et al., 2008). Rather, we observed rapid release of Arfs from Golgi membranes, concurrently with GBF1 accumulation. In the present study, we examined the recruitment of GBF1 on Golgi membranes using several independent approaches. Our findings indicate that GBF1 accumulation on membranes is sensitive to the Arf•GDP/ Arf•GTP ratio, which can explain the BFA effect. We propose that the recruitment of GBF1 to Golgi membranes is part of a homeostatic regulatory mechanism that functions to maintain proper Arf•GTP levels on *cis*-Golgi membranes.

3.3 Results

3.3.1 GBF1 accumulates on Golgi membranes in response to an increase in the ratio of Arf•GDP to Arf•GTP

The fact that Arf activation must occur at the membrane surface emphasizes the importance of studying the recruitment of GBF1 to Golgi membranes. Much of the information available on the function of ArfGEFs such as GBF1 is derived from use of the inhibitor BFA (Casanova, 2007; Melançon et al., 2003). Several *in vitro* studies established that the catalytic Sec7 domain of sensitive GEFs forms a stable, non-productive complex with BFA and substrate Arf•GDP (Mansour et al., 1999; Mossessova et al., 2003; Peyroche et al., 1999; Renault et al., 2003; Robineau et al., 2000; Sata et al., 1998). Furthermore, several groups reported that BFA treatment causes accumulation of GBF1 on Golgi membranes in live cells (Niu et al., 2005; Szul et al., 2005; Zhao et al., 2006). These results led to the hypothesis that release of GBF1 from membranes is linked to the completion of the nucleotide exchange reaction, a process that is blocked in the presence of BFA (Niu et al., 2005; Szul et al., 2005). We further observed that treatment of NRK cells with Exo1, a drug that reduces Arf•GTP levels but does not target the GEF, also caused recruitment of exogenous GBF1 to Golgi and ERGIC membranes (Feng et al., 2003). To confirm and extend these results, we tested the effect of Exo1 treatment on endogenous GBF1 localisation in HeLa cells. We first confirmed that in HeLa cells expressing mCherry-GBF1 and treated with 200 μM Exo1 for 1 minute, GBF1 is clearly recruited to Golgi and peripheral puncta (Figure 3.1A). No change in mCherry-GBF1 localisation and

recruitment was observed in control cells treated with DMSO for 1 minute. To ascertain that Exo1-dependent accumulation did not depend on overexpression of tagged-GBF1, we tested its effect on the endogenous protein. Treatment of HeLa cells with 200 μM Exo1 for one minute caused Golgi recruitment of endogenous GBF1 (Figure 3.1B) similar to that observed for exogenous mCherry-GBF1 (Figure 3.1A). Quantification of endogenous GBF1 recruitment, shown as a ratio of mean Golgi intensity to mean cytosol intensity, revealed a significant 2.5 fold increase in Golgi-localised GBF1 following 1-minute Exo1 treatment ($p < 0.001$, $n=3$) (Figure 3.1C). Changes in protein levels are not expected but were not measured.

To obtain independent evidence that the ratio of Arf•GDP to Arf•GTP influences GBF1 recruitment, we examined the impact of ArfGAP1 overexpression on GBF1 distribution. Previous studies established that ArfGAP1 localises to the Golgi where it promotes GTP hydrolysis on Arfs (Cukierman et al., 1995; Shiba et al., 2011; Szafer et al., 2001). Further characterization of the N-terminal GAP domain identified a critical "arginine finger" residue that participates in catalysis (Ismail et al., 2010; Szafer et al., 2000), and mutation of this arginine (residue 50 in human ArfGAP1) abrogated GAP activity *in vivo* (Shiba et al., 2011). To examine the potential role that the ratio of Arf•GDP to Arf•GTP played in GBF1 recruitment, we examined the distribution of endogenous GBF1 in HeLa cells transiently expressing low levels of wild-type (WT) or the catalytically dead R50Q point mutant EGFP-GAP1. This experiment revealed an increase in Golgi-localised GBF1 in cells expressing WT EGFP-GAP1. Interestingly, expression of inactive EGFP-GAP1 R50Q

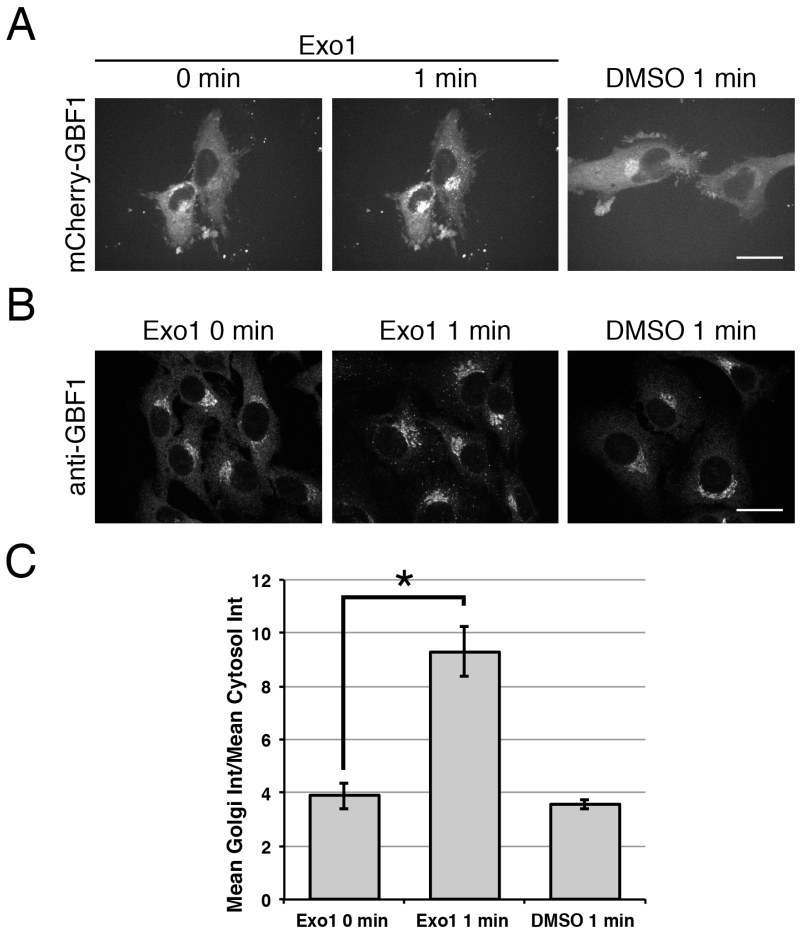

Figure 3.1 Exo1-mediated changes in cellular Arf·GTP:Arf·GDP ratio causes GBF1 recruitment and accumulation on Golgi membranes. (**A**) HeLa cells expressing mCherry-GBF1 were treated with 200 μM Exo1 or DMSO as control and imaged by live cell spinning disc confocal microscopy as described in Chapter 2. Cells from a representative experiment (n=6) are displayed as focal projections of all z-slices. (**B**) HeLa cells were treated with 200 μM Exo1 or DMSO as control then stained with mouse anti-GBF1 monoclonal antibody and imaged by fixed cell spinning disc confocal microscopy. Cells from a representative experiment (n=3) are displayed as focal projections of all z-slices. (**C**) Quantification of GBF1 recruitment in Exo1 and DMSO-only treated cells was performed by measuring the ratio of mean intensity (Int) of GBF1 staining at the Golgi to mean intensity of GBF1 staining in the cytosol. A minimum of 8 cells similar to those shown in panel B were quantitated in each of three separate experiments. Error bars represent the standard deviation between each of three replicate experiments. Unpaired two-tailed t-tests were performed, *$p < 0.001$ (n=3). Scale bars = 26 μm.

resulted in a clear and significant decrease in membrane associated GBF1 relative to mock-transfected control cells (Figure 3.2A). Quantification of the ratio of Golgi-bound to free cytosolic GBF1 showed that expression of WT ArfGAP1 resulted in a significant 2.5-fold increase in ratio of Golgi-associated to free GBF1 relative to mock-transfected control ($p < 0.01$, n=3) (Figure 3.2B). In contrast, expression of ArfGAP1 R50Q caused a 50% reduction in this ratio, which was found to be statistically significant ($p < 0.001$, n=3). This unexpected observation suggests that expression of catalytically inactive ArfGAP decreases the Arf•GDP:Arf•GTP ratio. Altogether, our results suggest that GBF1 recruitment responds to re-establish steady state Arf•GTP level, and is sensitive to both increases and decreases of the cellular ratio of Arf•GDP to Arf•GTP.

3.3.2 Arf•GDP promotes accumulation of GBF1 on Golgi membranes

Sensing a change in the ratio of Arf•GDP to Arf•GTP can result from responding to either the GDP- or the GTP-bound form of Arf. The potential involvement of Arf•GDP could be readily tested utilizing the well-characterized T31N point mutation that interferes with GTP binding and maintains Arf in an inactive state (Dascher and Balch, 1994). In order to perform this experiment, we first had to develop a method that would allow expression of dominant inactive Arf1 T31N-EGFP while maintaining the integrity of the Golgi since expression of this dominant negative mutant causes a collapse of the Golgi and a block in protein traffic (Dascher and Balch, 1994; Donaldson et al., 2005). To achieve this, we first optimized transfection

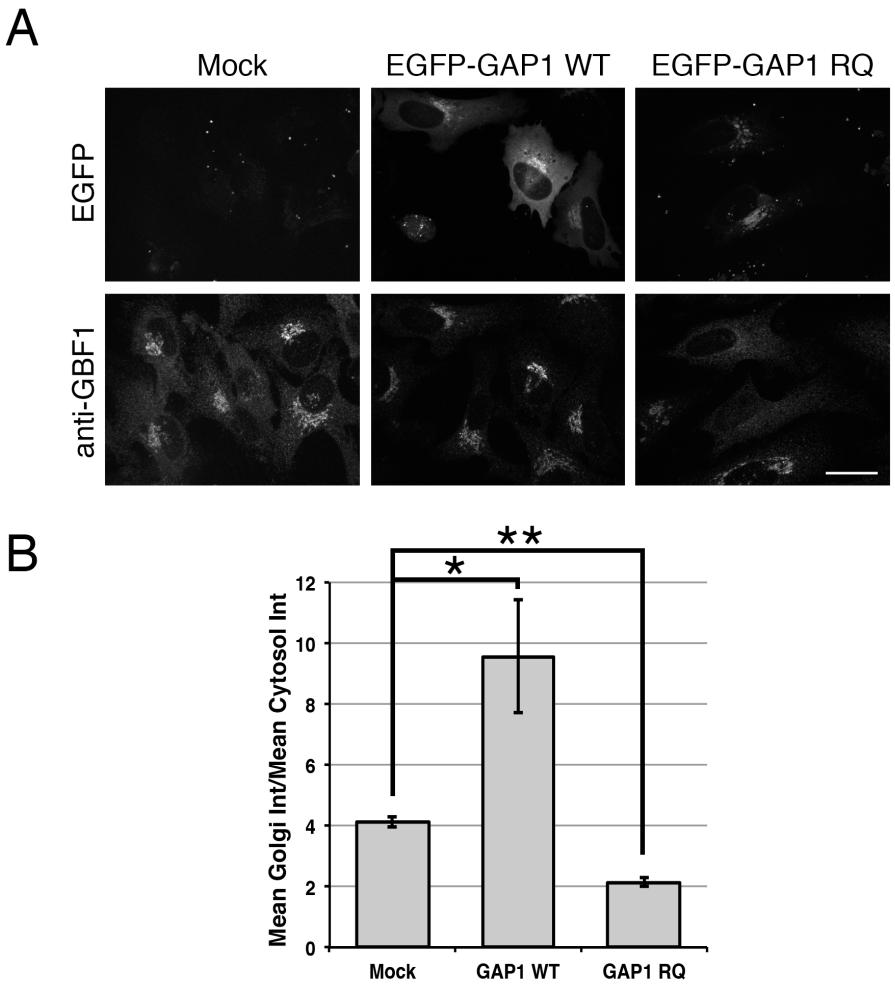

Figure 3.2 ArfGAP1-mediated changes in cellular Arf·GTP:Arf·GDP ratio alters GBF1 recruitment and accumulation on Golgi membranes. (**A**) HeLa cells were mock transfected or transfected with plasmids encoding EGFP-GAP1 WT or EGFP-GAP1 RQ. Cells were then fixed and stained with mouse anti-GBF1 monoclonal antibody and imaged by spinning disc confocal microscopy. Cells from a representative experiment (n=3) are displayed as focal projections of all z-slices. (**B**) Quantification of GBF1 recruitment in EGFP-ArfGAP expressing cells was performed by measuring the ratio of mean intensity (Int) of GBF1 staining at the Golgi to mean intensity of GBF1 staining in the cytosol. A minimum of 8 cells were quantitated in each of 3 separate experiments. Error bars represent the standard deviation between each of three replicate experiments. Unpaired two-tailed t-tests were performed, *$p < 0.01$, **$p < 0.0001$ (n=3).
Scale bars = 26 μm.

conditions to achieve low levels of Arf expression. To reduce the probability of Golgi collapse, we co-expressed myc-membrin, a Golgi SNARE that can recruit Arf1•GDP to the Golgi. Overexpression of either GBF1 (Claude et al., 1999) or membrin (Honda et al., 2005) had previously been shown to interfere with BFA-induced Golgi collapse. This effect is thought to result from maintenance of sufficient Arf•GTP production to prevent Golgi collapse; we speculated that membrin would similarly prevent Golgi collapse in the presence of Arf1•GDP. The distribution of GBF1 was therefore examined in HeLa cells co-expressing myc-membrin, and either WT or T31N mutant forms of Arf1-EGFP. To assess relative Arf over-expression in our experiment, we performed quantitative western blot analysis. We observed that relative band intensities of the exogenously expressed Arf-EGFP (about 45 kDa) and endogenous Arf (about 20 kDa) were similar (Figure 3.3A). The anti-GFP panels confirm that our Arf antibody detects the over-expressed protein. We determined that the fold over-expression of Arf1 WT-EGFP and Arf1 T31N-EGFP was 1.4-fold and 0.9-fold, respectively (Figure 3.3B).

We then examined GBF1 distribution in cells expressing low levels of WT and mutant Arf1. Initial experiments focused on the distribution of mCherry-GBF1. As predicted by Honda *et al*. (2005), the integrity of the Golgi was maintained in a significant fraction of cells co-expressing myc-membrin, mCherry-GBF1 and low levels of Arf1 T31N (Figure 3.4A). Significantly, we observed a clear accumulation of GBF1 on Golgi membranes and dramatic loss of cytoplasmic GBF1 in cells expressing Arf1 T31N relative to those expressing WT Arf1 (Figure 3.4A). Note that although the presence of myc-membrin allowed for a higher proportion of cells with

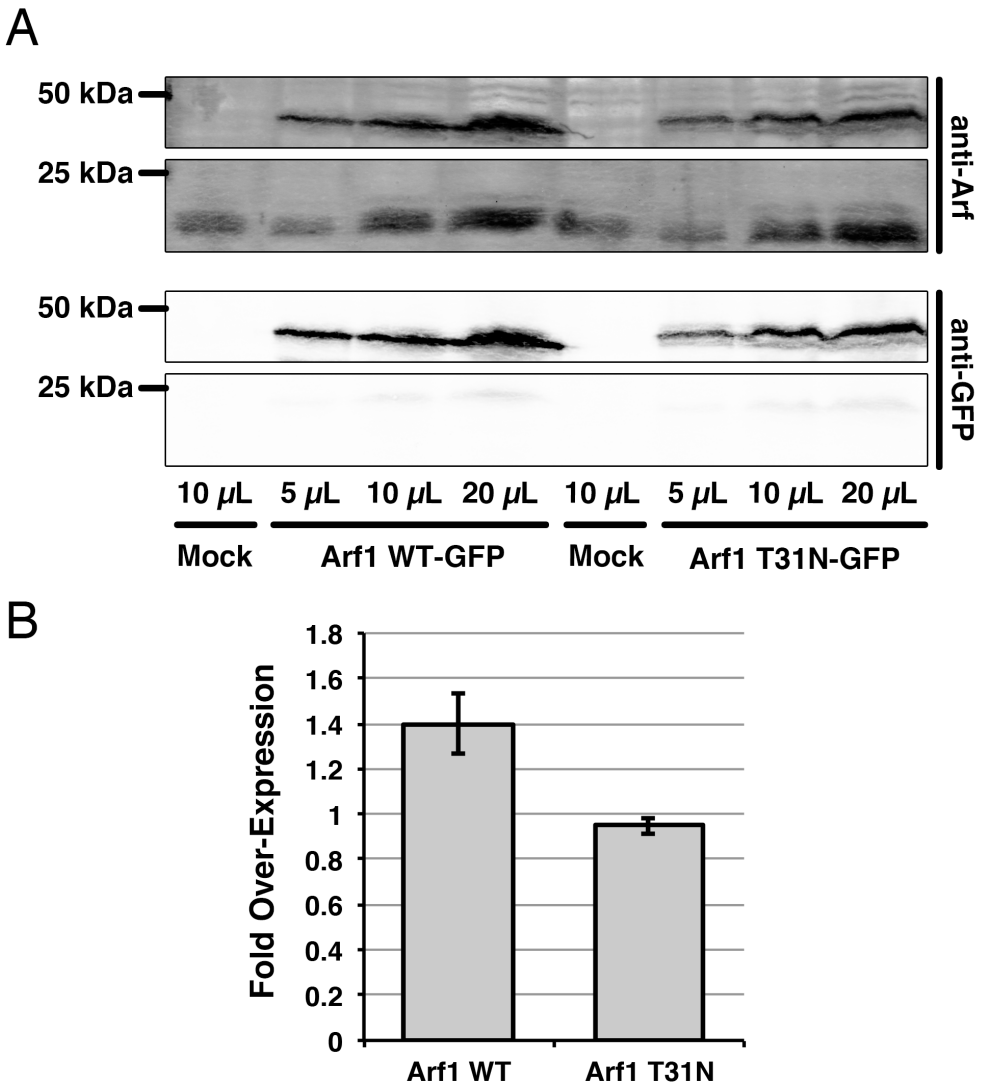

Figure 3.3 Transient expression of Arf-EGFP chimeras confer a moderate over-expression, relative to endogenous Arf. (**A**) Western blot analysis of post-nuclear extracts prepared from HeLa cells transfected with plasmids encoding mCherry-GBF1, myc-membrin, and either WT or T31N forms of Arf1-EGFP. Different volumes of each sample were analyzed to ensure that signal remained within linear range of detection. Membranes were incubated with mouse anti-Arf 1D9 and rabbit anti-GFP and were developed and analyzed. A representative western blot from four separate experiments is shown. (**B**) Quantification of the fold over-expression of exogenous Arf-EGFP over endogenous Arf levels was performed by comparing amount of signal in each band using Odyssey software.

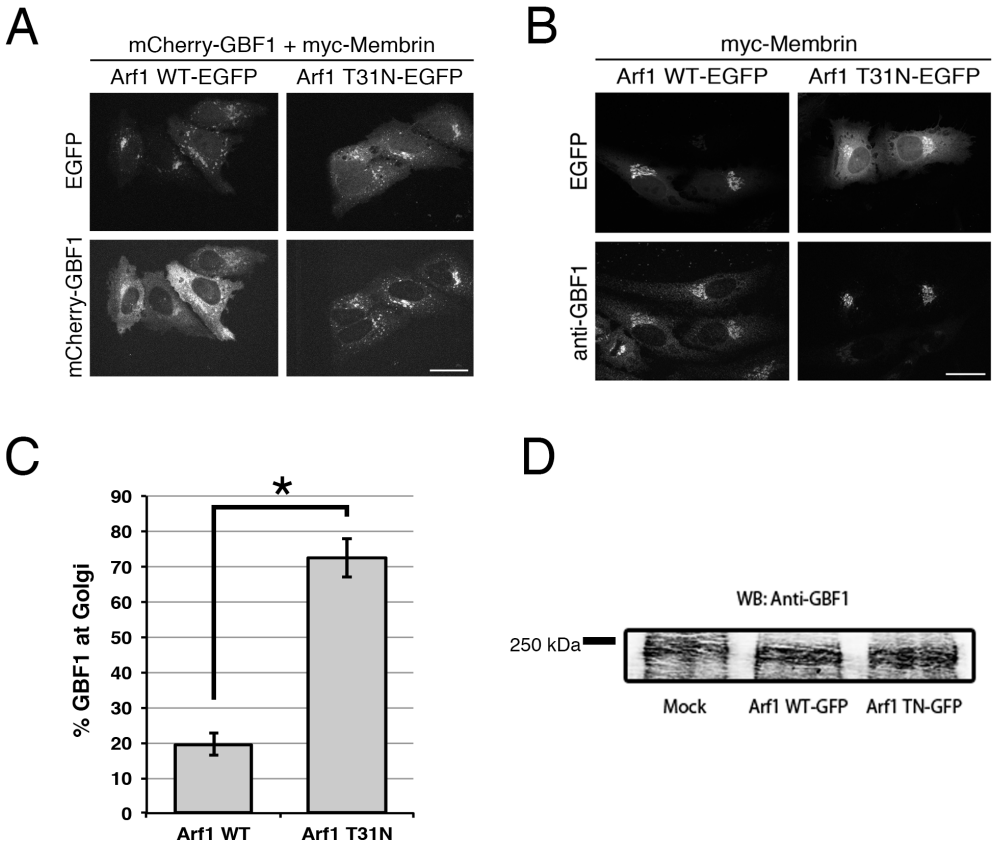

Figure 3.4 Increased Arf·GDP level causes GBF1 recruitment and accumulation on Golgi membranes. (**A**) HeLa cells were co-transfected with plasmids encoding mCherry-GBF1, myc-membrin, and either WT or T31N forms of Arf1-EGFP and imaged after fixation as for Figure 3.1 (n=3). (**B**) HeLa cells were co-transfected with plasmids encoding myc-membrin and either WT or T31N forms of Arf1-EGFP as for panel A. Cells were then fixed and stained with mouse anti-GBF1 monoclonal antibody and imaged as for Figure 3.1 (n=3). (**C**) Quantification of GBF1 recruitment in Arf1 WT and T31N expressing cells was performed by measuring the percent of total GBF1 staining at the Golgi. Error bars represent the standard deviation between each of three replicate experiments. Unpaired two-tailed t-tests were performed, *$p < 0.0005$ (n=3). (**D**) Expression of tagged Arfs does not alter the level of endogenous GBF1. Western blot analysis of post-nuclear extracts prepared from HeLa cells transfected as described in (**B**). Membrane was incubated with mouse anti-GBF1 and was then developed and analyzed. Scale bars = 26 μm.

intact Golgi, it was clearly not required for the Arf1 T31N-dependent accumulation of GBF1 (Figure 3.5). More importantly, Arf1 T31N was able to induce redistribution of untagged endogenous GBF1 from cytosol to Golgi (Figure 3.4B). Loss of cytosolic GBF1 did not result from lower expression/degradation of GBF1 in cells expressing T31N Arf1 (Figure 3.4D). The results obtained for endogenous GBF1 were quantitated as percent of total GBF1 signal at the Golgi and the results are shown in Figure 4C. This analysis revealed a significant 3.5-fold increase in membrane associated GBF1 in T31N Arf1 transfected cells compared to WT Arf1 transfected cells ($p < 0.0005$, $n=3$) (Figure 3.4C). These findings provide strong evidence that Arf•GDP can regulate GBF1 localisation to Golgi membranes.

3.3.3 GBF1 accumulates on *cis*-Golgi membranes in a catalytically active form

The results presented above suggest recruitment of GBF1 to the Golgi in response to elevated levels of its Arf•GDP substrate. This suggests a potentially novel mechanism to ensure homeostatic levels of Arf•GTP on *cis*-Golgi membranes by recruitment of GBF1. To assess whether GBF1 accumulated in an active form, we first determined whether the Golgi remained polarized. Current evidence suggests that the characteristic segregation of *cis*- and *trans*-markers results from continuous Arf- and coat-dependent sorting events and requires recruitment of GBF1 to *cis*-Golgi membranes (Manolea et al., 2008). We first confirmed that the *cis*-Golgi marker p115 and *trans*-Golgi network marker TGN46 remained well resolved in cells expressing both inactive Arf1 T31N and myc-membrin (Figure 3.6A). Although

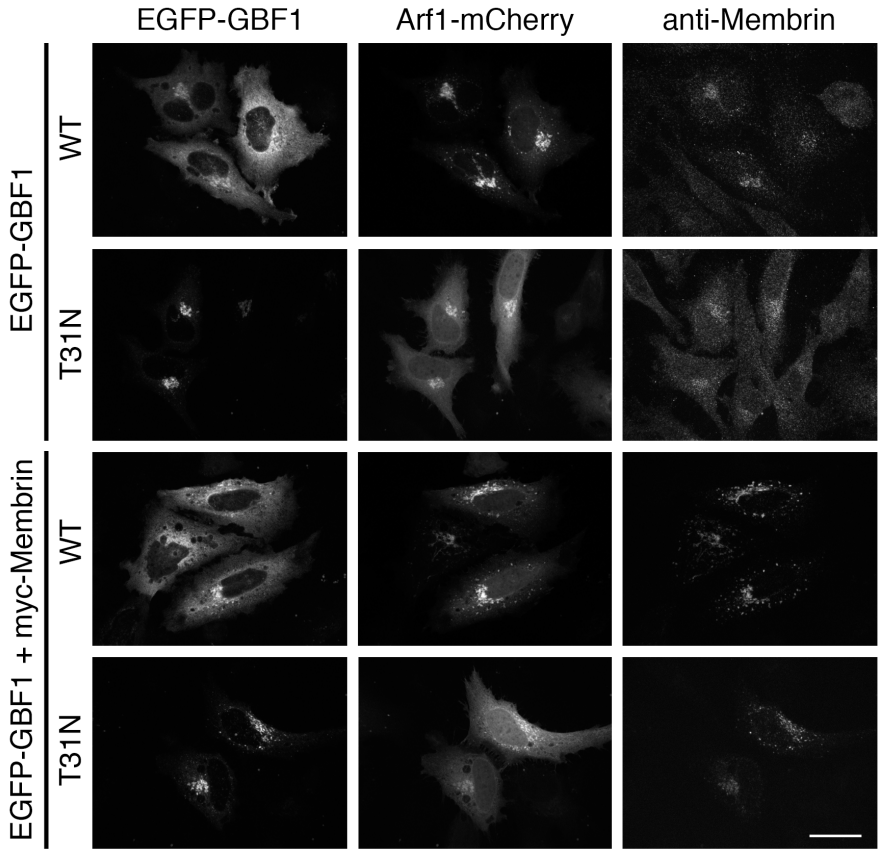

Figure 3.5 Exogenous expression of myc-membrin does not alter the ability for Arf•GDP to promote GBF1 accumulation on Golgi membranes. HeLa cells were co-transfected with plasmids encoding mCherry-GBF1 with or without myc-membrin, and either Arf1 WT-EGFP or Arf1 T31N-EGFP. Cells were then fixed and stained with mouse anti-membrin monoclonal antibody and imaged as for Figure 3.1 (n=3). Scale bars = 26 μm. These images indicate that the presence or absence of exogenously expressed myc-membrin has no effect on GBF1 localization and does not alter the recruitment phenotype observed with the expression of TN mutant Arf1. Further, it does not appear that myc-membrin expression increases the amount of Arf1 TN-EGFP associated with Golgi membranes, as one may expect if membrin is a strong binder of Arf1•GDP. Images obtained of endogenous membrin staining required at least 20x longer exposure time compared to those expressing exogenous myc-membrin, suggesting significant over-expression of the myc-membrin.

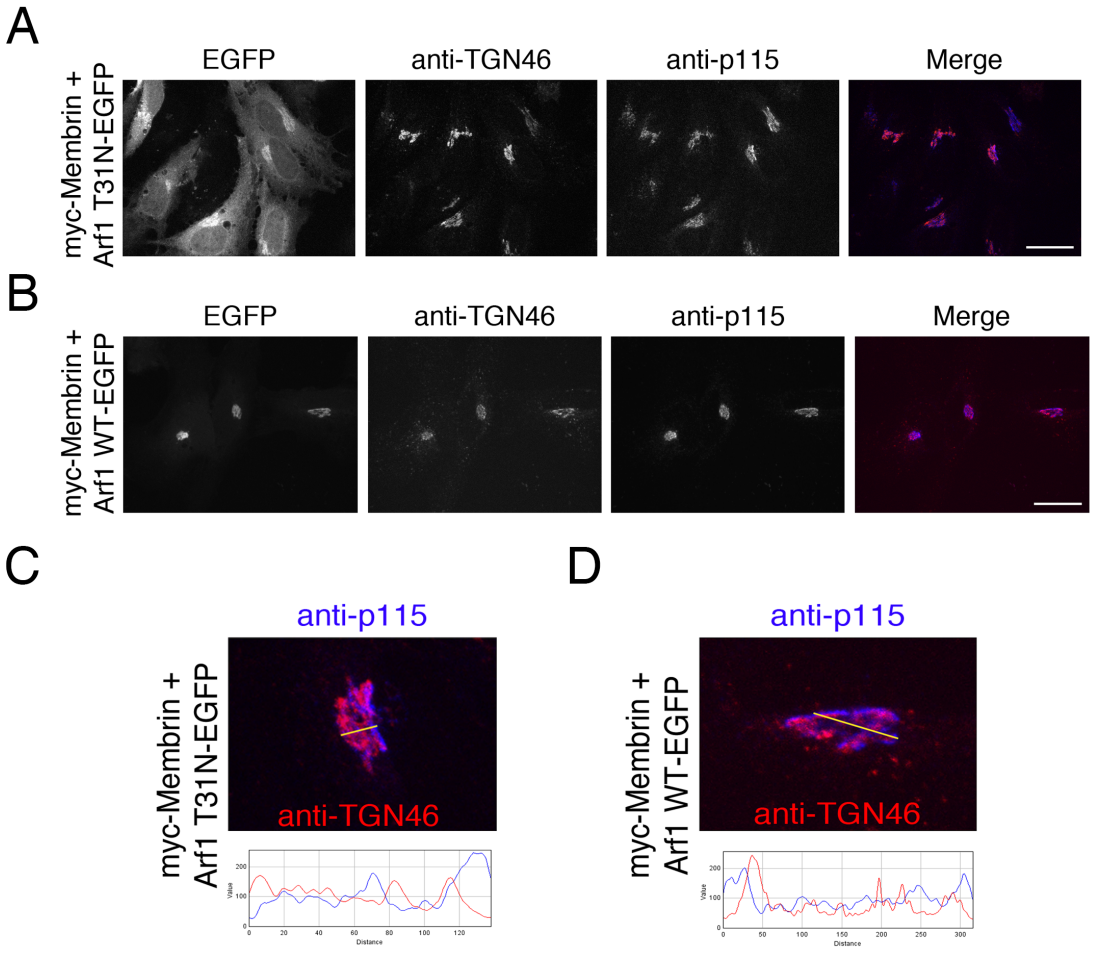

Figure 3.6 Arf•GDP-dependent GBF1 accumulation does not alter Golgi polarity. (**A**) HeLa cells were co-transfected with plasmids encoding myc-membrin and Arf1 T31N-EGFP, fixed and stained with sheep anti-TGN46 and mouse anti-p115 and then imaged as for Figure 3.1. (n=3). (**B**) HeLa cells were co-transfected with plasmids encoding myc-membrin and Arf1 WT-EGFP, fixed and stained with sheep anti-TGN46 and mouse anti-p115 and then imaged as for Figure 3.1 (n=3). (**C**) Line scan analysis was performed on cells expressing myc-membrin and Arf1 T31N-EGFP and stained with sheep anti-TGN46 and mouse anti-p115. A magnified image of a representative Golgi from (A) is shown. (**D**) Line scan analysis was performed on cells expressing myc-membrin and Arf1 WT-EGFP and stained with sheep anti-TGN46 and mouse anti-p115. A 4-fold magnification of a representative Golgi from (B) is shown.

it was clear that both markers localised to the juxta-nuclear Golgi region, the patterns were clearly different (Figure 3.6A), as observed in cells expressing WT Arf1 (Figure 3.6B). Merging of the p115 and TGN46 panels reveals distinct red and blue signals. Line-scan analysis of a representative Golgi from the merge image in panel A confirms the significant separation observed between TGN46 (red) and p115 (blue) signal peaks (Figure 3.6C), which was also observed in WT Arf1 expressing cells (Figure 3.6D). To assess whether GBF1 accumulated on *cis*-Golgi membranes, we repeated this analysis by comparing the distribution of endogenous GBF1 with *cis*-Golgi and TGN markers in cells expressing T31N mutant Arf1 (Figure 3.7A). We observed clear co-localisation of endogenous GBF1 with p115 but not with TGN46. This was also confirmed by line scan analysis (Figure 3.7B).

To obtain more direct evidence that accumulated GBF1 remained active, we first determined whether COPI, a well-established effector of Arf•GTP, associated with Golgi membranes in a BFA-sensitive and therefore GBF1-dependent manner. HeLa cells were co-transfected with plasmids encoding mCherry-GBF1 and myc-membrin as well as Arf1 T31N-EGFP to promote recruitment of GBF1. The COPI distribution was then examined in transfectants treated with either BFA or DMSO by staining for β-COP, a sub-unit of the COPI coat. Results established that a large fraction of COPI associates with juxtanuclear membranes in the presence of Arf1T31N (Figure 3.8A), as was observed for WT Arf1 expressing cells (Figure 3.8B). Significantly, BFA treatment completely dispersed COPI (Figure 3.8A, right panels), suggesting that accumulated GBF1 was active and remained BFA sensitive. Likewise,

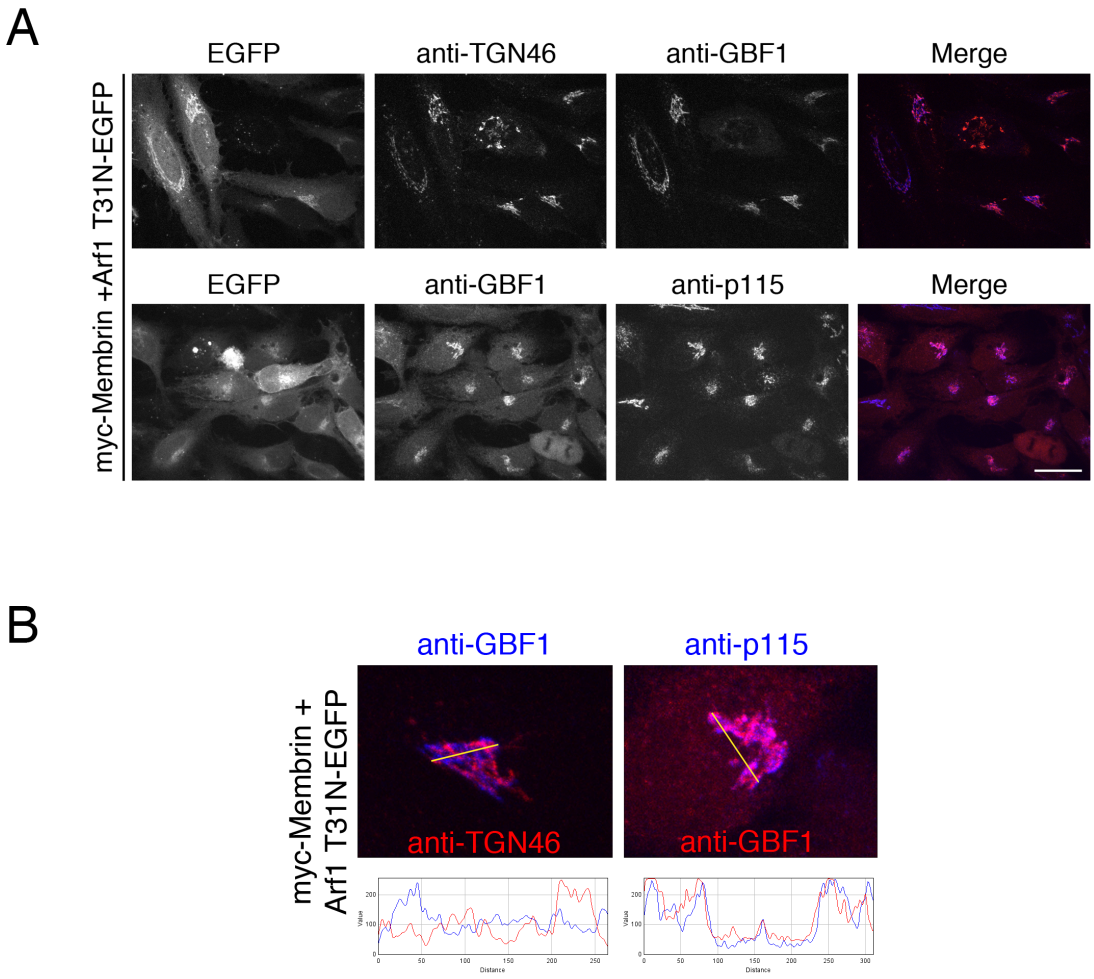

Figure 3.7 GBF1 accumulates specifically on the *cis*-Golgi in Arf•GDP-stimulated recruitment. (**A**) HeLa cells were co-transfected with plasmids encoding myc-membrin and Arf1 T31N-EGFP, fixed and stained with either sheep anti-TGN46 and mouse anti-GBF1 or rabbit anti-GBF1 and mouse anti-p115 and then imaged as for Figure 3.1 (n=3). (**B**) Line scan analysis was performed on cells expressing myc-membrin and Arf1 T31N-EGFP and stained with either sheep anti-TGN46 and mouse anti-GBF1 or rabbit anti-GBF1 and mouse anti-p115. A magnified image of a representative Golgi from (A) is shown. Scale bars = 26 μm.

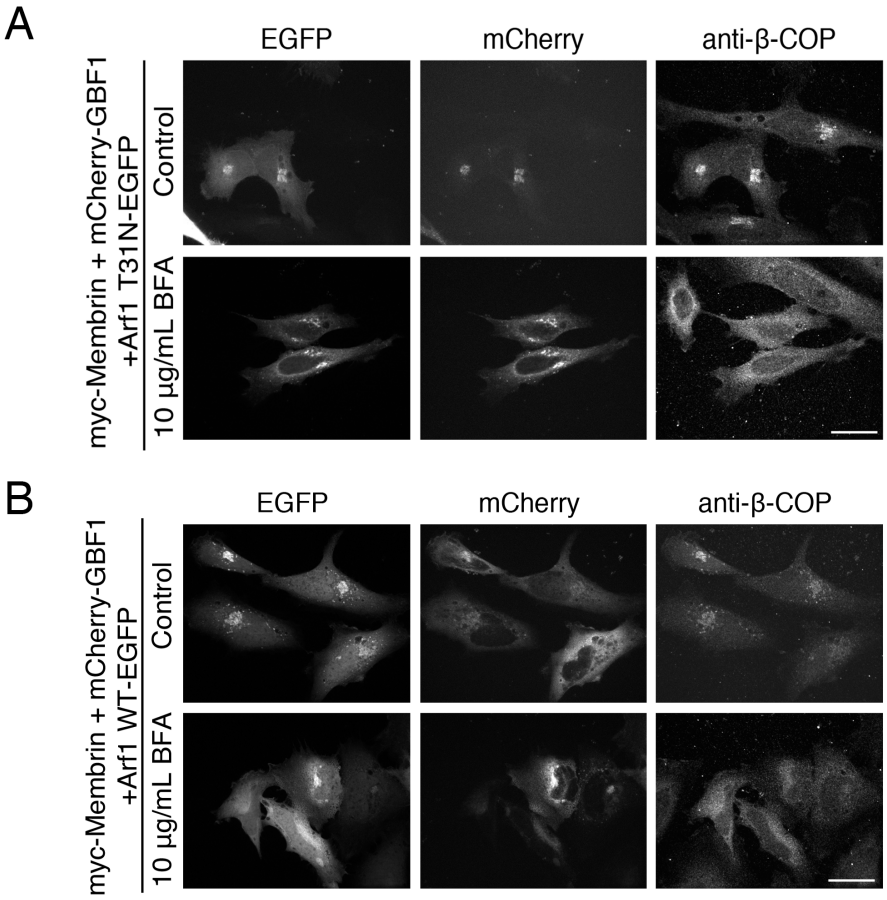

Figure 3.8 Arf•GDP-stimulated accumulation of GBF1 supports COPI association with *cis*-Golgi membranes in BFA-sensitive manner. (**A**) HeLa cells were co-transfected with plasmids encoding myc-membrin and Arf1 T31N-EGFP and treated with either 10 μg/mL BFA or DMSO control for 20 min then fixed and stained with mouse anti-β-COP and imaged as for Figure 3.1. (**B**) HeLa cells co-transfected with plasmids encoding myc-membrin and Arf1 WT-EGFP were treated with either 10 μg/mL BFA or DMSO control for 20 min. They were then fixed, stained with mouse anti-β-COP, and imaged as for Figure 3.1.

COPI in WT Arf1 expressing cells was sensitive to BFA treatment (Figure 3.8B, right panels).

To directly establish that recruitment of GBF1 leads to elevated Arf activation on Golgi membranes, we quantified the levels of Arf1 WT-mCherry on Golgi membranes in cells co-expressing either WT or the T31N mutant forms of Arf1-EGFP (Figure 3.9). Previous work established that Arf association with membranes is an indirect measure of Arf activation since treatments that block Arf nucleotide exchange results in rapid redistribution of Arf to cytosol (Donaldson et al., 1992; Helms and Rothman, 1992). The experimental set up and predicted results are illustrated in Figure 9. We first confirmed that GBF1 accumulates on Golgi membranes in cells co-expressing both WT and mutant Arf1 (Figure 3.10). Live cell imaging clearly indicated that Arf1 WT-mCherry was efficiently activated and Golgi-associated whether the cells co-expressed WT or mutant Arf1-EGFP (Figure 3.11 A and B). In contrast, T31N Arf1-EGFP associated weakly with membranes. Most of the WT Arf1 dispersed in response to BFA treatment, leaving a small fraction on Golgi membranes similar to that observed for the T31N mutant form of Arf1 (Figure 3.11 A, B, C). As expected if accumulated GBF1 is active, we observed a decrease in cytosolic WT Arf1-mCherry in cells expressing T31N Arf1-EGFP relative to those expressing WT Arf1-EGFP (Figure 3.12A). This observation suggests greater Arf1 activation and association with membranes in cells containing accumulated GBF1. Quantification of several experiments similar to that in Figure 12A revealed a 50% increase in active, membrane associated Arf in cells expressing low levels of inactive Arf (Figure 3.12B). This result is not only conclusive evidence that GBF1 remains

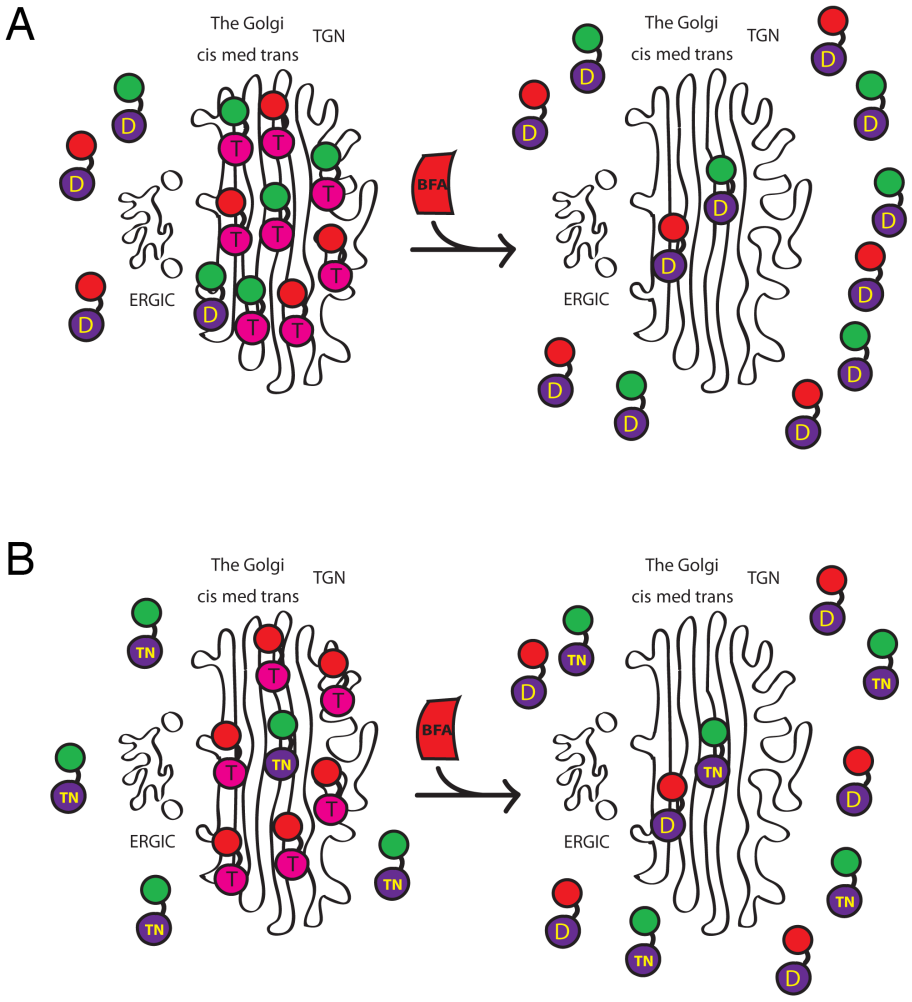

Figure 3.9 Diagram illustrating expected experimental outcomes with cells expressing both mCherry and GFP-tagged Arfs. (**A**) Cells expressing both WT Arf1-GFP and WT Arf1-mCherry are depicted before (left) and after (right) treatment with BFA. Before BFA treatment the majority of tagged Arfs accumulate in the GTP-bound form on Golgi membranes. BFA treatment causes conversion of tagged-Arfs to the GDP-bound form that redistributes predominantly to cytosol. (**B**) Cells expressing both WT Arf1-mCherry and T31N Arf1-GFP are depicted before (left) and after (right) treatment with BFA. Before BFA treatment the majority of mCherry-tagged WT Arfs accumulate in the GTP-bound form on Golgi membranes while mutant GFP-tagged Arf is predominantly cytosolic. BFA treatment causes conversion of mCherry-tagged WT Arf to the GDP-bound form that redistributes predominantly to cytosol. In all cases, some tagged-Arfs remain Golgi-localised in a GDP-bound form.

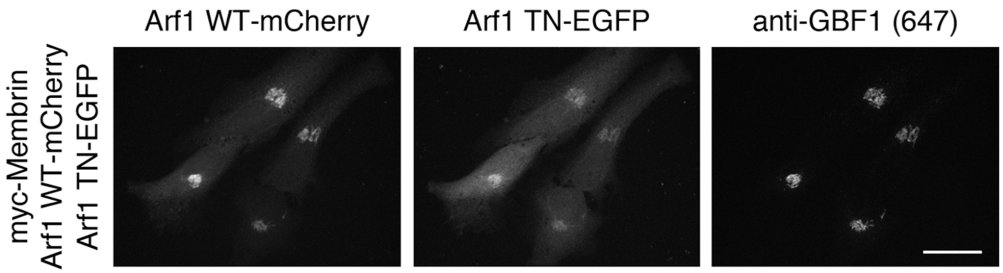

Figure 3.10 GBF1 is recruited to Golgi membranes in cells expressing both wild-type and T31N mutant Arf1. (**A**) HeLa cells were co-transfected with plasmids encoding myc-membrin and both WT Arf1-mCherry and T31N Arf1-EGFP. Cells were then fixed and stained with mouse anti-GBF1 monoclonal antibody and imaged as for Figure 3.1 (n=3).

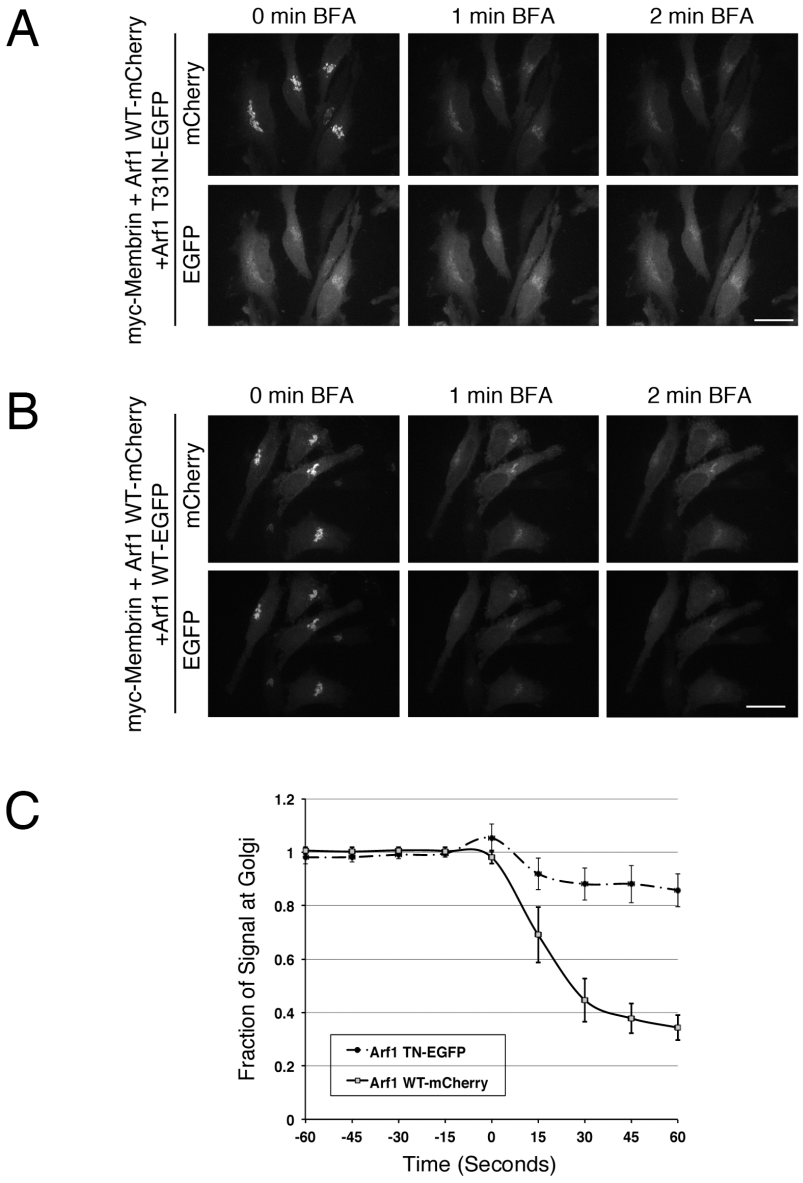

Figure 3.11 GBF1 remains catalytically active following Arf·GDP-dependent recruitment. (**A**) Live HeLa cells expressing Arf1 T31N-EGFP and Arf1 WT-mCherry were treated with 5 μg/mL BFA and imaged as for Figure 3.1. (**B**) Live HeLa cells expressing Arf1 WT-mCherry and Arf1 WT-EGFP were treated with 5 μg/mL BFA and imaged as for Figure 3.1. (**C**) Quantification of the normalized fraction of Arf signal at the Golgi was performed on cells expressing Arf1 WT-mCherry and either Arf1 WT-EGFP or Arf1 T31N-EGFP treated with 5 μg/mL BFA. A minimum of 2 cells similar to those shown in panel (B) were quantitated in each of 4 separate experiments. Images from panels (A) and (B) obtained before BFA addition were used to assemble Figure 3.12. Error bars represent the standard deviation between each of three replicate experiments (n = 4).

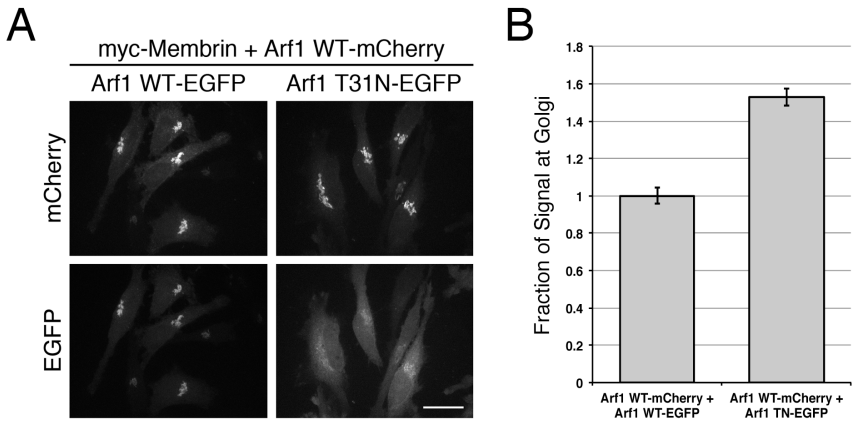

Figure 3.12 Arf•GDP-stimulated accumulation of GBF1 results in increased activation of Arf. (**A**) Live HeLa cells expressing myc-membrin, Arf1 WT-mCherry, and either the WT or T31N form of Arf1-EGFP were imaged as for Figure 3.1. Images shown in panel (A) were extracted from the experiments shown in Figure 3.11 (A) and (B).(**B**) Quantification of the fraction of Arf1 WT-mCherry signal at the Golgi in cells expressing Arf1 T31N-EGFP was performed and normalized to cells expressing Arf1 WT-EGFP. A minimum of 2 cells similar to those shown in panel A were quantitated in each of 4 separate experiments. Error bars represent the standard deviation between each of three replicate experiments (n = 4). Images shown in panel (A) were extracted from the experiments shown in Figure 3.11 (A) and (B). Scale bars = 26 μm.

active following recruitment, but also suggests that recruitment of GBF1 directly increases the amount of Arf activation at the Golgi.

3.3.4 Arf•GDP-dependent recruitment of GBF1 does not require PtdIns4P

The recent demonstration that PtdIns4*P*, through the activity of PI4KIIIα, is required for the association of GBF1 with *cis*-Golgi membranes (Dumaresq-Doiron et al., 2010) suggests a readily testable mechanism in which increases in Arf•GDP could result in recruitment of GBF1 by elevating levels of PtdIns4*P*. To test this possibility, we utilized a chimera containing the PtdIns4*P* binding PH domain of (EYFP-PH^{FAPP}) to visually monitor intracellular PtdIns4*P* levels (De Matteis and Luini, 2008; Godi et al., 2004). The best-characterized approach to rapidly increase Arf•GDP is BFA treatment, which allowed us to simultaneously monitor relative changes in GBF1 and PtdIns4*P* levels by live cell imaging. HeLa cells co-expressing mCherry-GBF1 and EYFP-PH^{FAPP} were treated with BFA and changes in GBF1 and PtdIns4*P* levels at Golgi membranes were monitored. As expected, treatment with carrier DMSO had no impact on distribution of either GBF1 or EYFP-PH^{FAPP} (Figure 3.13A). Treatment with BFA caused the expected recruitment of GBF1 to Golgi membranes, but contrary to the prediction of the hypothesis above, caused a rapid loss of EYFP-PH^{FAPP} from Golgi membranes (Figure 3.13B).

BFA inhibits both the *cis*-Golgi localised GBF1 and the TGN-localised BIGs (Saenz et al., 2009). To more specifically assess a potential role for PtdIns4*P* on *cis*-membranes where GBF1 is localised, we turned to the more selective drug Golgicide

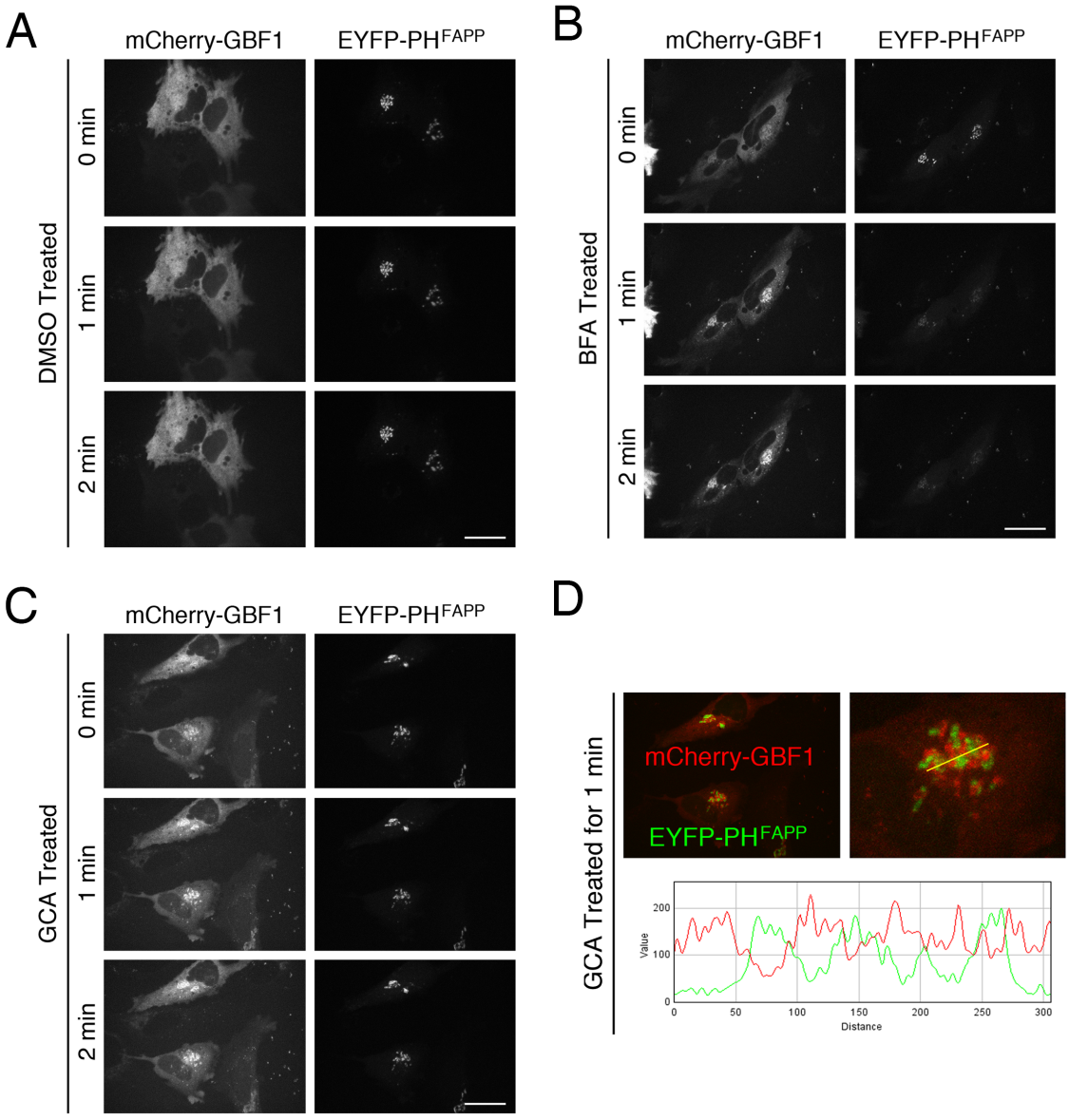

Figure 3.13 Arf·GDP-dependent GBF1 recruitment to *cis*-Golgi membranes is independent of PI4P levels. (**A**) HeLa cells expressing mCherry-GBF1 and EYFP-PH$_{FAPP}$ were treated with carrier DMSO at the same final concentration as in panels (B) and (C) and imaged by live cell spinning disc confocal microscopy as for Figure 3.1 (n=6). (**B**) HeLa cells expressing mCherry-GBF1 and EYFP-PH$_{FAPP}$ were treated with 5 μg/mL BFA and imaged by live cell spinning disc confocal microscopy (n=6) as for Figure 3.1. (**C**) Live HeLa cells expressing mCherry-GBF1 and EYFP-PHF$_{APP}$ were treated with 10 μM GCA and imaged as for Figure 3.1 (n=6). (**D**) Line scan analysis was performed on images of cells expressing mCherry-GBF1 and EYFP-PH$_{FAPP}$ obtained following 1 min treatment with 10 μM GCA. Merge image and four-fold magnification of a representative Golgi from (C) are shown. Scale bars = 26 μm.

A (GCA). The bulkier GCA inhibits GBF1 activity but is excluded from the BIGs binding site (Saenz et al., 2009). GCA treatment of HeLa cells co-expressing mCherry-GBF1 and EYFP-PH^{FAPP} caused obvious recruitment of GBF1 on Golgi membranes (Figure 3.13C). However, despite this clear increase in GBF1 signal there was no change in EYFP-PH^{FAPP} intensity in all-replicate experiments suggesting that PtdIns4*P* levels remained constant. The dramatic decrease in PtdIns4*P* levels observed following BFA treatment (Figure 3.13B) likely resulted from inhibition of BIGs activity, as could be predicted from the well established localisation of PI4P (Bankaitis et al., 2012; D'Angelo et al., 2008) and BIGs (Manolea et al., 2008; Shinotsuka et al., 2002b; Zhao et al., 2002) to the TGN. This interpretation is further supported by our observation that accumulated mCherry-GBF1 is well resolved from EYFP-PH^{FAPP} (Figure 3.13C). The clear separation of GBF1 and PtdIns4*P* signal is most apparent in the magnified image and line scan (Figure 3.13D). Together, these data suggest that the mechanism by which Arf•GDP recruits GBF1 to *cis*-Golgi membranes is independent of PtdIns4*P* level and that contrary to previous reports (Dumaresq-Doiron et al., 2010), GBF1 recruitment does not require PtdIns4*P* for membrane binding.

3.3.5 Most Golgi-associated Arfs can regulate recruitment of GBF1

Experiments to date focused on the more abundant Arf1 isoform. However, all Arf isoforms but Arf6 associate to some extent with *cis*-Golgi membranes and must therefore be activated by GBF1 *in vivo*. For this reason, we predict that GBF1

recruitment should respond to all isoforms to maintain adequate levels of each distinct Arf isoform. To test this prediction, HeLa cells expressing mCherry-GBF1, myc-membrin, and various Arf T31N-EGFP mutants were examined for accumulation of GBF1 on Golgi membranes. The left panels in Figure 14 show the distribution of overexpressed GBF1 in cells co-expressing either Class I (Arf1 or Arf3) or Class II (Arf4 or Arf5) Arf mutants. Expression of inactive forms of both Class I Arfs caused dramatic recruitment of GBF1 on a juxta-nuclear Golgi (Figure 3.14). Expression of Arf5 T31N caused reproducible fragmentation of the Golgi, and in every case examined, GBF1 accumulated on the Golgi fragments. In contrast, expression of the mutant form of the other Class II Arf, Arf4 T31N, failed to caused GBF1 recruitment. Interestingly, Arf4 T31N also fails to display a dominant negative phenotype with respect to Golgi morphology, suggesting that this mutant may not be GDP-arrested or may have folding defects. These results indicate that most inactive Arf isoforms can promote GBF1 recruitment, and suggest a substrate-driven recruitment mechanism by which GBF1 can maintain active levels of all Arf isoforms at the Golgi.

3.3.6 Arf•GDP-dependent accumulation of GBF1 requires membrane association of Arf•GDP

Recruitment of GBF1 to the Golgi most likely involves a putative compartment-specific membrane bound receptor and regulation of its activity should occur at the membrane. To begin addressing the mechanism by which Arf•GDP recruits GBF1 to

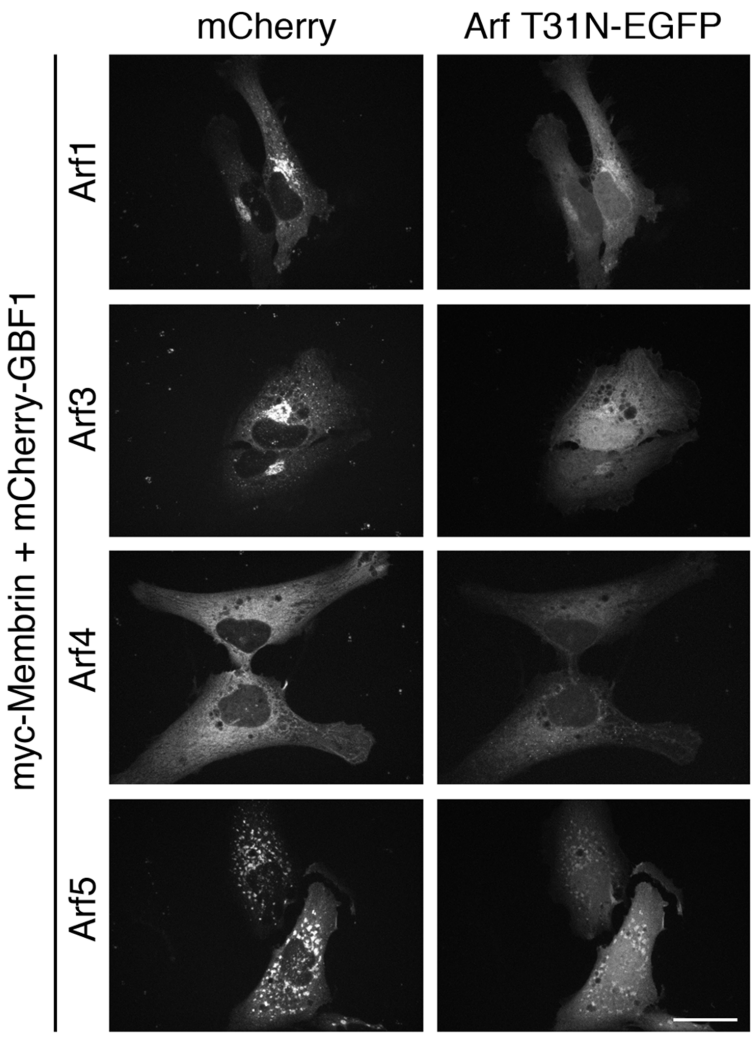

Figure 3.14 Arf•GDP-dependent recruitment of GBF1 to *cis*-Golgi membranes is not Arf isoform specific. Live HeLa cells were co-transfected with plasmids encoding mCherry-GBF1, myc-membrin, and either Arf1, 3, 4, or 5 T31N-EGFP and imaged as for Figure 3.1. Images are repreesentative of three replicate experiments. Scale bars = 26 μm.

cis-Golgi membranes, we therefore examined whether association of Arf•GDP with membranes was required. Several studies demonstrated that N-terminal myristoylation of Arf proteins is required for efficient binding to membranes since mutation of the myristoylation site from glycine to alanine (G2A) abolishes membrane binding (Franco et al., 1993; Haun et al., 1993; Kahn et al., 1995). A double mutant of inactive Arf lacking the essential myristoylation site [G2A,T31N] provided us with a tool with which to readily test our hypothesis.

HeLa cells expressing myc-membrin and low levels of either WT, T31N, or T31N,G2A forms of Arf1-EGFP were stained for endogenous GBF1 (Figure 3.15A). As observed previously (Figure 3.4B and C), expression of WT Arf1 failed to accumulate GBF1 while that of the T31N mutant led to significant recruitment of GBF1 ($p < 0.005$, n=3). As expected, the T31N,G2A double mutant did not associate to any detectable extent with Golgi membranes. More importantly, the T31N,G2A double mutant did not cause significant accumulation of GBF1 on Golgi membranes in any of the transfectants examined. GBF1 failed to accumulate even in cells expressing significantly higher levels of the Arf1 T31N,G2A double mutant (Figure 3.15A, cell in center of bottom right panel). These results indicate that membrane association of Arf•GDP is required for subsequent GBF1 recruitment. Quantification of GBF1 signal at the Golgi from several similar experiments established that expression of T31N,G2A Arf1 did not cause a significant increase in GBF1 at the Golgi. The percentage of GBF1 signal at the Golgi in the T31N,G2A Arf1 expressing cells is very similar to that observed with WT Arf1, whereas expression of T31N Arf1 causes a 3.5-fold increase in GBF1 level at the Golgi (Figure 3.15B), as previously observed

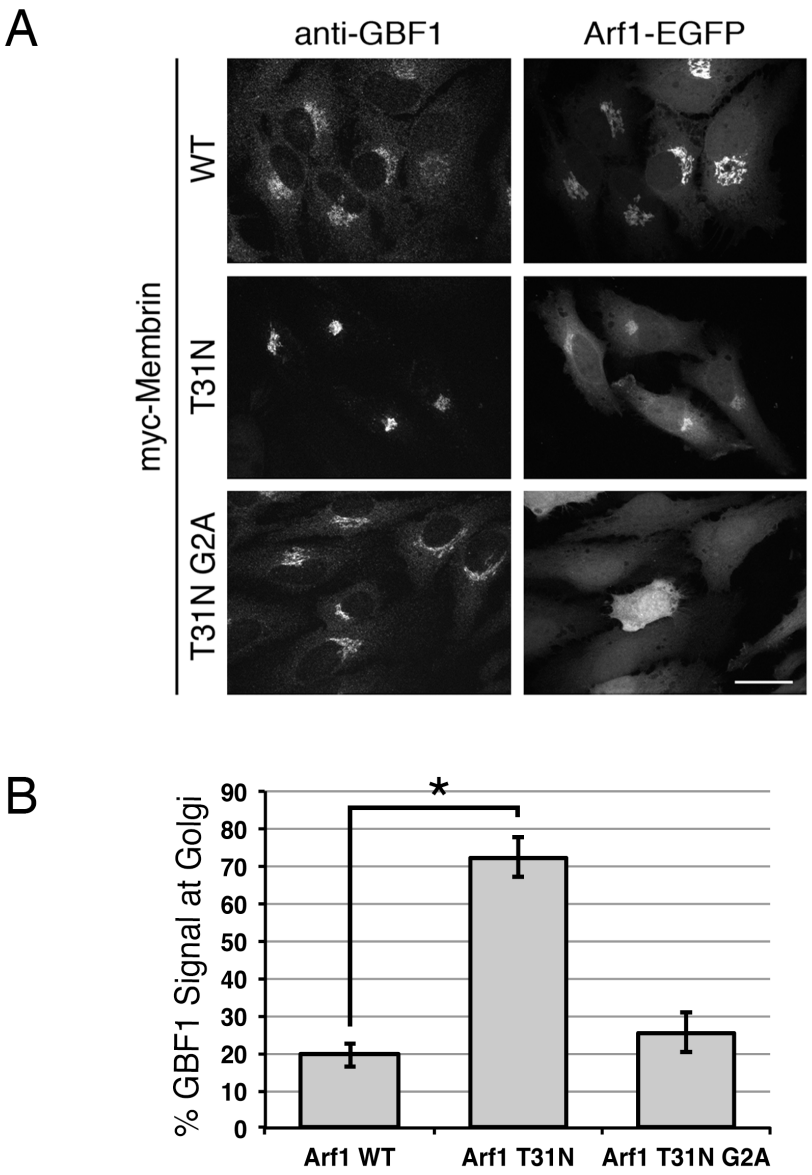

Figure 3.15 Arf·GDP-dependent GBF1 recruitment requires Arf·GDP association with Golgi membranes. (**A**) HeLa cells were co-transfected with plasmids encoding myc-membrin and Arf1 WT-EGFP, Arf1 T31N-EGFP, or Arf1 T31N G2A-EGFP. Cells were then fixed and stained with mouse anti-GBF1 monoclonal antibody and imaged as for Figure 3.1. (**B**) Quantification of GBF1 recruitment at the Golgi in Arf1 WT, T31N, and T31N G2A expressing cells was performed by measuring the percent of total GBF1 staining at the Golgi. A minimum of 8 cells similar to those shown in panel (A) were quantitated in each of 3 separate experiments. Error bars represent the standard deviation between each of three replicate experiments (n = 3). Unpaired two-tailed t-tests were performed, *$p < 0.0005$ (n=3). Scale bar = 26 μm.

(Figure 4B). In summary, these results demonstrate that membrane association of Arf•GDP is required for subsequent recruitment of GBF1 on a *cis*-Golgi localised factor.

3.4 Discussion

3.4.1 GBF1 is recruited to Golgi membranes in response to increases in Arf•GDP

It has been hypothesized (Niu et al., 2005; Szul et al., 2007) that treatment of cells with BFA results in accumulation of GBF1 on Golgi membranes due to the formation of an "abortive complex", first observed biochemically *in vitro* using purified components (Beraud-Dufour et al., 1998; Peyroche et al., 1999; Renault et al., 2003). More recently, our laboratory tested this hypothesis and found no coincident recruitment of GBF1 and Arf to Golgi membranes following BFA treatment (Chun et al., 2008). This result suggested that BFA inhibition *in vivo* induces a physiological response resulting in GBF1 recruitment to Golgi membranes in a form that no longer binds Arf to form a stable Arf•BFA•GBF1 complex. In this study, we further tested the hypothesis and discovered that various treatments that decrease Arf•GTP, resulting in a corresponding increase in Arf•GDP, cause GBF1 recruitment and accumulation. For example, as shown in Figure 3.2, overexpression of active ArfGAP1 led to clear accumulation of GBF1 on Golgi membranes. In contrast, expression of an inactive mutant ArfGAP1 caused significant reduction of GBF1 recruitment to Golgi membranes compared to control cells, suggesting that

this mutant interferes with Arf•GTP hydrolysis and thus the production of Arf•GDP. This, in turn, results in a lesser requirement for GBF1 to produce Arf•GTP achieved by lower levels of recruited GBF1.

As predicted, expression of even very low levels of the inactive T31N mutant of several Arfs was sufficient to induce the recruitment and accumulation of both over-expressed and endogenous GBF1 (Figure 3.4). To further define the mechanism by which Arf•GDP promotes GBF1 recruitment to membranes we assessed if specific Golgi-associated Arf isoform played a regulatory role. These experiments established that expression of inactive mutants of Arf1, 3, and 5 caused GBF1 accumulation on Golgi membranes; only Arf4T31N failed to do so (Figure 3.14). Arf4 T31N does not disrupt the Golgi and may not properly mimick the GDP-bound form. We expect that the true GDP-bound form of all class I and class II Arfs can regulate the recruitment of GBF1. Our results suggest that GBF1 has evolved to respond equally to the production of most Golgi-associated Arf species.

The experiments discussed above led us to propose that Arf•GDP plays a regulatory role by activating a putative GBF1 receptor found specifically on membranes of the *cis*-Golgi and ERGIC (Figure 3.16). In this model, cells can monitor levels of Arf•GDP at the membrane and respond by adjusting GBF1 recruitment to cis-Golgi membranes in order to maintain homeostasis by nucleotide exchange. Several lines of evidence discussed below support the possibility that accumulation of Arf•GDP promotes selective recruitment of active GBF1 on *cis*-Golgi membranes.

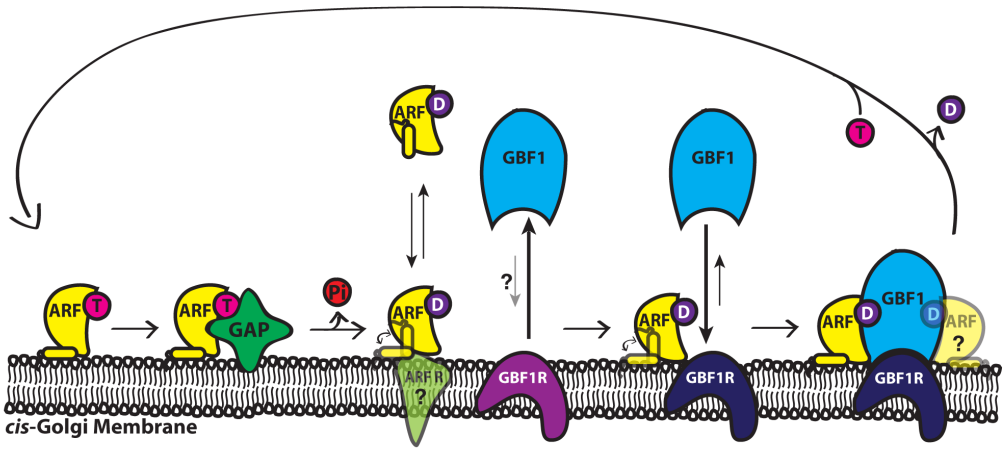

Figure 3.16 Diagram depicting the novel "Arf•GDP Increase" model for regulation of GBF1 recruitment to cis-Golgi membranes. Arf•GDP acts as a trigger for GBF1 recruitment. Regulatory Arf•GDP can arise through hydrolysis of Arf•GTP by GAP or be recruited directly from cytosol. Arf•GDP may be either free or bound to an unknown receptor. GBF1 is recruited from cytosol to a no/low affinity receptor (light colour) that likely requires Arf•GDP for activation (dark colour). The nature of the binding site for regulatory Arf•GDP remains unknown but must be at the membrane, possibly the GBF1 receptor itself. However, we cannot eliminate the possibility that Arf•GDP is regulating a lipid-modifying enzyme to cause GBF1 recruitment. This self-limiting model provides a mechanism to maintain homeostatic levels of Arf•GTP.

3.4.2 GBF1 enriched on membranes remains catalytically active and maintains Golgi polarity and function

For our model to be physiological relevant, Arf•GDP-dependent recruitment of GBF1 must result in increased GBF1 activity at the *cis*-Golgi. Specifically, we would expect to observe selective recruitment of GBF1 to membranes of the early secretory pathway, as well as subsequent Arf activation and maintenance of a polarized Golgi. Under conditions that caused GBF1 enrichment, we indeed observed that GBF1 was recruited specifically to *cis*-Golgi membranes on a Golgi that remained polarized with clearly resolved *cis*-Golgi and TGN elements (Figure 3.6). The activity of accumulated GBF1 was confirmed by the dual observations that COP1 was efficiently recruited to Golgi structures and that elevated GBF1 levels yielded 50% greater Arf activation relative to control conditions (Figure 3.12). As expected if COP1 and Arf membrane association required GBF1 activity, COPI recruitment and Arf activation remained BFA-sensitive in each assay (Figure 3.8). These data establish that Arf•GDP-dependent recruitment of GBF1 occurs specifically on *cis*-Golgi membranes, results in GBF1 activity, and demonstrate a novel and physiologically relevant model for regulation of GBF1 recruitment.

3.4.3 Arf•GDP must be membrane-associated to regulate recruitment of GBF1 to membranes

To examine the mechanism through which Arf•GDP regulates GBF1 recruitment we first examined its potential involvement in modulating PtdIns4*P* levels using the well-characterized biosensor EYFP-PH^{FAPP} (De Matteis and Luini,

2008; Godi et al., 2004). LeFrancois and colleagues hypothesized that production of PtdIns4*P* was required for recruitment of GBF1 to Golgi membranes (Dumaresq-Doiron et al., 2010). However, experiments involving treatment with BFA or GCA revealed no correlation between GBF1 recruitment and PtdIns4*P* levels (Figure 3.13). Treatment with BFA, which targets both GBF1 and BIGs, caused GBF1 accumulation and almost complete loss of PI4P signal from the Golgi. In contrast, treatment with the GBF1-specific inhibitor GCA also caused GBF1 accumulation but had no impact on PtdIns4*P* levels. More importantly, GBF1 recruitment occurred on membranes that appeared clearly distinct from membranes positive for PtdIns4*P*. Whereas those experiments failed to reveal a link between GBF1 and PtdIns4*P*, they established a predicted but to date uncharacterized link between production of the TGN-localised PtdIns4*P* (D'Angelo et al., 2008; De Matteis et al., 2005; Odorizzi et al., 2000) and the BFA-sensitive but GCA-resistant BIGs, also localised at the TGN (Manolea et al., 2008; Shinotsuka et al., 2002a; Zhao et al., 2002). Furthermore, these results confirm that GBF1 localisation occurs primarily on *cis*-Golgi membranes (Kawamoto et al., 2002; Zhao et al., 2002).

As an alternate to the candidate approach summarized above, we turned to the more basic question of whether Arf•GDP must be membrane-associated to regulate recruitment of GBF1 to membranes. Two plausible mechanisms appeared reasonable. Arf•GDP could interact with its target in cytoplasm, possibly GBF1 itself, to modulate its affinity for the membrane. Alternatively, Arf•GDP could interact with its target at the membrane, possibly a putative GBF1 receptor, to modulate its affinity for GBF1. Such information not only helps define the regulatory mechanism

but also provides avenues for identification of putative receptors. To distinguish between these two potential mechanisms, we took advantage of a well-characterized Arf G2A mutation that abrogates myristoylation of the N-terminal helix of Arf that is required for membrane association (Franco et al., 1993; Haun et al., 1993; Kahn et al., 1995). As shown in Figure 3.6, expression of the Arf1 T31N G2A double mutant failed to induce GBF1 recruitment, even in cells over-expressing the putative Arf•GDP receptor, membrin. These results demonstrate that myristate-dependent membrane association of Arf•GDP is required to elicit recruitment of GBF1, potentially to an unknown *cis*-Golgi bound factor.

3.4.4 Arf•GDP-dependent recruitment of GBF1 to *cis*-Golgi membranes may establish and maintain homeostatic levels of Arf•GTP

ArfGEF recruitment to membranes is a critical step in initiating guanine nucleotide exchange on Arf proteins at the Golgi (Paris et al., 1997). Our model for the regulation of GBF1 recruitment to *cis*-Golgi membranes centers on the cell's response to changes in Arf•GDP levels (Figure 3.16). This model accounts for our observation that increasing Arf•GDP levels promotes GBF1 membrane association, while decreasing Arf•GDP levels results in reduced GBF1 association with membranes. More importantly, this self-limiting model provides a simple mechanism to maintain homeostatic levels of Arf•GTP. Indeed, increases in substrate Arf•GDP promote recruitment of GBF1 and subsequent Arf activation. Conversely, ongoing activation eventually leads to a local reduction in Arf•GDP levels that decreases GBF1 recruitment and establishes the desired steady-state level of

Arf•GTP. Stimulation of ArfGEF recruitment by Arf•GTP has been previously reported for members of the BIGs (Lowery et al., 2013; Richardson and Fromme, 2012; Richardson et al., 2012) and cytohesin families (Cohen et al., 2007; Hofmann et al., 2007). The mechanisms reported here for GBF1 appears novel since it involves Arf•GDP.

The model also takes into account our demonstration that association of Arf•GDP with membranes is critical for regulation (Figure 3.15). Such results suggest the presence of a membrane-associated target, either a non-catalytic domain of GBF1 or possibly the GBF1 receptor itself. Whether Arf•GDP simply increases the affinity of GBF1 for the membrane or its receptor, or is actually required for its activation remains unknown. Our observation that overexpression of GAP-dead mutant which will reduce production of Arf•GDP leads to near elimination of GBF1 recruitment (Figure 3.2), suggests that the GBF1 receptor has no or extremely low affinity for GBF1 in absence of Arf•GDP.

Our data allows us to also speculate on the regulation of ArfGAP1, whose activity opposes that of GBF1 at *cis*-Golgi membranes. Previous studies reported that the expression of catalytically dead mutants of ArfGAP1 did not lead to observable phenotypes on the Golgi (Liu et al., 2005). Our data can now explain this unexpected result through modulation of GBF1 recruitment. For example, expression of the ArfGAP1 R50Q mutant decreases GBF1 recruitment by roughly 50% (Figure 3.2A and B), thereby reducing Arf•GTP production and likely compensating for the loss of ArfGAP activity. In other words, our results suggest that cells adjust GBF1 recruitment to correct for decreased GAP activity. Cells could establish homeostatic

Arf•GTP levels by regulating GAP and/or GEF activity. Our results also suggest that cells do not readily modulate endogenous GAP activity. This conclusion is based on the fact that accumulation of GBF1 to Golgi membranes results in a 50% greater activation of Arf (Figure 3.12A and B), and therefore appears not to be compensated by increased GAP activity. Together these results suggest that whereas the GEF is extremely sensitive to alterations in Arf•GTP:Arf•GDP ratio, the GAP appears to be largely unresponsive.

Chapter 4: ArfGAP1 produced Arf•GDP stimulates recruitment of GBF1 to Golgi membranes via a Golgi-localised protein receptor

The work comprising this chapter has not been published. Katie Yurkiw assisted in performing replicate experiments that resulted in Figures 4.1, 4.2, and 4.3 as part of an undergraduate research project. Calvin Chan assisted in performing replicate experiments and experimental planning that resulted in Figures 4.11 and 4.12 as part of an undergraduate research project.

4.1 Abstract

We previously proposed a novel mechanism by which GBF1 is recruited to the membranes of the *cis*-Golgi based on *in vivo* experiments. Here, we provide additional supportive data through the establishment and testing of an *in vitro* GBF1 recruitment assay. Specifically, we have demonstrated that GBF1 recruitment is positively regulated by Arf•GDP as previously described *in vivo*. In addition, we have characterized a critical role for ArfGAP1 in the production of Arf•GDP that stimulates GBF1 recruitment. Interestingly, ArfGAP2/3 do not appear to play such a role based on our *in vivo* assay. We have also been able to establish that Arf•GDP localisation is critical as a GDP-arrested mutant form of a TGN-localised Arf fails to positively influence GBF1 recruitment. Importantly, we provide the first study that suggests that a Golgi-localised protein is essential for GBF1 recruitment and localisation to Golgi membranes. This interaction with Golgi membranes via a putative receptor appears to be mediated through the HDS1 and HDS2 domains of GBF1. Lastly, we have identified a roughly 30 kDa novel GBF1 interacting partner in Golgi-enriched fractions. Further identification and characterization of this interacting partner will allow us to determine if it may be the highly sought after GBF1 receptor.

4.2 Background

As mentioned in the first chapter of this thesis, the secretory pathway is required for the correct modification and targeting of secretory cargoes. This pathway is composed of a series of membrane bound compartments with varying characteristics and functions. The exact mechanism through which individual compartments are created and maintained remains unknown, but it is generally assumed that the recruitment of protein factors to specific compartment is required to establish and define each compartment (Lippincott-Schwartz, 2011). Within the secretory pathway, the Golgi functions as a central organizing organelle (Emr et al., 2009; Farquhar and Palade, 1998). This central Golgi stack processes and facilitates the targeting of newly synthesized cargo proteins as they emerge from the ERGIC and traffic through the TGN.

The Arf family proteins can be subdivided into three classes. Class I (Arfs 1-3; primates do not express Arf 2) and Class II (Arfs 4 and 5) Arfs localise differentially through the Golgi complex (Chun et al., 2008; Dejgaard et al., 2007; Manolea et al., 2010), while the sole Class III (Arf 6) Arf functions at the endosomes and plasma membrane (Donaldson and Jackson, 2011). Interestingly, analysis of chimeras between Arf1 and Arf6 identified residues critical for Arf1 localisation to early Golgi compartments (Honda et al., 2005). These studies yielded an Arf1-6-1 chimera that displays a predominantly TGN localisation. Further work suggests that initial Arf association with membranes depends not only on N-terminal myristoylation (Franco et al., 1993; Haun et al., 1993; Kahn et al., 1995) but also on Arf receptors that are present in the Golgi membrane (Gommel et al., 2001; Honda et al., 2005).

In mammalian cells, Arf activation at Golgi and ERGIC membranes is dependent on the Golgi-localised ArfGEF GBF1. Therefore, GBF1 recruitment to Golgi membranes is required for Golgi maintenance and function, and thus it remains important to understand how GBF1 recruitment is regulated. In chapter three of this thesis, we used *in vivo* imaging experiments to identify a novel Arf•GDP-stimulated mechanism for GBF1 recruitment to ERGIC and Golgi membranes. The proposed mechanism allows for GBF1 to respond to increasing or decreasing levels of Arf•GDP to maintain a homeostatic Arf•GTP at the Golgi. To date, the identity of a putative Golgi-localised GBF1 receptor remains unknown. However, increasing our knowledge on the regulation of GBF1 recruitment to target membranes will provide us with the tools required for identification of a putative GBF1 receptor. We propose that this receptor is critical in establishing the identity of the Golgi and ERGIC compartments through the membrane-specific recruitment of GBF1.

4.3 Results

4.3.1 GBF1 recruitment is linked specifically to ArfGAP1 produced Arf•GDP

Previously published *in vivo* experiments (Chapter 3) revealed that the over-expression of ArfGAP1, wild-type (WT) or catalytically inactive R50Q mutant, altered the amount of GBF1 bound to Golgi membranes. Specifically, ArfGAP1 WT expression resulted in increased GBF1 recruitment to Golgi membranes, likely through the increased production of Arf•GDP (Parnis et al., 2006). Likewise, the expression of a catalytically inactive mutant of ArfGAP1 resulted in a significant

decrease in Golgi associated GBF1, due to an expected decrease in Arf•GDP. Here, we examined in more detail the ability of ArfGAPs to modulate GBF1 recruitment. We first tested whether ArfGAP1 altered GBF1 recruitment preferentially relative to the Golgi-localised ArfGAP2 and ArfGAP3 (Weimer et al., 2008). To determine if ArfGAP2 and/or 3 play a role in the production of regulatory Arf•GDP, we transfected HeLa cells with WT or RQ mutant forms of ArfGAP1, 2, and 3. As previously observed (Chapter 3.2; (Quilty et al., 2014)), expression of ArfGAP1 WT caused a clear increase in GBF1 levels on Golgi membranes, while the ArfGAP1 RQ mutant expression had the opposite effect and resulted in a striking loss of GBF1 signal on Golgi membranes (Figure 4.1A). Representative images displayed also contain untransfected cells to better illustrate the striking effect of ArfGAP1 expression.

To ascertain the reproducibility and significance of those observations, we quantified imaging results by calculating the percent of endogenous GBF1 signal found within the Golgi area for each of 10 cells from three separate replicate experiments (30 cells total for each condition) (Figure 4.1B). This approach yields a more accurate quantitation than the simpler Golgi:cytoplasm ratio previously reported (Figure 3.2). This analysis demonstrated that overexpression of the WT construct conferred a 2.5-fold increase in Golgi-localised GBF1 staining while the RQ mutant resulted in a 50% reduction in Golgi-localised GBF1 staining, relative to mock-transfected cells. Interestingly, while the ArfGAP1 WT induced increase in GBF1 recruitment was statistically significant ($p < 0.05$, $n=3$), the ArfGAP1 RQ induced 50% reduction Golgi-localised GBF1 was not statistically supported.

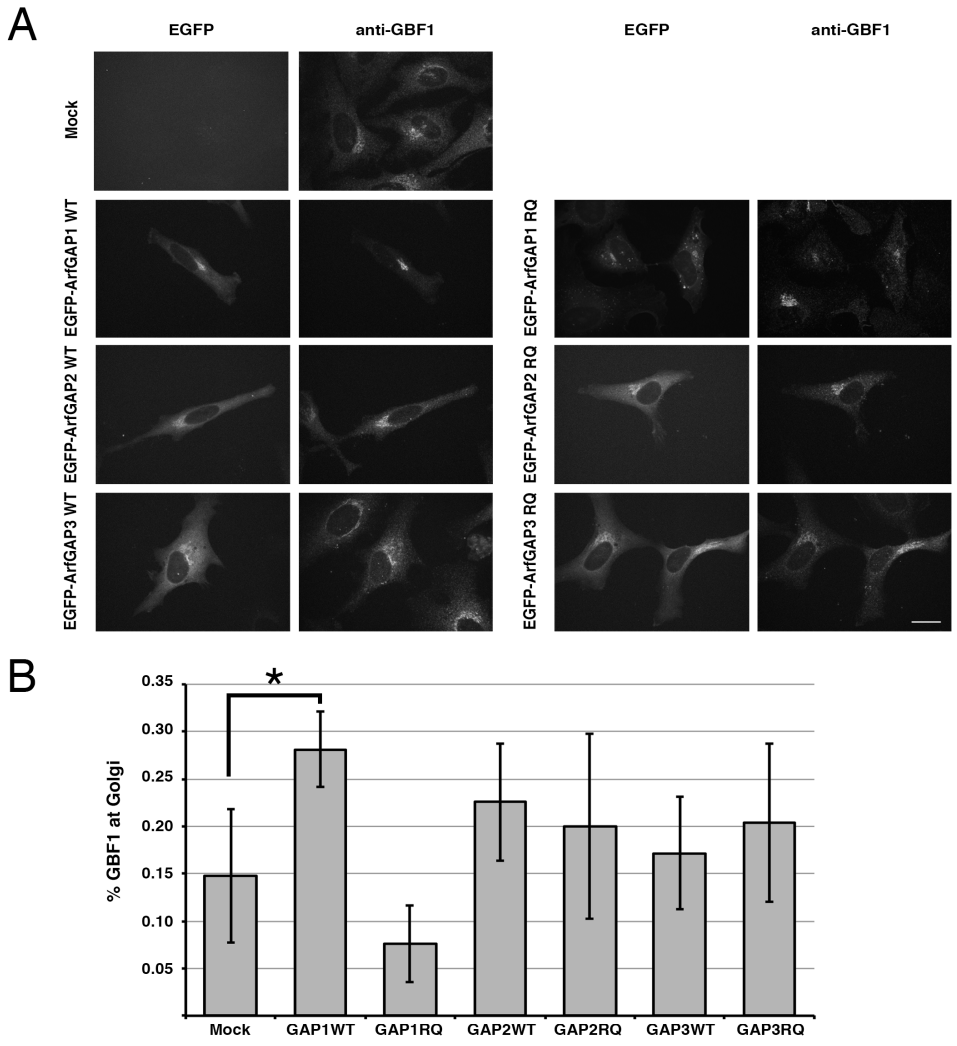

Figure 4.1 ArfGAP1 expression alters GBF1 recruitment to Golgi membranes. (**A**) HeLa cells were mock transfected or transfected with EGFP tagged constructs of ArfGAP1 WT, ArfGAP1 RQ, ArfGAP2 WT, ArfGAP2 RQ, ArfGAP3 WT or ArfGAP3 RQ. Cells were fixed and stained with mouse anti-GBF1 and imaged using spinning-disc confocal microscopy. Representative images are shown as projections of all z-slices. (**B**) Quantification was carried out by selecting a minimum of 10 cells from each condition from each of three independent experiments. The graph reports the percent of GBF1 localised to the Golgi in cells that were mock transfected or transfected with wild-type or mutant ArfGAP constructs. Error bars represent the standard deviation between each replicate experiment. Unpaired two-tailed t-tests were performed, *$p < 0.05$ (n=3). Scale bar = 26 μm.

In contrast, expression of ArfGAP2 and 3 WT to similar levels failed to result in a significant increase in GBF1 staining at the Golgi (Figure 4.1A). More importantly, expression of the catalytically inactive RQ mutant form of ArfGAP2 and 3 did not cause a decrease in GBF1 staining at the Golgi, as observed with ArfGAP1 RQ. Quantification of the fraction of GBF1 on Golgi structures indicates there was a slight, but not statistically significant change in GBF1 localisation when either WT or RQ mutant ArfGAP2/3 proteins were expressed. However, there does appear to be a modest increase in GBF1 recruitment to Golgi membranes in these samples relative to control. Failure of ArfGAP2/3 to significantly impact GBF1 levels at the Golgi suggests they do not produce regulatory Arf•GDP. This could be due to either lack of proximity to Arf•GDP-regulated elements or due to specialized functions of ArfGAP2/3 that precludes the production of pools of Arf•GDP capable of regulating GBF1 recruitment.

4.3.2 TGN-localised Arf•GDP does not alter GBF1 recruitment

The results of the ArfGAP experiments suggest that Arf•GDP must either be produced on a specific Golgi sub-compartment or micro-domain in order to regulate GBF1 recruitment. Such conclusion is consistent with our previous demonstration that regulatory Arf•GDP must be membrane-associated since N-terminal myristoylation was essential to promote GBF1 recruitment (Figure 3.15). To more definitively test if the localisation of Arf•GDP influences whether it regulates GBF1 recruitment, we proposed that a TGN-localised Arf•GDP would not stimulate GBF1 recruitment. To achieve this we utilized an Arf 1-6-1 chimera that has been shown to

localise predominantly to the TGN (Honda et al., 2005). We constructed a GFP-tagged version of the Arf1-6-1 chimera and confirmed TGN localisation by transient expression in HeLa cells. Following transfection, cells were fixed and stained with markers for the *cis*-Golgi (P115) and TGN (TGN46) (Figure 4.2A). There was a clear co-localisation of the Arf1-6-1 chimera with the TGN marker. A basic line-scan analysis was performed which confirmed that the Arf1-6-1-GFP preferentially localised to the TGN, consistent with published data (Figure 4.2B) (Honda et al., 2005).

Having confirmed that the Arf1-6-1-GFP was TGN-localised, we assessed if the GDP-arrested T31N mutant form would promote GBF1 recruitment. HeLa cells were transfected with both the WT and T31N mutant forms of Arf1-6-1-GFP and Arf1-GFP as controls. Cells were fixed and stained with anti-GBF1 antibodies to determine if GBF1 localisation to Golgi membranes was altered (Figure 4.3A). Imaging results confirmed that Arf1 T31N expression results in a striking increase in GBF1 recruitment to Golgi membranes relative to the Arf1 WT control. However, we observed that the Arf1-6-1 T31N construct failed to induce obvious GBF1 recruitment (compare Arf1-6-1 T31N expressing cells with surrounding untransfected cells). Quantitation of the percent of total GBF1 found on Golgi membranes in these cells confirms that there was no significant increase in Golgi-localised GBF1 in the Arf1-6-1 T31N expressing cells relative to Arf1-6-1 WT transfected control (Figure 4.3B). As expected, we observed a robust and statistically significant 2.5-fold increase in Golgi-localised GBF1 in cells expressing Arf1 T31N,

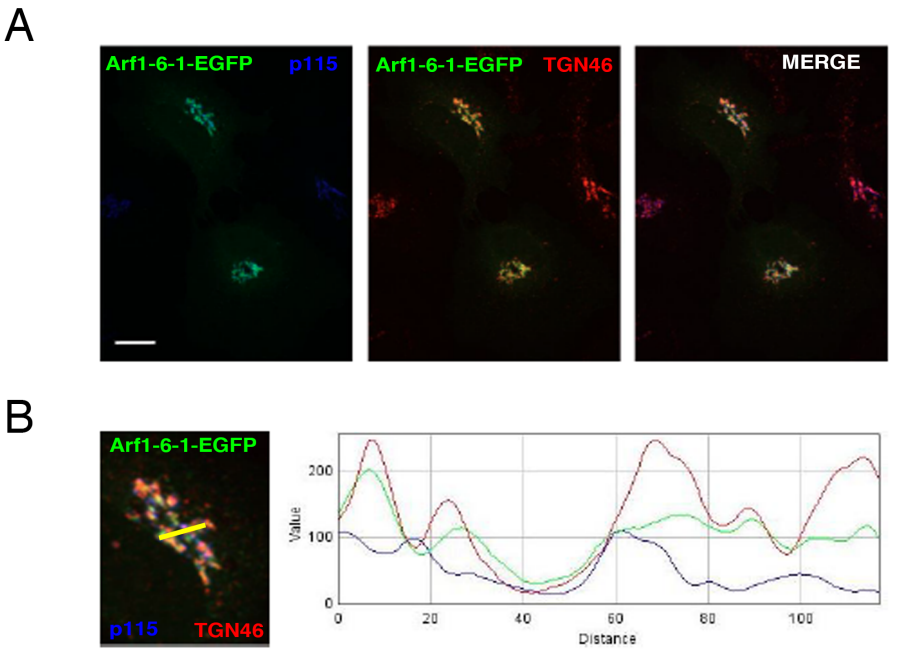

Figure 4.2 Arf1-6-1-EGFP localises predominantly to TGN membranes.
(**A**) HeLa cells were transfected with wild-type Arf1-6-1-EGFP (green). Cells were fixed and stained with mouse anti-p115 (blue) and sheep anti-TGN46 (red). Imaging was performed using spinning-disc confocal microscopy.
(**B**) Magnified (4x) representative Golgi images were used for line scan analysis was performed on extended focus images for a minimum of five Golgi images from each of three independent replicates. Scale bar = 26µm.

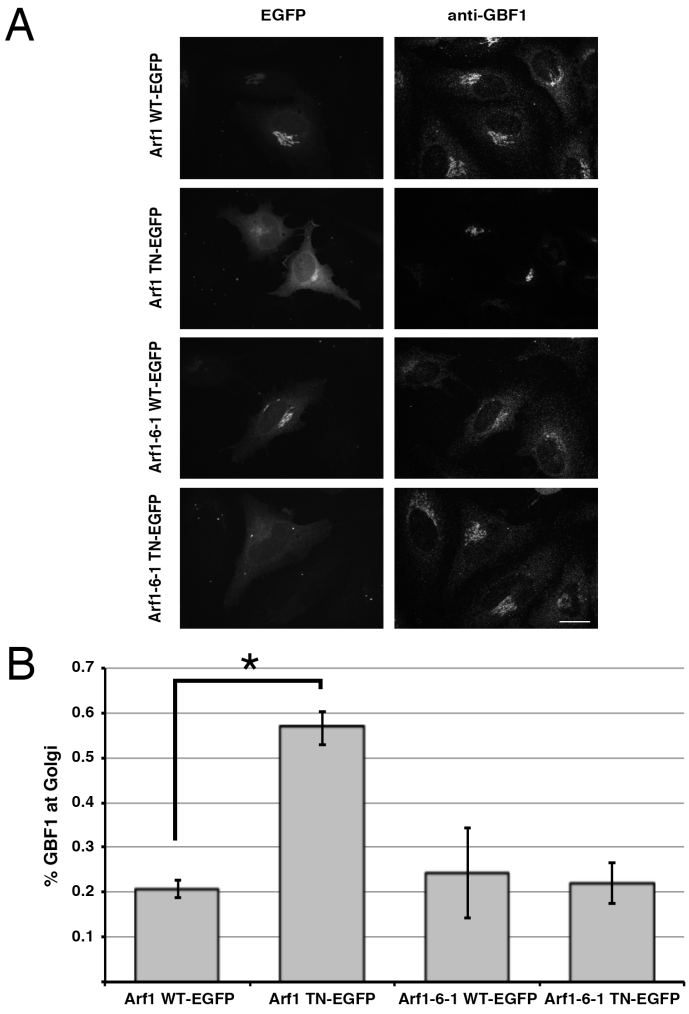

Figure 4.3 TGN-localised Arf1-6-1 expression has no effect on GBF1 recruitment to Golgi membranes. (**A**) HeLa cells were transfected with EGFP tagged wild-type or mutant Arf1 or Arf1-6-1. Cells were fixed and stained with mouse anti-GBF1 antibody and images were collected using spinning-disc confocal microscopy. Representative images are shown as projections of all z-slices. (**B**) Quantification was carried out by selecting a minimum of 10 cells from each condition from each of three separate experiments. The graph reports the percent of GBF1 localised to the Golgi in cells that were transfected with wild-type or mutant Arf1 or Arf1-6-1 constructs. Error bars represent the standard deviation between each replicate experiment. Unpaired two-tailed t-tests were performed, *$p < 0.0005$ (n=3). Scale bar = 26 µm.

relative to the Arf1 WT expressing control ($p < 0.0005$, n=3). These data indicate that regulatory Arf•GDP must not only interact with membranes via the N-terminal myristate, but associate specifically with *cis*-Golgi membranes in order to promote GBF1 recruitment to the Golgi membranes.

4.3.3 Characterization of WNG membranes

To provide further evidence for a role for Arf•GDP in the regulation of GBF1 recruitment to Golgi membranes, we performed *in vitro* GBF1 recruitment experiments. To establish an *in vitro* GBF1 recruitment assay, we utilized a Golgi membrane preparation from rat liver nuclei (WNG) that was found to be highly stacked (Dominguez et al., 1999) and contain significant levels of bound GBF1 (Gilchrist et al., 2006). We first confirmed that WNG membranes contained bound GBF1 using centrifugation and anti-GBF1 western blot (Figure 4.4). This analysis established that the WNG (Total) contained an immuno-reactive band running just below the 250 kDa molecular weight standard, the expected size of GBF1. Moreover, the GBF1 found in WNG fractions was found almost exclusively in the membrane fraction. These data indicate that WNG fractions contain significant levels of membrane-associated GBF1 and are a viable membrane for use in an *in vitro* GBF1 recruitment assay.

4.3.4 GBF1 recruitment to Golgi membranes *in vitro* is temperature sensitive

In order to perform an *in vitro* GBF1 binding assay, we require a source of

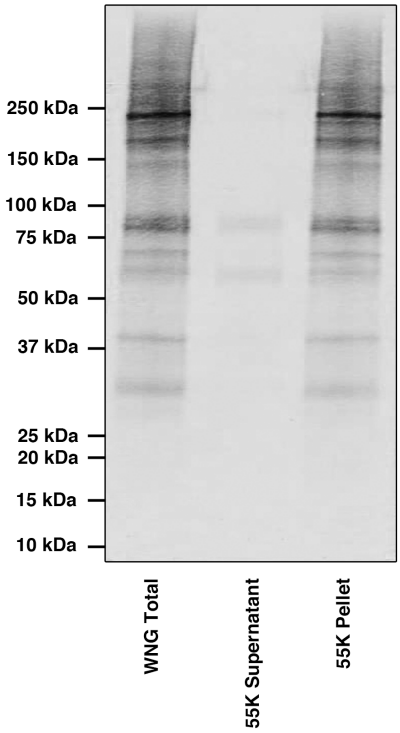

Figure 4.4: GBF1 is present in WNG and found exclusively in the membrane fraction. Total WNG membranes along with WNG that were separated into 55K pellet and supernatant were separated by SDS-Page. Proteins were transferred to nitrocellulose and immunoblotted with a mouse anti-GBF1 monoclonal antibody and donkey anti-mouse Alexa 750 secondary and was then scanned in a Licor Odyssey scanner. The resulting western blot is displayed above.

GBF1. For this purpose, we used cytosol produced from a well-studied normal rat kidney (NRK) cells expressing GFP-GBF1 (Zhao et al., 2006) as a source of GBF1 for the assay since full-length GBF1 cannot be produced recombinantly in our hands. Lastly, binding assays were carried out in the presence of excess protease inhibitors since both endogenous and exogenous GBF1 proved extremely sensitive to proteolysis.

To measure recruitment of GFP-GBF1 from cytosol onto the WNG membranes, we mixed GFP-GBF1 NRK cytosol with WNG for 5 minutes either on ice or at 37° Celsius as described in Methods. Following incubation, samples were separated by centrifugation and analysed by immunoblotting with an anti-GBF1 antibody as described in Chapter 2. In order to normalize results to the amount of membrane present in each assay, we also probed the blots with antibodies raised against the Golgi protein Mannosidase II (ManII). 10% cytosol and WNG alone loading controls were included for the purpose of comparison. The resulting western blots demonstrate that GFP-GBF1 (Arrow) could be recruited to WNG membranes when incubated at 37° Celsius, while there was much weaker recruitment of GFP-GBF1 in samples incubated on ice (Figure 4.5A). ManII levels in these samples were not obviously discrepant. These data suggest that GBF1 recruitment to Golgi membranes can be reconstituted in an *in vitro* assay.

Quantitation of band intensity using Licor Odyssey software allowed for corrected measure of GFP-GBF1 recruitment across three replicate experiments. The ratio of GFP-GBF1 intensity to ManII band intensity was calculated for each replicate and mean values are displayed along with standard deviation error bars (n=3)

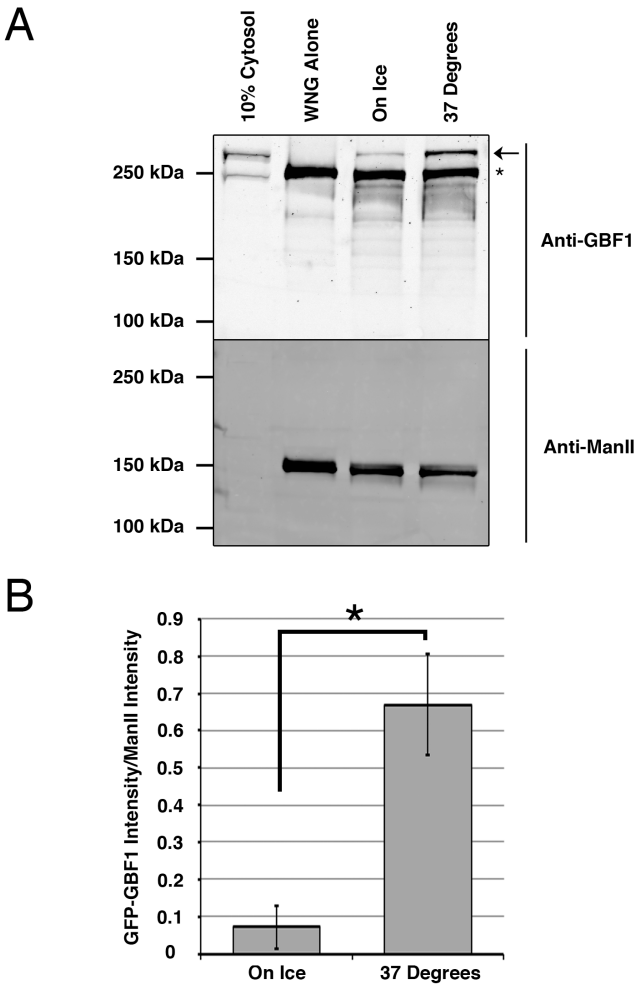

Figure 4.5: GBF1 is recruited to WNG at physiological temperature and not on ice. (**A**) WNG membranes were incubated with GFP-GBF1 NRK cytosol at 37° Celsius or on ice for 5 minutes and then separated into membrane and supernatant fractions by centrifugation. Resulting pellets were run by SDS-Page along with 10% cytosol and WNG alone controls. Proteins were transferred to nitrocellulose and western blotted with a mouse anti-GBF1 monoclonal antibody and rabbit anti-ManII antibodies then incubated in donkey anti-mouse Alexa 750 and donkey anti-rabbit alexa 680 secondary antibodies. The resulting western blot was then scanned in a Licor Odyssey scanner. A representative western blot is displayed above. Arrow indicates GFP-GBF1 band and asterisk indicates GBF1 band. (**B**) GFP-GBF1 band intensity was quantified and corrected for amount of WNG present through comparison to ManII band intensity. Error bars represent the standard deviation between each replicate experiment. The resulting quantitation is displayed (n=3). Unpaired two-tailed t-tests were performed, *$p < 0.005$ (n=3).

(Figure 4.5B). The quantitation indicates that there was significant 6.5-fold more GFP-GBF1 recruited to membranes incubated at 37° Celsius relative to those incubated on ice ($p < 0.005$, n=3). These data indicate that we can reconstitute GBF1 recruitment to Golgi membranes *in vitro.* Additionally, we can conclude that this recruitment is not due to non-specific hydrophobic interactions, as these interactions would be stabilized in samples incubated on ice.

4.3.5 GBF1 recruitment to Golgi membranes *in vitro* is sensitive to presence of guanine nucleotide

We have demonstrated that Arf•GDP positively regulates GBF1 recruitment to *cis*-Golgi membranes through an unknown mechanism *in vivo* (Chapter 3; (Quilty et al., 2014)). We hypothesize that GBF1 recruitment to Golgi membranes *in vitro* will respond to changes in Arf•GDP level. In order to assess the effect of Arf•GDP on GBF1 recruitment *in vitro* we added 5 mM GTP or 10 mM GTP and examined the effect on recruitment. A representative western blot (n=3) shows that, when either 5 or 10 mM GTP is added to the *in vitro* GBF1 recruitment assay, significantly less GFP-GBF1 (Arrow) is recruited to the Golgi membranes (Figure 4.6A). The ratio of GFP-GBF1 intensity to ManII band intensity was calculated for each replicate and normalized to the value obtained with the control reaction (n=3) (Figure 4.6B). The quantitation indicates that there is an approximately 90% reduction in the amount of GFP-GBF1 recruited to Golgi membranes in the presence of 5 or 10 mM GTP, relative to control samples. These data suggest that GBF1 recruitment to Golgi

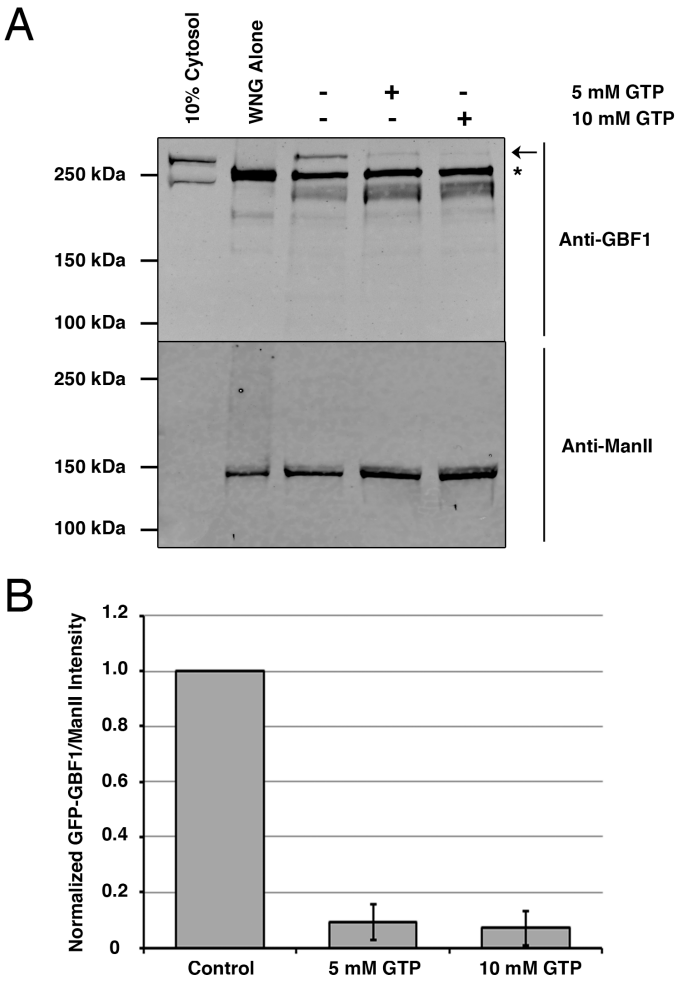

Figure 4.6: GBF1 recruitment to WNG is inhibited by the addition of GTP. (**A**) WNG membranes were incubated with GFP-GBF1 NRK cytosol at 37° Celsius with or without the addition of GTP and then separated into membrane and supernatant fractions by centrifugation. Resulting pellets were run by SDS-Page along with 10% cytosol and WNG alone controls. Proteins were transferred to nitrocellulose and western blotted with a mouse anti-GBF1 monoclonal antibody and rabbit anti-ManII antibodies then incubated in donkey anti-mouse Alexa 750 and donkey anti-rabbit Alexa 680 secondary antibodies. The resulting western blot was then scanned in a Licor Odyssey scanner. A representative western blot is displayed above. Arrow indicates GFP-GBF1 band and asterisk indicates GBF1 band. (**B**) GFP-GBF1 band intensity was quantified and corrected for amount of WNG present through comparison to ManII band intensity. Values obtained were then normalized to Control values to determine the fold change relative to Control. Error bars represent the standard deviation between each replicate experiment. The resulting quantitation is displayed (n=3).

membranes *in vitro* is sensitive to guanine nucleotide, likely through the activation of Arf and consequent reduction in Arf•GDP. This finding is consistent with our previously published work *in vivo* demonstrating that reducing Arf•GDP levels will result in a reduction in Golgi membrane-associated GBF1.

4.3.6 Recombinant ArfGAP1 addition alters GBF1 recruitment to Golgi membranes *in vitro*

Having shown that GBF1 recruitment is reduced in the presence of high concentrations of GTP suggests a role for Arf•GDP in regulating GBF1 recruitment *in vitro*, as we would expect based on our *in vivo* data discussed in Chapter 3. To confirm that the reduction in GBF1 recruitment in the presence of excess GTP results from Arf activation, we determined whether addition of recombinant ArfGAP1 would reverse the effect of GTP. We performed *in vitro* GBF1 recruitment assays in the presence of 5 mM GTP alone or with either 20 or 40 μg/mL recombinant ArfGAP1. A representative western blot (n=3) indicates that GFP-GBF1 was efficiently recruited to the Golgi membranes in our control assay, while we observe a clear reduction in this recruitment in the sample where 5 mM GTP had been added (Figure 4.7A). Interestingly, while addition of 20 μg/mL recombinant ArfGAP1 caused little change in recruitment, addition of recombinant ArfGAP1 to 40 μg/mL resulted in a partial recovery in GFP-GBF1 recruitment. The ratio of GFP-GBF1 intensity to ManII band intensity was calculated for each replicate and normalized to the control. The mean values of the calculated fold-change are displayed along with standard error bars

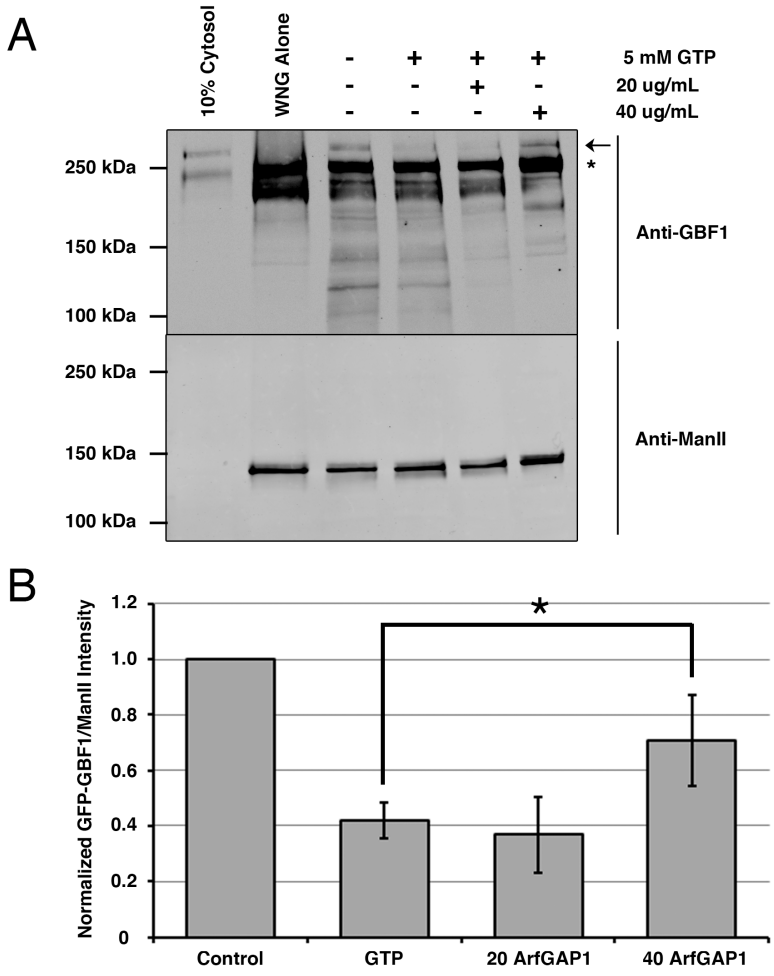

Figure 4.7 GBF1 recruitment to WNG is promoted by the addition of ArfGAP1. (**A**) WNG membranes were incubated with GFP-GBF1 NRK cytosol at 37° Celsius with 5 mM GTP with or without the addition of ArfGAP1 and then separated into membrane and supernatant fractions by centrifugation. Resulting pellets were run by SDS-Page along with 10% cytosol and WNG alone controls. Proteins were transferred to nitrocellulose and western blotted with a mouse anti-GBF1 monoclonal antibody and rabbit anti-ManII antibodies then incubated in donkey anti-mouse Alexa 750 and donkey anti-rabbit Alexa 680 secondary antibodies. the resulting western blot was then scanned in a Licor Odyssey scanner. A representative western blot is displayed above. Arrow indicates GFP-GBF1 band and asterisk indicates GBF1 band. (**B**) GFP-GBF1 band intensity was quantified and corrected for amount of WNG present through comparison to ManII band intensity. Values obtained were then normalized to Control values to determine the fold change relative to Control. The resulting quantitation is displayed (n=3). Error bars represent the standard deviation between each replicate experiment. Unpaired two-tailed t-tests were performed, *$p < 0.05$ (n=3).

(n=3) (Figure 4.7B). The quantitation indicates that addition of 40 µg/mL recombinant ArfGAP1 conferred a roughly 50% recovery in GFP-GBF1 recruitment relative to control and 5 mM GTP conditions, which was statistically significant ($p < 0.05$, n=3). These data further suggest that increasing Arf•GDP levels positively regulates *in vitro* recruitment of GBF1 to Golgi membranes.

4.3.7 Establishing a role for a Golgi-localised protein in GBF1 recruitment to Golgi membranes

To date we have hypothesized that GBF1 is recruited specifically to membranes of the *cis*-Golgi and ERGIC through a putative GBF1 receptor. The nature of this receptor remains unknown and could be a lipid, a soluble protein, a transmembrane protein, or a combination of any of the above. We postulate that there is likely a proteinaceous factor that facilitates GBF1 recruitment to *cis*-Golgi membranes. To test this possibility, we proposed that treatment of WNG membranes with high heat would denature the proteins found on these Golgi membranes and potentially impact GBF1 recruitment. WNG membranes were incubated either on ice or at 95° Celsius for 5 minutes and then assayed for *in vitro* GBF1 recruitment, as previously described. A representative western blot of three replicates is displayed (Figure 4.8A). As seen previously, our control assay recruited a significant amount of GFP-GBF1 (Arrow) to the membrane fraction. More importantly, we observed a striking reduction in GFP-GBF1 recruitment to membranes that had been denatured by heat. Quantitation of three replicate experiments was performed as before

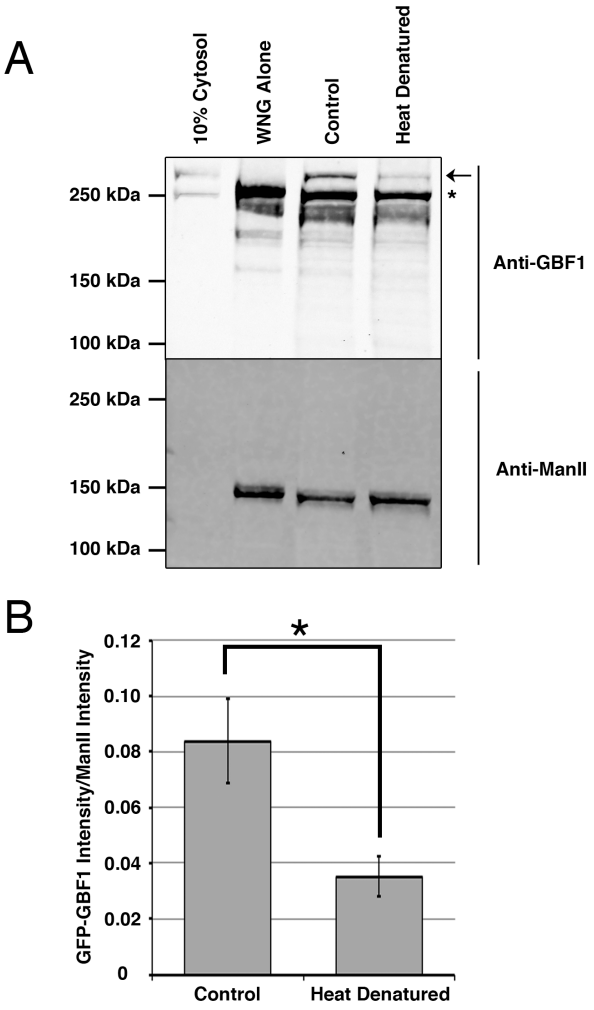

Figure 4.8 GBF1 recruitment to WNG is inhibited by heat denaturation of WNG. (**A**) WNG membranes were incubated with GFP-GBF1 NRK cytosol at 37° Celsius following incubation at 95 degrees Celsius or on ice and then separated into membrane and supernatant fractions by centrifugation. Resulting pellets were run by SDS-Page along with 10% cytosol and WNG alone controls. Proteins were transferred to nitrocellulose and western blotted with a mouse anti-GBF1 monoclonal antibody and rabbit anti-ManII antibodies then incubated in donkey anti-mouse Alexa 750 and donkey anti-rabbit Alexa 680 secondary antibodies. the resulting western blot was then scanned in a Licor Odyssey scanner. A representative western blot is displayed above. Arrow indicates GFP-GBF1 band and asterisk indicates GBF1 band. (**B**) GFP-GBF1 band intensity was quantified and corrected for amount of WNG present through comparison to ManII band intensity. Error bars represent the standard deviation between each replicate experiment. The resulting quantitation is displayed (n=3). Unpaired two-tailed t-tests were performed, *$p < 0.01$ (n=3).

(n=3) (Figure 4.8B). The quantitation indicates a significant 50% reduction in GFP-GBF1 recruitment in samples in which WNG were denatured by heating prior to performing the recruitment assay, relative to control ($p < 0.01$, n=3). These data provide the first evidence that a Golgi-localised protein mediates GBF1 recruitment to Golgi membranes.

To more directly test the presence of a Golgi-localised GBF1 protein receptor, we treated WNG membranes with trypsin prior to performing the recruitment assay. We incubated WNG membranes for 5 minutes at 37° Celsius either with or without 0.5 mg/mL trypsin. Following incubation, 1.0 mg/mL soybean trypsin inhibitor was then added to control and trypsin treated WNG membranes and incubated on ice. Resulting membranes were then used in the *in vitro* GBF1 recruitment assay as previously described. A representative western blot of three replicates is displayed (Figure 4.9A). As seen previously, the control assay recruited a significant amount of GFP-GBF1 (Arrow) to the membrane fraction. However, in samples containing membranes pre-treated with trypsin, we observed a near complete loss in GFP-GBF1 recruitment. In order to ensure we had not degraded all of the GFP-GBF1 protein found in cytosol, we assessed the level of GFP-GBF1 remaining in supernatant fractions. While we did observe evidence of minor GFP-GBF1 degradation, the striking reduction in GFP-GBF1 recruitment observed cannot be attributed to this degradation. These data indicate that trypsin treatment of WNG abrogates GBF1 recruitment. Quantitation of three replicate experiments was performed as before (Figure 4.9B). The quantitation indicates a statistically significant 85% reduction in

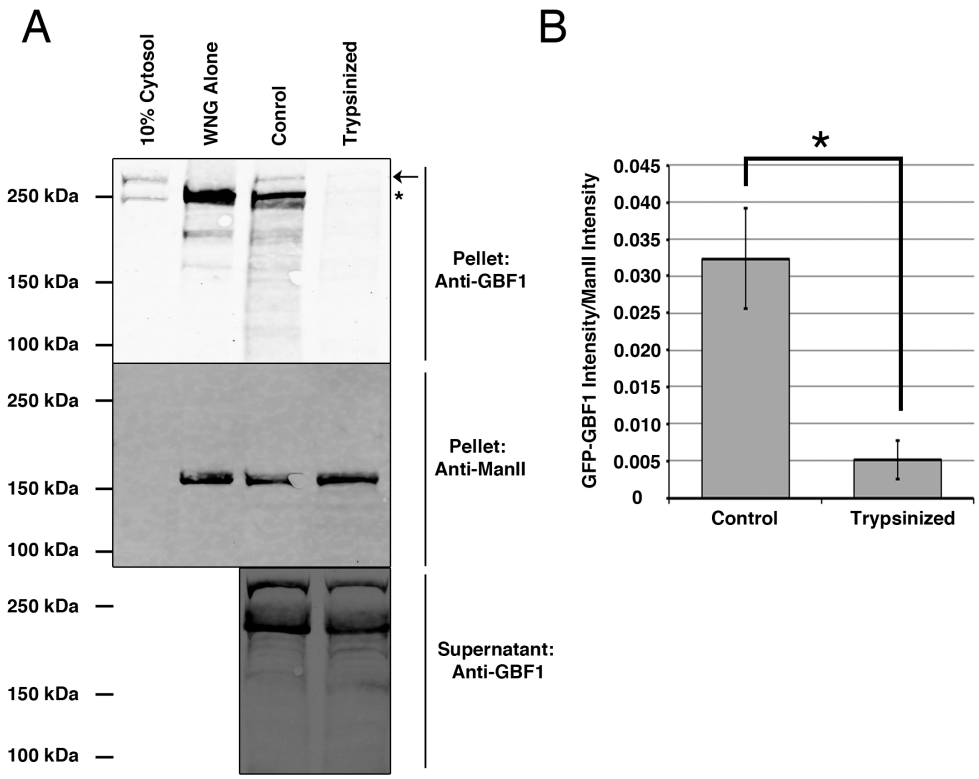

Figure 4.9 GBF1 recruitment to WNG is inhibited by trypsin treatment of WNG. (**A**) WNG membranes were incubated with GFP-GBF1 NRK cytosol at 37° Celsius following incubation with or without trypsin and then separated into membrane and supernatant fractions by centrifugation. Resulting pellets and supernatants were run by SDS-Page along with 10% cytosol and WNG alone controls. Proteins were transferred to nitrocellulose and western blotted with a mouse anti-GBF1 monoclonal antibody and rabbit anti-ManII antibodies then incubated in donkey anti-mouse Alexa 750 and donkey anti-rabbit Alexa 680 secondary antibodies. the resulting western blot was then scanned in a Licor Odyssey scanner. A representative western blot is displayed above. Arrow indicates GFP-GBF1 band and asterisk indicates GBF1 band. (**B**) GFP-GBF1 band intensity was quantified and corrected for amount of WNG present through comparison to ManII band intensity. Error bars represent the standard deviation between each replicate experiment. The resulting quantitation is displayed (n=3). Unpaired two-tailed t-tests were performed, *$p < 0.005$ (n=3).

GFP-GBF1 recruitment in samples in which WNG were treated with trypsin prior to performing the recruitment assay, relative to control ($p < 0.005$, $p=3$). These data, together with those in Figure 4.8, indicate that a Golgi-localised protein(s) is required for efficient recruitment of GBF1 to Golgi membranes. It remains unclear, however, if this unknown protein(s) functions as a direct binding partner or an enzyme required for modifications that promote GBF1 recruitment.

4.3.8 Identification of a putative GBF1 receptor

In an attempt to identify an interacting partner, we performed a far western in which we separated 5 and 10 µL of WNG proteins by SDS-PAGE and transferred to nitrocellulose and subsequently incubated the membrane in GFP-GBF1 NRK cytosol. As a control, an identical membrane was probed with 20-fold excess recombinant GFP protein, relative to the amount of GFP-GBF1 in 1 mL based on fluorescence signal. The membranes were then incubated with anti-GFP antibody, followed by fluorescently labeled secondary antibody and imaged. The resulting far western blot is displayed (Figure 4.10). In our GFP-GBF1 incubated blot we observed two bands of interest (Arrows), one running at about 48 kDa (just below the 50 kDa molecular weight standard) and the other at about 32 kDa (just below the 37 kDa molecular weight standard). The roughly 48 kDa band we observed was not pursued further because this band could be detected prior to incubation with cytosol, suggesting this region of the nitrocellulose membrane displayed auto-fluorescence.

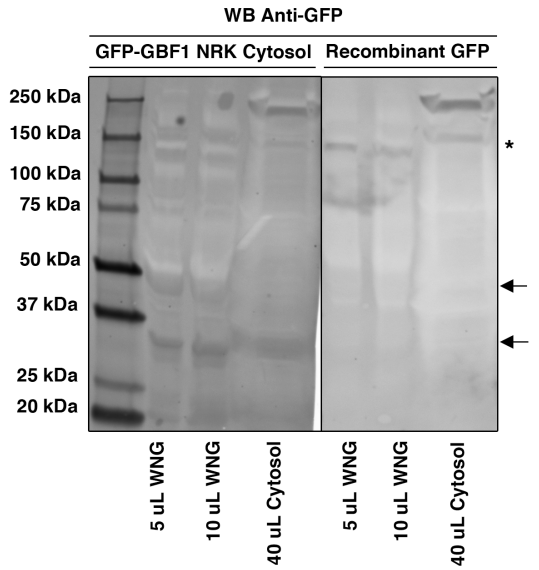

Figure 4.10 GFP-GBF1 far western suggests an approximately 32 kDa GBF1 interacting partner. WNG membranes were run by SDS-Page and proteins were transferred to nitrocellulose and incubated in GFP-GBF1 NRK cytosol or recombinant GFP. Membranes were then western blotted with a rabbit anti-GFP antibody then incubated with donkey anti-rabbit Alexa 647 secondary antibody. The resulting Far Western blot was then imaged in a FluorChemQ system (Cell Biosciences). A representative western blot prepared using Alphaview softaware (Cell Biosciences) is displayed above. Arrows indicate GFP-GBF1 positive bands. Asterisk indicates a GFP positive band on our control membrane.

To begin identification of a potential interacting partner of approximately 32 kDa, we ran an identical gel to that used for the far western and excised the region that corresponds to the GFP-GBF1 positive band. The results of mass spectrometry analysis are displayed (Table 4.1). Within this data set are a number of Golgi-localised proteins that could be potential GBF1 receptors and therefore should be further tested.

4.3.9 Identifying the minimal Golgi-binding domain of GBF1

We propose that GBF1 is recruited to Golgi membranes via a putative GBF1 receptor. As a practical first step towards characterizing the interaction of GBF1 with *cis*-Golgi membranes, we chose to identify domains of GBF1 required for this process. We constructed a GFP-tagged GBF1 truncation library based on the borders of the DCB, HUS, Sec7, HDS1, HDS2, HDS3 domains initially published by Cherfils and colleagues (Mouratou et al., 2005). This resulted in the construction of nine N-terminal truncations and nine C-terminal truncations. A cartoon map representation of the GBF1 truncation library is shown (Figure 4.11A). To assess the ability for each truncation to be recruited to Golgi membranes, HeLa cells were transfected with the truncation library along with GBF1 WT and GFP-alone controls. We determined that it was critical to perform the imaging in live cells as we observed an inconsistent loss in Golgi localisation when performing fixed-cell imaging experiments. Therefore, cells were then imaged by live cell epifluorescence microscopy to assess whether each truncation localised to a juxta-nuclear Golgi structure. A summary of the

Table 4.1 List of proteins identified by mass spectrometry

UniProt Accession Number	**Description** *ProteinName* **OS=***OrganismName* **GN=***GeneName* **PE=***ProteinExistence* **SV=***SequenceVersion*
P09118	Uricase OS=Rattus norvegicus GN=Uox PE=1 SV=3 - [URIC_RAT]
P02650	Apolipoprotein E OS=Rattus norvegicus GN=Apoe PE=1 SV=2 - [APOE_RAT]
P04797	Glyceraldehyde-3-phosphate dehydrogenase OS=Rattus norvegicus GN=Gapdh PE=1 SV=3 - [G3P_RAT]
Q9WVK3	Peroxisomal trans-2-enoyl-CoA reductase OS=Rattus norvegicus GN=Pecr PE=2 SV=1 - [PECR_RAT]
Q9ERE4	Golgi phosphoprotein 3 OS=Rattus norvegicus GN=Golph3 PE=1 SV=1 - [GOLP3_RAT]
P54921	Alpha-soluble NSF attachment protein OS=Rattus norvegicus GN=Napa PE=1 SV=2 - [SNAA_RAT]
P16232	Corticosteroid 11-beta-dehydrogenase isozyme 1 OS=Rattus norvegicus GN=Hsd11b1 PE=1 SV=2 - [DHI1_RAT]
Q5PPL3	Sterol-4-alpha-carboxylate 3-dehydrogenase, decarboxylating OS=Rattus norvegicus GN=Nsdhl PE=2 SV=1 - [NSDHL_RAT]
P04636	Malate dehydrogenase, mitochondrial OS=Rattus norvegicus GN=Mdh2 PE=1 SV=2 - [MDHM_RAT]
P06866	Haptoglobin OS=Rattus norvegicus GN=Hp PE=1 SV=3 - [HPT_RAT]
Q08851	Syntaxin-5 OS=Rattus norvegicus GN=Stx5 PE=1 SV=2 - [STX5_RAT]
Q5XFW8	Protein SEC13 homolog OS=Rattus norvegicus GN=Sec13 PE=1 SV=1 - [SEC13_RAT]
P19945	60S acidic ribosomal protein P0 OS=Rattus norvegicus GN=Rplp0 PE=1 SV=2 - [RLA0_RAT]
P13803	Electron transfer flavoprotein subunit alpha, mitochondrial OS=Rattus norvegicus GN=Etfa PE=1 SV=4 - [ETFA_RAT]
P29147	D-beta-hydroxybutyrate dehydrogenase, mitochondrial OS=Rattus norvegicus GN=Bdh1 PE=1 SV=2 - [BDH_RAT]

Q5M875	17-beta-hydroxysteroid dehydrogenase 13 OS=Rattus norvegicus GN=Hsd17b13 PE=1 SV=1 - [DHB13_RAT]
P20070	NADH-cytochrome b5 reductase 3 OS=Rattus norvegicus GN=Cyb5r3 PE=1 SV=2 - [NB5R3_RAT]
P55006	Retinol dehydrogenase 7 OS=Rattus norvegicus GN=Rdh7 PE=2 SV=1 - [RDH7_RAT]
Q9WVK7	Hydroxyacyl-coenzyme A dehydrogenase, mitochondrial OS=Rattus norvegicus GN=Hadh PE=2 SV=1 - [HCDH_RAT]
P24329	Thiosulfate sulfurtransferase OS=Rattus norvegicus GN=Tst PE=1 SV=3 - [THTR_RAT]
P09895	60S ribosomal protein L5 OS=Rattus norvegicus GN=Rpl5 PE=1 SV=3 - [RL5_RAT]
Q6AYS8	Estradiol 17-beta-dehydrogenase 11 OS=Rattus norvegicus GN=Hsd17b11 PE=2 SV=1 - [DHB11_RAT]
Q499P3	C1GALT1-specific chaperone 1 OS=Rattus norvegicus GN=C1galt1c1 PE=1 SV=1 - [C1GLC_RAT]
P00481	Ornithine carbamoyltransferase, mitochondrial OS=Rattus norvegicus GN=Otc PE=1 SV=1 - [OTC_RAT]
Q5PQP2	Receptor-binding cancer antigen expressed on SiSo cells OS=Rattus norvegicus GN=Ebag9 PE=1 SV=1 - [RCAS1_RAT]
P63245	Guanine nucleotide-binding protein subunit beta-2-like 1 OS=Rattus norvegicus GN=Gnb2l1 PE=1 SV=3 - [GBLP_RAT]
Q5XIH7	Prohibitin-2 OS=Rattus norvegicus GN=Phb2 PE=1 SV=1 - [PHB2_RAT]
Q9Z2M4	Peroxisomal 2,4-dienoyl-CoA reductase OS=Rattus norvegicus GN=Decr2 PE=2 SV=1 - [DECR2_RAT]
P04642	L-lactate dehydrogenase A chain OS=Rattus norvegicus GN=Ldha PE=1 SV=1 - [LDHA_RAT]
Q9Z2L0	Voltage-dependent anion-selective channel protein 1 OS=Rattus norvegicus GN=Vdac1 PE=1 SV=4 - [VDAC1_RAT]
P21533	60S ribosomal protein L6 OS=Rattus norvegicus GN=Rpl6 PE=1 SV=5 - [RL6_RAT]
P07154	Cathepsin L1 OS=Rattus norvegicus GN=Ctsl PE=1 SV=2 - [CATL1_RAT]
Q9QUH3	Apolipoprotein A-V OS=Rattus norvegicus

	GN=Apoa5 PE=1 SV=1 - [APOA5_RAT]
P27952	40S ribosomal protein S2 OS=Rattus norvegicus GN=Rps2 PE=1 SV=1 - [RS2_RAT]
P55159	Serum paraoxonase/arylesterase 1 OS=Rattus norvegicus GN=Pon1 PE=1 SV=3 - [PON1_RAT]
P0C6B1	Solute carrier family 35 member E1 OS=Rattus norvegicus GN=Slc35e1 PE=3 SV=1 - [S35E1_RAT]
P62909	40S ribosomal protein S3 OS=Rattus norvegicus GN=Rps3 PE=1 SV=1 - [RS3_RAT]
Q63416	Inter-alpha-trypsin inhibitor heavy chain H3 OS=Rattus norvegicus GN=Itih3 PE=2 SV=1 - [ITIH3_RAT]
P43428	Glucose-6-phosphatase OS=Rattus norvegicus GN=G6pc PE=2 SV=1 - [G6PC_RAT]
P97852	Peroxisomal multifunctional enzyme type 2 OS=Rattus norvegicus GN=Hsd17b4 PE=1 SV=3 - [DHB4_RAT]
P21743	Insulin-like growth factor-binding protein 1 OS=Rattus norvegicus GN=Igfbp1 PE=1 SV=2 - [IBP1_RAT]
Q7TPJ0	Translocon-associated protein subunit alpha OS=Rattus norvegicus GN=Ssr1 PE=1 SV=1 - [SSRA_RAT]
Q5RJR8	Leucine-rich repeat-containing protein 59 OS=Rattus norvegicus GN=Lrrc59 PE=1 SV=1 - [LRC59_RAT]
B2GUZ5	F-actin-capping protein subunit alpha-1 OS=Rattus norvegicus GN=Capza1 PE=1 SV=1 - [CAZA1_RAT]
P57760	Serine/threonine-protein kinase 16 OS=Rattus norvegicus GN=Stk16 PE=2 SV=2 - [STK16_RAT]
P08081	Clathrin light chain A OS=Rattus norvegicus GN=Clta PE=1 SV=1 - [CLCA_RAT]
P56603	Secretory carrier-associated membrane protein 1 OS=Rattus norvegicus GN=Scamp1 PE=1 SV=1 - [SCAM1_RAT]
P55260	Annexin A4 OS=Rattus norvegicus GN=Anxa4 PE=1 SV=3 - [ANXA4_RAT]
Q5I0E7	Transmembrane emp24 domain-containing protein 9 OS=Rattus norvegicus GN=Tmed9 PE=1 SV=1 - [TMED9_RAT]
P81155	Voltage-dependent anion-selective channel protein 2 OS=Rattus norvegicus GN=Vdac2 PE=1 SV=2 - [VDAC2_RAT]

P97532	3-mercaptopyruvate sulfurtransferase OS=Rattus norvegicus GN=Mpst PE=1 SV=3 - [THTM_RAT]
P00507	Aspartate aminotransferase, mitochondrial OS=Rattus norvegicus GN=Got2 PE=1 SV=2 - [AATM_RAT]
Q5FVQ4	Malectin OS=Rattus norvegicus GN=Mlec PE=2 SV=1 - [MLEC_RAT]
D3ZTX0	Transmembrane emp24 domain-containing protein 7 OS=Rattus norvegicus GN=Tmed7 PE=1 SV=1 - [TMED7_RAT]
P54311	Guanine nucleotide-binding protein G(I)/G(S)/G(T) subunit beta-1 OS=Rattus norvegicus GN=Gnb1 PE=1 SV=4 - [GBB1_RAT]
Q9Z2Z8	7-dehydrocholesterol reductase OS=Rattus norvegicus GN=Dhcr7 PE=2 SV=1 - [DHCR7_RAT]
Q5HZX7	Lipid droplet-associated hydrolase OS=Rattus norvegicus GN=Ldah PE=2 SV=1 - [LDAH_RAT]
Q6PCU2	V-type proton ATPase subunit E 1 OS=Rattus norvegicus GN=Atp6v1e1 PE=1 SV=1 - [VATE1_RAT]
P14668	Annexin A5 OS=Rattus norvegicus GN=Anxa5 PE=1 SV=3 - [ANXA5_RAT]
Q07936	Annexin A2 OS=Rattus norvegicus GN=Anxa2 PE=1 SV=2 - [ANXA2_RAT]
P57093	Phytanoyl-CoA dioxygenase, peroxisomal OS=Rattus norvegicus GN=Phyh PE=1 SV=2 - [PAHX_RAT]
Q5BK17	Iodotyrosine deiodinase 1 OS=Rattus norvegicus GN=Iyd PE=2 SV=1 - [IYD1_RAT]
P29266	3-hydroxyisobutyrate dehydrogenase, mitochondrial OS=Rattus norvegicus GN=Hibadh PE=1 SV=3 - [3HIDH_RAT]
Q4V899	Transmembrane protein 165 OS=Rattus norvegicus GN=Tmem165 PE=2 SV=1 - [TM165_RAT]
Q8R431	Monoglyceride lipase OS=Rattus norvegicus GN=Mgll PE=1 SV=1 - [MGLL_RAT]
P23457	3-alpha-hydroxysteroid dehydrogenase OS=Rattus norvegicus GN=Akr1c9 PE=1 SV=1 - [DIDH_RAT]
Q68FR9	Elongation factor 1-delta OS=Rattus norvegicus GN=Eef1d PE=1 SV=2 - [EF1D_RAT]
P48199	C-reactive protein OS=Rattus norvegicus GN=Crp PE=1 SV=1 - [CRP_RAT]
P06757	Alcohol dehydrogenase 1 OS=Rattus norvegicus

	GN=Adh1 PE=1 SV=3 - [ADH1_RAT]
P02651	Apolipoprotein A-IV OS=Rattus norvegicus GN=Apoa4 PE=1 SV=2 - [APOA4_RAT]
P60711	Actin, cytoplasmic 1 OS=Rattus norvegicus GN=Actb PE=1 SV=1 - [ACTB_RAT]
Q63041	Alpha-1-macroglobulin OS=Rattus norvegicus GN=A1m PE=1 SV=1 - [A1M_RAT]
P35435	ATP synthase subunit gamma, mitochondrial OS=Rattus norvegicus GN=Atp5c1 PE=1 SV=2 - [ATPG_RAT]
P62755	40S ribosomal protein S6 OS=Rattus norvegicus GN=Rps6 PE=1 SV=1 - [RS6_RAT]
P49242	40S ribosomal protein S3a OS=Rattus norvegicus GN=Rps3a PE=1 SV=2 - [RS3A_RAT]
P85970	Actin-related protein 2/3 complex subunit 2 OS=Rattus norvegicus GN=Arpc2 PE=1 SV=1 - [ARPC2_RAT]

localisation analysis is displayed (Figure 4.11B). Image analysis clearly showed that, of the 18 truncations queried, four truncations displayed a clear juxta-nuclear localisation (Figure 4.12). Specifically, the N205-1856, N390-1856, N885-1856, and C1-1275 constructs all displayed juxta-nuclear localisation, suggestive of Golgi recruitment. Interestingly, the only domains in common for the four constructs of interest are the HDS1 and HDS2 domains. Furthermore, our minimum Golgi-associated GBF1 truncation is the N885-1856 truncation. Efforts to further establish a minimum Golgi binding construct were unsuccessful as any further deletion from the N885-1856 truncation rendered the mutant incapable of Golgi association.

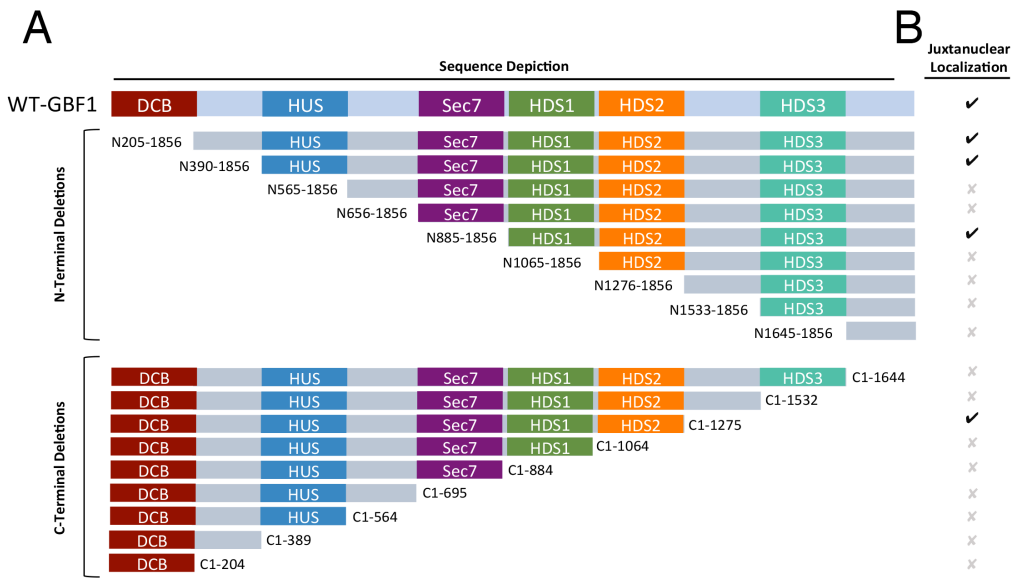

Figure 4.11 The N-terminal half of GBF1 is not required for recruitment to Golgi membranes.
(**A**) A cartoon map of the pEGFP-GBF1 truncation library. Constructs were generated by PCR and inserted into a modified pEGFP-SbfI vector. All constructs were sequenced and correct size was confirmed by immuno blot.
(**B**) HeLa cells were transfected with plasmids encoding each of the GBF1 truncations pictured in (A) and imaged by live cell wide-field fluorescence microscopy. An extended focus view of all acquired z-slices, that was deconvolved, was used to determine if the truncations displayed juxtanuclear-localisation. Chimeras that demonstrated Golgi localisation in each cell imaged across three replicate experiments are marked with a check mark, while those that failed to display such localisation are marked and an “x”.

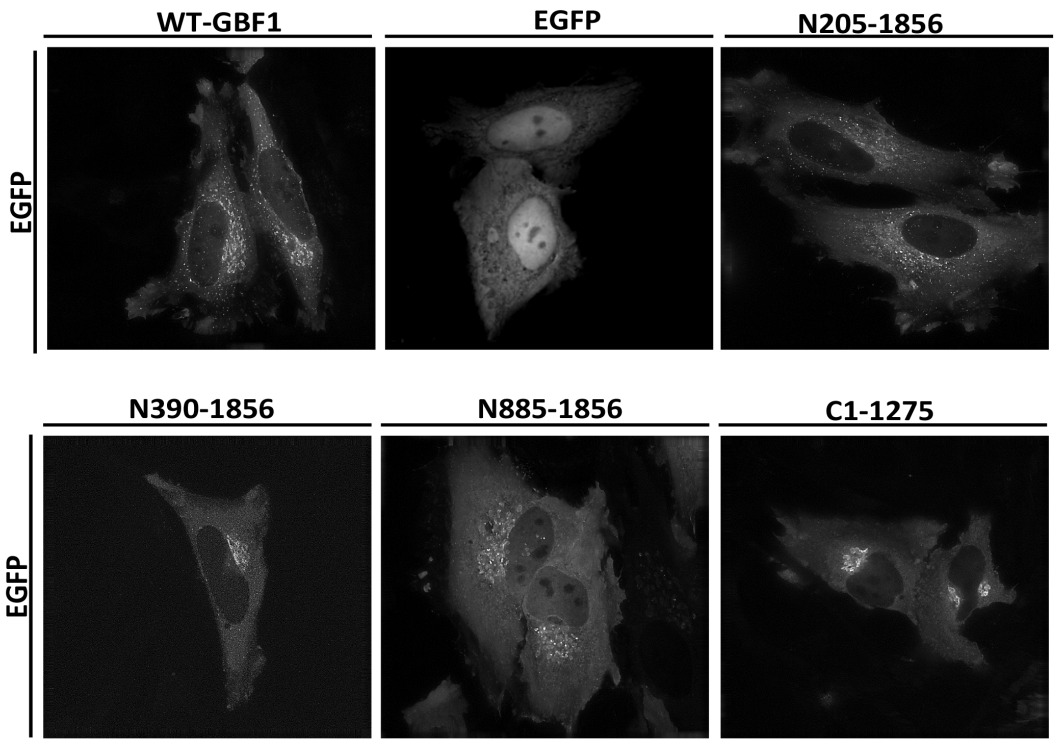

Figure 4.12 The N-terminal half of GBF1 is not required for recruitment to Golgi membranes.
HeLa cells were transfected with plasmids encoding each of the GBF1 truncations pictured in Figure 4.12B and imaged by live cell wide-field fluorescence microscopy. An extended focus view of all acquired z-slices, that was deconvolved, are displayed here. Images displayed are representative of a minimum of 10 cells from each of three replicate experiements and used for the summary shown in Figure 4.11.

4.4 Discussion

4.4.1 ArfGAP1 produces regulatory Arf•GDP

The results presented in Chapter 3 suggest that ArfGAP1 WT over-expression resulted in increased GBF1 recruitment to *cis*-Golgi membranes, *in vivo*. Moreover, here we have confirmed these observations using more sophisticated quantitation of the percent of GBF1 signal at the Golgi. This effect is most likely due to increased hydrolysis of Arf•GTP to Arf•GDP, as we have shown that increasing Arf•GDP levels in the cell promotes GBF1 recruitment. Interestingly, transfection of the catalytically inactive RQ mutant of ArfGAP1 caused a striking reduction in Golgi-localised GBF1. This was surprising since studies of other inactive mutants failed to demonstrate defects in Golgi morphology and function (Liu et al., 2005). We have now provided a reasonable explanation for this lack of phenotype. Specifically, we have shown that in the context of over-expressing WT or RQ ArfGAP1, the regulated recruitment of GBF1 to Golgi membranes by Arf•GDP allows for compensation for the effects of the ArfGAP proteins. At the time of these assays, we tested ArfGAP1 first somewhat arbitrarily. To extend these results, we wanted to determine if this ability to promote GBF1 recruitment was restricted to ArfGAP1, or if Golgi-localised ArfGAP2 and/or 3 would also exhibit positive regulation GBF1 recruitment.

We hypothesized that production of Arf•GDP from any ArfGAP protein would likely influence GBF1 recruitment. This theory was based on our understanding of Arf•GDP localisation in live cells. Arf•GDP is predominantly cytosolic and we assumed that recruitment of Arf•GDP to Golgi membranes through binding via

interaction with Golgi-localised Arf•GDP receptors, such as membrin, or the N-terminal myristate moiety would be sufficient to allow for GBF1 recruitment. Our data, however, suggest that Arf•GDP produced by different ArfGAP species has different impacts on GBF1 recruitment. What remains to be determined is if overexpression of the GFP-tagged ArfGAPs generates equal levels of Arf•GDP. It is possible that ArfGAP1 is more efficient at promoting hydrolysis of Arf•GTP to Arf•GDP, which would provide a simple explanation for our results. Therefore, we have updated our model of GBF1 recruitment to illustrate that importance of ArfGAP1 in the production of Arf•GDP (Figure 4.13). It also remains possible that specific localisation of ArfGAP proteins may determine whether product Arf•GDP would be capable of promoting GBF1 recruitment, while this would only potentially explain the ArfGAP3 result. This is due to the fact that ArfGAP3 is localised predominantly to the TGN, not the *cis*-Golgi compartment where GBF1 is recruited (Shiba et al., 2013). Alternatively, it is also likely that ArfGAP2/3 have specialized roles, distinct from ArfGAP1 that would preclude them from producing Arf•GDP that would serve to promote GBF1 recruitment (Kartberg et al., 2010). An alternate explanation is that ArfGAP1 may reside in close proximity to regulatory elements that promote the likelihood that Arf•GDP molecules promote GBF1 recruitment.

4.4.2 Arf•GDP stimulates GBF1 recruitment to Golgi membranes *in vitro*

Chapter 3 presented an *in vivo* study of the regulation of GBF1 recruitment to *cis*-Golgi membranes. We elucidated a substrate-stimulated, feed-forward mechanism in which Arf•GDP promoted GBF1 recruitment by an unknown

mechanism for maintenance of Arf•GTP homeostasis. To further strengthen our results, we proposed to develop an *in vitro* GBF1 recruitment assay. To solve this problem, we proposed the usage of cytosol generated from well-characterized GFP-GBF1 stably expressing NRK cells as a source of GBF1 for our recruitment assay. In addition, we acquired WNG, a highly stacked Golgi preparation, from the laboratory of Dr. John Bergeron as a target membrane for GBF1 recruitment. These membranes were chosen due to published proteomic data indicating that GBF1 was identified on these membranes, suggesting that they would likely be capable of GBF1 binding. We were subsequently able to demonstrate *in vitro* recruitment of GFP-GBF1 to Golgi membranes in a temperature-dependent manner, minimizing concerns that Golgi binding was due to non-specific hydrophobic interactions. Using this assay we were able to perform assays that supported *in vivo* results. Specifically, we confirmed that GBF recruitment is tightly linked to Arf•GDP level through addition of GTP and ArfGAP1 to binding assays. Our data indicate that addition of significant levels of GTP to binding assay significantly suppressed GBF1 recruitment, and while indirect this suggests a role for Arf•GDP in *in vitro* GBF1 recruitment as seen *in vivo*. To further link *in vitro* GBF1 recruitment to Arf•GDP we demonstrated that addition of sufficient ArfGAP1 could alleviate the inhibitory effect of GTP. Our model for GBF1 recruitment predicts that addition of GTP resulted in Arf activation and thus a conversion of Arf•GDP to Arf•GTP, while the subsequent addition of ArfGAP1 would efficiently hydrolyze activated Arf•GTP back to Arf•GDP that would positively regulate GBF recruitment. Confirmation that *in vitro* GBF1 recruitment is Arf•GDP-

dependent further supports our proposed mechanism for GBF1 recruitment (Figure 4.13).

4.4.3 HDS1 and HDS2 domains appear to mediate Golgi localisation and potentially interaction with a GBF1 receptor

We have hypothesized that GBF1 is recruited to *cis*-Golgi membranes through interaction with a Golgi-localised protein receptor. To date, we have been unable to provide conclusive evidence that a protein is indeed required for GBF1 recruitment. Establishing an *in vitro* GBF1 recruitment assay afforded us an opportunity to test this hypothesis. We demonstrated that when WNG membranes were either heat denatured or exposed to trypsin prior to GBF1 recruitment there was significant impairment in GBF1 recruitment. These results suggest that GBF recruitment to *cis*-Golgi membranes is dependent on a Golgi-localised protein. We hypothesize that this protein is likely an uncharacterized GBF1 receptor that is positively regulated by Arf•GDP.

Classically, characterization of protein-protein interactions often involved the identification of minimal domains that facilitate a proposed interaction. To this end, we proposed to generate a GBF1 truncation library that would allow us to identify the minimal Golgi-binding domain, while also providing us with a valuable tool for future characterization of GBF1 interacting partners, using the published domain boundaries based on sequence homology studies (Mouratou et al., 2005). Interestingly, we determined that the N-terminal half of GBF1, including the Sec7 domain, was dispensable with respect to GBF1 recruitment to membranes. This

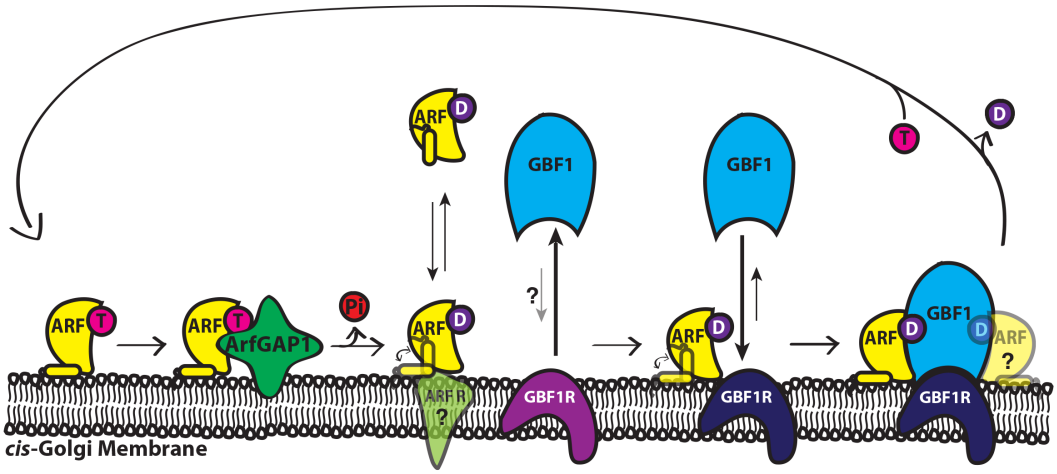

Figure 4.13 Diagram depicting Arf•GDP stimulated recruitment of GBF1 to cis-Golgi membranes. Arf•GDP stimulates GBF1 recruitment to *cis*-Golgi membranes. Regulatory Arf•GDP can be recruited directly through hydrolysis of Arf•GTP by ArfGAP1 specifically or be recruited from cytosol by Arf•GDP receptors. Arf•GDP may be either free or bound to an unknown receptor. GBF1 is recruited from cytosol to a no/low affinity receptor (Purple) that likely requires Arf•GDP for activation (Navy). We have confirmed that a Golgi-localised protein is required for GBF1 recruitment. Currently, the nature of the binding site for regulatory Arf•GDP remains unknown but must be at the membrane, possibly the GBF1 receptor itself. However, we cannot eliminate the possibility that Arf•GDP is regulating a lipid-modifying enzyme to cause GBF1 recruitment. This substrate stimulated model provides a mechanism for GBF1 to maintain homeostatic levels of Arf•GTP in the cell.

result was surprising as previous reports indicated that the N-terminal DCB and HUS were required for Golgi binding (Bouvet et al., 2013). However, these experiments were done in fixed cells and therefore likely did not capture localisation of these GBF1 truncations to the Golgi. Further, more recent reports have confirmed our findings suggesting that the N-terminal DCB domain is not required for Golgi recruitment (Bhatt et al., 2016). Analysis of additional GBF1 truncations suggests that the HDS1 and HDS2 domains are critical for GBF1 association with Golgi membranes. Identification of the HDS1 and HDS2 domains as critical for Golgi association is consistent with previous reports (Bouvet et al., 2013). We propose that these domains facilitate GBF1 interaction with Golgi membranes, potentially through a putative GBF1 receptor or through interaction with lipids. All attempts to solve localisation issues resulting from fixation were unsuccessful, so our attempts to confirm truncation localisation to the *cis*-Golgi were not fruitful. Use of fluorescent live-cell markers for the *cis*-Golgi and TGN will allow us to confirm *cis*-Golgi localisation of truncated GBF1 constructs.

4.4.4 Identification of a potential GBF1 interacting partner by far western

Lastly, we have determined that a roughly 34 kDa protein by GFP-GBF1 far western that could be a novel GBF1 interacting partner. Ideally, this protein would be the putative GBF1 receptor that we have trying to identify for many years. Of the proteins identified in our mass spectrometry analysis, we must consider each Golgi protein carefully and disregard the strength or abundance due to the fact that a low abundance protein may be sufficient to bind GFP-GBF1 in this assay. It is quite

possible the protein of interest may be a low abundance protein, relative to other irrelevant proteins identified. Candidates will be tested by reciprocal far western and shRNA knockdown followed by assessment of GBF1 recruitment. A putative GBF1 receptor will display a significant impairment in GBF1 recruitment when partially knocked down. This topic will be further discussed in Chapter 5.7.

Chapter 5: General Discussion

5.1 Synopsis

The primary focus of the work presented here was elucidation of the Arf•GDP-dependent regulatory mechanism responsible for triggering GBF1 recruitment and maintenance of Arf activation at *cis*-Golgi membranes. Results of *in vivo* imaging experiments that utilized pharmacological agents and GDP-arrested Arf mutants led to our current model of Arf•GDP-stimulated GBF1 recruitment (Figure 3.16). These experiments also confirmed that Arf•GDP-stimulated GBF1 recruitment resulted in proper *cis*-Golgi localisation, Golgi structure organization, COPI recruitment, and Arf activation as would be expected of a physiologically relevant mechanism. Subsequent development of an *in vitro* GBF1 recruitment assay provided further support for a link between Arf•GDP and the stimulation of GBF1 recruitment. Moreover, the *in vitro* GBF1 recruitment assay allowed us to provide the first evidence for the requirement of a *cis*-Golgi-localised protein, or putative receptor, in GBF1 recruitment to Golgi membranes. The work presented here also provides us with tools that should lead to the identification of the putative GBF1 receptor. The recruitment of GBF1 could be mediated by interactions with several factors such as phosphoinositides (Dumaresq-Doiron et al., 2010), rab1 (Alvarez et al., 2003) and receptor abundance/modification, as proposed for other ArfGEFs (Richardson et al., 2012). Current work towards identification of a receptor will greatly add to our understanding of GBF1 function and could potentially lead to discovery of therapeutics for the treatment of diseases resulting for GBF1 dysfunction and those caused by viruses that manipulate GBF1 function and localisation to ensure successful replication. The work described in this thesis

identified a novel mechanism of GBF1 recruitment regulation, for the first time attributed a role for Arf•GDP in the cell, potentially identified a novel role for ArfGAP1, yielded novel insight into how BFA acts *in vivo*, and established the requirement for a Golgi-localised protein in GBF1 recruitment.

5.2 Arf•GDP stimulates GBF1 recruitment to Golgi membranes in order to maintain Arf•GTP homeostasis by a currently unknown mechanism

This thesis reports both *in vivo* and *in vitro* data that support our model for Arf•GDP-stimulated GBF1 recruitment to Golgi membranes. We have determined that in order for Arf•GDP to promote GBF1 recruitment it must associate with membranes, specifically those of the *cis*-Golgi and ERGIC, based on results obtained with the soluble G2A Arf mutation (Figure 3.15) and TGN-restricted Arf1-6-1 chimera (Figure 4.3), respectively. Additionally, examination of the effect of overexpressing wild-type or catalytically inactive forms of Golgi-localised ArfGAPs demonstrates that the source of the Arf•GDP may matter. Expression of active and inactive ArfGAP1 had opposite effects on GBF1 recruitment (Figure 3.2; Figure 4.1), whereas expression of wt and mutant ArfGAP2 and ArfGAP3 had no significant effect on GBF1 (Figure 4.1). One possible explanation for these observations is that ArfGAP3 failed to have a significant impact on GBF1 recruitment because it localises predominantly to the TGN (Shiba et al., 2013).

One potential hypothesis based on these data is that Arf•GDP associates with GBF1 in the cytoplasm leading to co-recruitment of both proteins to target membranes, presumably through interactions with Arf•GDP receptors and/or membrane association of the N-terminal myristate. This model is largely based on

the assumption that the GDP-arrested Arf T31N mutant stably binds GBF1 non-productively, and may cause GBF1 recruitment due to the formation of these complexes. This appears improbable for several reasons. First, Arf•GDP displays low affinity for membranes and therefore would be a poor candidate to translocate GBF1 from the cytosol to membranes. Second, we failed to observe an increase in capacity to recruit GBF1 to Golgi membranes in the presence of over-expressed membrin (Figure 3.4 and Figure 3.5), a proposed Arf1•GDP receptor. More importantly, we demonstrated that Arf activation not only continues in cells expressing GDP-arrested Arf1 (Figure 3.12), but also supports both Golgi morphology (Figure 3.6) and COPI coat recruitment (Figure 3.8). These results indicate that, in the presence of GDP-arrested Arf, GBF1 is recruited and accumulates on target membranes in a manner that supports Arf activation. This is not consistent with the notion that GBF1 binds GDP-arrested Arf in a stable non-productive complex. Instead, we hypothesize that a putative *cis*-Golgi localised GBF1 receptor is Arf•GDP-sensitive and becomes "activated" when Arf•GDP levels rise to promote GBF1 recruitment (Figure 4.13). The nature of this "activation" remains unclear.

The molecular mechanisms that mediate the "activation" of the GBF1 receptor at *cis*-Golgi membranes remain elusive. The simplest scenario one could propose would be that Arf•GDP directly regulates a Golgi-localised, proteinaceous GBF1 receptor to promote GBF1 recruitment by inducing a conformational change. The requirement for a Golgi-localised protein, potentially the GBF1 receptor(s), was confirmed *in vitro* (Figure 4.8 and 4.9). These data led to a proposed model for Arf•GDP-dependent recruitment of GBF1 to Golgi and ERGIC membranes (Figure

4.13). This putative GBF1 receptor could be comprised of multiple proteins, including both transmembrane and peripheral *cis*-Golgi proteins.

Understanding the mechanism of GBF1 recruitment will be a critical step in the identification and characterization of the putative GBF1 receptor(s). We suspect that altering the cellular conditions to high Arf•GDP will promote interaction of GBF1 with its membrane receptor. A putative receptor is likely to undergo a post-translational modification and/or conformation change in the presence of Arf•GDP. The simplest hypothesis would be for Arf•GDP to associate directly with a putative receptor and elicit a conformational change that would confer an increase in affinity for GBF1. However, GBF1 recruitment could result from integration of multiple signals from a variety of proteins and/or lipids. Such a mode involving multiple signals, also called "coincidence detection" (Wright et al., 2014), would likely require a protein receptor with unique localisation to ensure specific recruitment to the membranes of the *cis*-Golgi and ERGIC. This mechanism may be supported by the fact that GBF1 is such a large protein with many conserved domains, most of which do not have defined functions. Moreover, coincidence detection mechanisms have been proposed for other ArfGEFs, which is further discussed in section 5.4.

Remaining open to various alternate models will ensure we do not bias our search in a manner that would result in missing an important discovery. Another possibility consistent with the kinetics, temperature and protease sensitivity is that Arf•GDP positively regulates an enzyme at the *cis*-Golgi that then promotes GBF1 recruitment to *cis*-Golgi membranes. Multiple enzymatic processes could potentially play a regulatory role in GBF1 recruitment including, but not limited to,

phosphorylation. For example, Arf•GDP could regulate an enzyme(s) that post-translationally modifies a putative GBF1 receptor, altering its affinity for GBF1. Lastly, our data suggesting the requirement of a Golgi-localised protein for GBF1 recruitment (Figure 4.8 and 4.9) do not preclude the possibility that lipid remodeling could play a critical role. Specifically, it remains possible that Arf•GDP could promote activity of a lipid-modifying enzyme that would facilitate GBF1 recruitment by altering the lipid environment and activity of the "receptor". Ultimately, questions regarding the specifics of GBF1 recruitment will remain until we identify the *cis*-Golgi-localised proteins required for GBF1 recruitment.

5.3 GBF1 recruitment and function at non-classical subcellular localisations

In addition to the classical role of GBF1 in Arf activation at the ERGIC and Golgi, multiple alternate localisations and related functions have been proposed. Specifically, GBF1 has been implicated in GPI-APs enriched early endosomal compartment (GEEC) endocytosis at the plasma membrane and in lipid droplet homeostasis (Bouvet et al., 2013; Gupta et al., 2009). The mechanism that governs GBF1 recruitment and localisation at these subcellular compartments remains unclear. Interestingly, the role in GEEC type endocytosis has been proposed to be BFA resistant. Since BFA only requires interaction of GBF1 with Arf to create the BFA binding pocket, the notion of BFA resistant functions involving Arf1 remains unlikely. Moreover, under conditions where Arf•GDP levels are increased, either pharmacologically or by expression of a GDP-arrested Arf mutant, we never observed increased localisation of GBF1 to the plasma membrane (Figure 3.1 and

Figure 3.13). These observations suggest that any potential GBF1 localisation to the plasma membrane is not regulated by Arf•GDP level.

While multiple reports link GBF1 activity to the regulation and homeostasis of lipid droplets (Ellong et al., 2011; Guo et al., 2008), evidence suggesting GBF1 localisation to lipid droplets is not as convincing (Bartz et al., 2007b; Bouvet et al., 2013). Bouvet and colleagues reported that expression of a GBF1 truncation containing only the HDS1 domain localised to lipid droplets, however this was not demonstrated for the full-length protein. One possible explanation of alternate GBF1 localisations and functions is the presence of mRNAs that suggest splice variation in GBF1 transcripts (Claude et al., 1999; Claude et al., 2003). To date, it remains unclear if any of these variants are translated and if splice variants could support alternate functions for GBF1. Additional study of the potential relevance of splice variation and alternate GBF1 functions is required.

5.4 Potential role for Arf•GDP in recruitment of other ArfGEFs to membranes

The establishment of a novel mechanism for recruitment of GBF1 to Golgi membranes naturally leads to us to question whether this mechanism governs membrane recruitment of other ArfGEFs. Obvious candidates for Arf•GDP-dependent regulation are the BIGs, TGN-localised members of the large ArfGEFs with significant homology to GBF1. Interestingly, published work suggests the mechanism of BIGs recruitment is likely quite dissimilar to that of GBF1. Specifically, work performed on BIG1 and the highly related BIGs homologue in yeast, Sec7p, concluded that Sec7p was recruited to Golgi membranes through interactions with

the GTP-bound form of both Arf1 and Arl1 (Richardson and Fromme, 2012) (Galindo et al., 2016). Interestingly, in the case of regulation of Sec7p, Arf1•GTP alleviates an autoinhibitory conformation mediated by the HDS1 domain, like that observed for ARNO (Stalder et al., 2011). This is in sharp contrast to the Arf•GDP-stimulated recruitment of GBF1 to ERGIC and *cis*-Golgi membranes. In addition, imaging experiments suggest that a larger proportion of BIGs proteins reside on membranes than observed for GBF1 (Manolea et al., 2008). This observed difference predict that BIGs recruitment to membranes of the TGN should be less reactive to Arf•GDP level and regulated in a different manner than GBF1.

It remains interesting that Arf1•GTP, the product of enzymatic activity, recruits both Sec7p and ARNO. These proposed mechanisms would result in run-away ArfGEF activity due to Arf1•GTP stimulating a massive feed-forward recruitment further stimulated by enzymatic activity. These predictions fit with the observation that BIGs display high affinity for TGN membranes and do not have a significant cytosolic pool. In contrast, under conditions in which Arf1•GTP levels have been eliminated, such as during BFA treatment, the TGN and endosomal system would irreversibly fail. However, BFA can be washed out and the Arf activation system efficiently recovers at the Golgi and TGN, suggesting Arf1 activation may occur due to the activity of an alternate ArfGEF that thereby supports BIGs activity.

It is important to note that the models of Sec7 and ARNO recruitment are consistent with a mechanism in which GBF1 plays an essential, not only in the maintenance of ERGIC and Golgi compartments, but also potentially the TGN. Specifically, maintenance of Arf•GTP homeostasis in the Golgi stack by GBF1 would

ensure proper recruitment and activity of BIGs at the TGN. In other words, we hypothesize that, stimulation of GBF1 recruitment by Arf•GDP, would lead to Arf activation and ultimately stimulation of BIGs activity. This hypothesis fits recently published data suggesting that GBF1 activity is required for BIGs function at the TGN. However, our interpretation of these results are not in agreement with the interpretation published by the authors, specifically that GBF1 is present at the TGN (Lowery et al., 2013). This study relied extensively on the GBF1-specific inhibitor GCA which has no impact on the TGN, but causes TGN fragmentation and dispersal following prolonged treatment (Saenz et al., 2009) (Figure 3.13). In contrast, short treatment with GCA has no impact on the TGN. These studies provide further support for this functional link between GBF1 activity and the proper localisation and function of BIGs. I propose that GBF1 recruited to ERGIC and *cis*-Golgi membranes could reestablish Arf•GTP levels and therefore provide the required Arf1•GTP to regenerate the TGN through BIGs recruitment. This hypothesis is further supported by the reversibility of BFA inhibition of GBF1 and BIGs. This would implicate GBF1 in playing a critical role in not only the maintenance of the ERGIC and *cis*-Golgi as previously suggested, but also potentially the maintenance of the entire endosomal system by providing Arf1•GTP critical for recruitment of ArfGEFs of the late secretory pathway.

5.5 ArfGAP1 displays an unique ability to stimulate GBF1 recruitment, relative to ArfGAP2/3

The ability for ArfGAP1 to promote GBF1 recruitment, through increased Arf•GDP production (Cukierman et al., 1995), suggested a specific role for ArfGAP1

in the production of regulatory Arf•GDP. Testing of the other Golgi-localised ArfGAPs suggested that ArfGAP2 and 3 had no significant effect on GBF1 recruitment in several independent experiments (Figure 4.1). As mentioned above in section 5.1, our results for ArfGAP3 could easily be explained by the published observation that ArfGAP3 localises preferentially to the TGN (Shiba et al., 2013), not the *cis*-Golgi stack where regulated recruitment of GBF1 takes place. ArfGAP2 localisation studies suggest significant overlap with both the *cis*-Golgi stack and TGN, leaving it unclear as to why ArfGAP2 expression has a reduced effect on GBF1 recruitment to the Golgi, relative to ArfGAP1. One hypothesis for the role of ArfGAP1 in GBF1 recruitment is that ArfGAP1 functions in facilitating GTP hydrolysis that results in micro-domains of high Arf•GDP, sufficient to stimulate GBF1 recruitment. Alternatively, ArfGAP1 may produce Arf•GDP in a manner that allows for efficient binding to regulatory factors found at the Golgi membrane, due to proximity.

With respect to ArfGAP2/3, the proposed specialized function in the production of COPI vesicles may preclude these proteins from functioning as significant producers of regulatory Arf•GDP (Cukierman et al., 1995), although this link to vesicle production has also been made for ArfGAP1. Redundancy within the ArfGAPs is further supported by the fact that single and double knock down of ArfGAPs 1, 2 or 3 does not result in Golgi collapse, which is observed in a triple knock down (Frigerio et al., 2007; Saitoh et al., 2009). Although more recent knock down studies point to ArfGAP2 and 3 having functional redundancy in coat assembly, this was not observed for ArfGAP1 (Kartberg et al., 2010). Importantly, it appears that ArfGAP2/3 requires interaction with COPI coat proteins for Golgi

recruitment (Frigerio et al., 2007; Kliouchnikov et al., 2009). These results suggest that even under conditions of over-expression, the amount of Golgi-localised ArfGAP2/3 may be limited by COPI binding. Conversely, ArfGAP1 can interact directly with Golgi membranes via paired ALPS domains, potentially resulting in a greater amount of GAP activity at the Golgi. Of the models for ArfGAP function at the Golgi, our data support ArfGAP1 having non-overlapping functions with ArfGAP2/3. This hypothesis could be further queried by looking at the effects of expression of the Golgi-localised ArfGAPs on trafficking. Specifically, replicating assays outlined in Yang et al. (Yang et al., 2011a) would allow the use of VSV-G and VSV-G-KDEL to assess any enhancement or inhibition of trafficking in the presence of over-expressed wild-type and inactive RQ mutant versions of ArfGAP1, 2, and 3.

ArfGAP1 can produce significant levels of regulatory Arf•GDP capable of triggering GBF1 recruitment to *cis*-Golgi membranes. The critical evidence for this conclusion arises from the observation that the catalytically inactive R50Q point mutant form elicited a dominant negative response resulting in a significant decrease in the amount of GBF1 at *cis*-Golgi membranes. We propose that this reduction in Golgi-localised GBF1 was due to impaired activity of endogenous ArfGAP1 on Arf proteins, resulting in lower Arf•GDP levels. This would explain why inactive forms of ArfGAP1 had no effect on Golgi morphology and function (Liu et al., 2005). We surmise that the dominant-negative ArfGAP1 R50Q phenotype was masked by the reduction of GBF1 recruited to *cis*-Golgi membranes, and therefore a reduction in Arf activation. Our model of GBF1 recruitment predicts that GBF1 can modulate its recruitment to Golgi membranes in response to either increases or

decreases in Arf•GDP, maintaining homeostatic levels of Arf•GTP and thereby maintaining Golgi morphology and function. In other words, the dominant negative effect of expressing a catalytically inactive Arf-GTP binding ArfGAP1 mutant is significant reduction of GBF1 recruitment to Golgi membranes, due to a decreased Arf•GDP-dependent activation of putative GBF1 receptors. These results suggest GBF1 may serve as a master regulator of the homeostasis, maintenance, and establishment of the secretory pathway.

5.6 Incorporating the Arf•GDP-stimulated recruitment of GBF1 with current BFA paradigm

Initially, our interest in understanding GBF1 recruitment to Golgi membranes began as an effort to further understand the mechanism of BFA action in live cells. Work done by Dr. Justin Chun suggested that a stable "abortive" complex, which was well characterized *in vitro*, was elusive *in vivo* (Chun et al., 2008). It was suggested that the observed loss of Golgi-localised Arf as GBF1 recruitment to *cis*-Golgi membranes was occurring provided evidence for a lack of abortive stable complex formation *in vivo* (Chun et al., 2008). The authors proposed that GBF1 was recruited to Golgi membranes in the presence of BFA due to rapid reduction in Arf•GTP levels. The results presented in this thesis demonstrate that increasing cellular Arf•GDP levels, as opposed to decreasing Arf•GTP, stimulates GBF1 recruitment. This likely represents physiological regulation of GBF1 that allows maintenance of a homeostatic level of Arf activation.

Here we attempt to propose a parsimonious model for BFA action *in vivo*, which takes all the published data into account. In the presence of BFA, GBF1

proteins at the Golgi could form a complex with BFA and Arf•GDP. This complex will prevent Arf activation and therefore result in Arf•GDP levels quickly rising within the cell. Arf•GDP would then stimulate further GBF1 recruitment to Golgi membranes, likely by activating a putative GBF1 receptor and BFA would likely inhibit the recruited GBF1. This inhibitory cascade results in rapid, accumulation of GBF1 in a non-productive manner and subsequent Golgi collapse. The stability of the putative GBF1•BFA•Arf•GDP remains difficult to assess; whereas it can be crystallized, the effects of BFA are reversible *in vivo* and several researchers have failed to purify the proposed non-productive complex. To address the observed decrease of Golgi-localised Arf following BFA addition, we propose that only a small proportion of the total Arf in the cell is required to efficiently complex with GBF1 in the presence of BFA. Specifically, as Arf•GTP levels decreased following BFA addition, resulting in a significant reduction in Golgi-localised Arf, the small pool of remaining Arf•GDP is sufficient for BFA-induced impairment of GBF1 activity. While the acquisition parameters made it difficult to observe this remaining pool of Arf•GDP, we have imaged this pool in experiments presented here (Figure 3.11B). Moreover, we've also displayed data indicating that the "GDP-arrested" form of Arf also displays Golgi-localisation (Figure 3.11A).

5.7 Identification of GBF1 interacting partners and potential receptor proteins

To date, immunopurification approaches failed to identify GBF1 interacting partners, such as a putative GBF1 receptor. However, work in progress has identified a potential GBF1 interacting partner(s) by far western blots (Figure 4.10). To

identify interacting partners from the list of potential candidates (Table 4.1), we plan to perform additional far westerns. Specifically, for each candidate receptor we will generate recombinant protein that would allow us to perform a far western and probe membranes containing GBF1 to identify any candidates that bind the GBF1 band, which would serve as a first screen for true GBF1 interaction. As an alternate approach, we can perform a functional assay in which a putative GBF1 receptor is knocked-down by shRNA and GBF1 recruitment could be assayed *in vivo* pharmacologically by addition of GCA or BFA.

Performing a complementary experiment to identify novel GBF1 interacting partners will allow us to complete a comparative analysis of both lists of candidates and potentially narrow down to a small list of probable receptors. To this end, we propose to utilize the recently developed BioID technique (Roux et al., 2012) to identify proteins in close proximity to GBF1 and potentially the elusive *cis*-Golgi GBF1 receptor. BioID relies on a BirA biotin ligase bearing a point mutation that renders it incapable of specificity (Kim and Roux, 2016). Specifically, the point mutant form (BirA*) is incapable of holding activated biotin for specific labeling, and rather releases activated biotin (biotin-AMP) to generate a soluble cloud of biotin-AMP. When the BirA* is appended to a protein of interest it can create a cloud of biotin around the chimera, labeling the nearest neighboring proteins, allowing for immuno-isolation with streptavidin beads. Resulting products can then be identified by mass spectrometry analysis providing us with a list of candidates that could be used to test for potential receptors. This list of candidates could be cross-referenced against our table of potential candidates from the far western experiment discussed

above to narrow down our candidates to be tested functionally in *in vivo* and *in vitro* GBF1 recruitment assays.

Since a complex mechanism of Arf•GDP regulated GBF1 recruitment remains possible, we suggest that direct study of the role of Arf•GDP will allow us an alternate approach to identify the GBF1 receptor. Our data support the hypothesis that *cis*-Golgi membrane association is required for Arf•GDP to stimulate GBF1 recruitment (Figures 3.15 and 4.3), suggesting it must interact with a Golgi-resident protein. The requirement for such a protein was confirmed by demonstrating that pre-treatment of Golgi membranes with denaturing heat or trypsin significantly abrogated GBF1 recruitment *in vitro* (Figures 4.8 and 4.9). Arf•GDP directly regulating the GBF1 receptor to promote recruitment remains the simplest explanation. To begin characterization of potential interacting partners of Arf•GDP, or proteins in close proximity to Arf•GDP, we can utilize the BioID technique described above. While we suggest this unknown Golgi-resident protein may be the putative GBF1 receptor, alternate possibilities remain possible. Performing BioID requires tagging of wild-type Arf would be paired with pharmacological inhibition of Arf activation, ensuring the BioID-Arf chimera is GDP-bound. Similarly, we could tag T31N mutant forms of Arf and determine which proteins are in close proximity to Arf•GDP in the cell. To ensure we are looking at Golgi localised proteins, assays would be performed and followed by enrichment of Golgi to remove cytosolic proteins. Proteins required for GBF1 recruitment could be screened by performing *in vivo* GBF1 recruitment assays, as proteins of interest should confer decreased GBF1 recruitment when knocked down, as described above. The results of the

proteomics on the biotinylated proteins would provide a candidate list of Arf•GDP interacting partners, one of which could be the putative GBF1 receptor. However, it remains possible that Arf•GDP-stimulated GBF1 recruitment involves a multi-protein complex and that the methods described above may identify critical regulators of GBF1 recruitment that do not directly bind GBF1.

5.8 Concluding remarks

The work described here identified a novel mechanism of GBF1 recruitment regulation, and for the first time attributed a role for Arf•GDP in the cell. This novel activity of Arf•GDP is dependent on localisation to membranes of the *cis*-Golgi. In addition, this work has yielded novel insights into how BFA potentially acts *in vivo*. Expression of ArfGAP1 stimulated significant GBF1 recruitment, likely through Arf•GDP production, suggesting a specialized function at the Golgi. This work also provides us with tools that should lead to the identification of the putative GBF1 receptor. The recruitment of GBF1, as proposed for other GEFs (Richardson et al., 2012), could respond simultaneously to several stimuli such as phosphoinositide level, rab1 (Alvarez et al., 2003) and receptor abundance/modification. Preliminary efforts at GBF1 receptor identification have yielded a list from which candidates can be tested for viability as a putative receptor. Ongoing work towards identification of a receptor will greatly add to our understanding of GBF1 function and could potentially lead to discovery of therapeutics for the treatment of diseases resulting for GBF1 dysfunction and those caused by viruses that manipulate GBF1 function and localisation to ensure successful replication.

Chapter 6: References

Acharya, U., A. Mallabiabarrena, J.K. Acharya, and V. Malhotra. 1998. Signaling via mitogen-activated protein kinase kinase (MEK1) is required for Golgi fragmentation during mitosis. *Cell*. 92:183-192.

Allan, B.B., B.D. Moyer, and W.E. Balch. 2000. Rab1 recruitment of p115 into a cis-SNARE complex: programming budding COPII vesicles for fusion. *Science*. 289:444-448.

Alvarez, C., H. Fujita, A. Hubbard, and E. Sztul. 1999. ER to Golgi transport: Requirement for p115 at a pre-Golgi VTC stage. *J Cell Biol*. 147:1205-1222.

Alvarez, C., R. Garcia-Mata, E. Brandon, and E. Sztul. 2003. COPI Recruitment Is Modulated by a Rab1b-dependent Mechanism. *Mol Biol Cell*. 14:2116-2127.

Ambroggio, E., B. Sorre, P. Bassereau, B. Goud, J.B. Manneville, and B. Antonny. 2010. ArfGAP1 generates an Arf1 gradient on continuous lipid membranes displaying flat and curved regions. *EMBO J*. 29:292-303.

Anders, N., M. Nielsen, J. Keicher, Y.D. Stierhof, M. Furutani, M. Tasaka, K. Skriver, and G. Jurgens. 2008. Membrane association of the Arabidopsis ARF exchange factor GNOM involves interaction of conserved domains. *Plant Cell*. 20:142-151.

Antonny, B., S. Beraud-Dufour, P. Chardin, and M. Chabre. 1997. N-terminal hydrophobic residues of the G-protein ADP-ribosylation factor-1 insert into membrane phospholipids upon GDP to GTP exchange. *Biochemistry*. 36:4675-4684.

Aoe, T., E. Cukierman, A. Lee, D. Cassel, P.J. Peters, and V.W. Hsu. 1997. The KDEL receptor, ERD2, regulates intracellular traffic by recruiting a GTPase-activating protein for ARF1. *EMBO J*. 16:7305-7316.

Aoe, T., I. Huber, C. Vasudevan, S.C. Watkins, G. Romero, D. Cassel, and V.W. Hsu. 1999. The KDEL receptor regulates a GTPase-activating protein for ADP-ribosylation factor 1 by interacting with its non-catalytic domain. *Journal of Biological Chemistry*. 274:20545-20549.

Appenzeller-Herzog, C., and H.P. Hauri. 2006. The ER-Golgi intermediate compartment (ERGIC): in search of its identity and function. *J Cell Sci*. 119:2173-2183.

Arakel, E.C., K.P. Richter, A. Clancy, and B. Schwappach. 2016. delta-COP contains a helix C-terminal to its longin domain key to COPI dynamics and function. *Proceedings of the National Academy of Sciences of the United States of America*. 113:6916-6921.

Balch, W.E. 2004. Vesicle traffic in vitro. *Cell*. 116:S17-19, 12 p following S19.

Balsinde, J., M.V. Winstead, and E.A. Dennis. 2002. Phospholipase A(2) regulation of arachidonic acid mobilization. *FEBS letters*. 531:2-6.

Bankaitis, V.A., R. Garcia-Mata, and C.J. Mousley. 2012. Golgi membrane dynamics and lipid metabolism. *Curr Biol*. 22:R414-424.

Bannykh, S.I., N. Nishimura, and W.E. Balch. 1998. Getting into the Golgi. *Trends Cell Biol*. 8:21-25.

Bartz, R., J. Seemann, J.K. Zehmer, G. Serrero, K.D. Chapman, R.G. Anderson, and P. Liu. 2007a. Evidence that mono-ADP-ribosylation of CtBP1/BARS regulates lipid storage. *Molecular biology of the cell*. 18:3015-3025.

Bartz, R., J.K. Zehmer, M. Zhu, Y. Chen, G. Serrero, Y. Zhao, and P. Liu. 2007b. Dynamic activity of lipid droplets: protein phosphorylation and GTP-mediated protein translocation. *Journal of proteome research*. 6:3256-3265.

Bechler, M.E., P. de Figueiredo, and W.J. Brown. 2011. A PLA1-2 punch regulates the Golgi complex. *Trends in cell biology*. 22:116-124.

Bechler, M.E., A.M. Doody, E. Racoosin, L. Lin, K.H. Lee, and W.J. Brown. 2010. The phospholipase complex PAFAH Ib regulates the functional organization of the Golgi complex. *The Journal of cell biology*. 190:45-53.

Beck, R., F. Adolf, C. Weimer, B. Bruegger, and F.T. Wieland. 2009. ArfGAP1 Activity and COPI Vesicle Biogenesis. *Traffic*. 10:307-315.

Beller, M., C. Sztalryd, N. Southall, M. Bell, H. Jackle, D.S. Auld, and B. Oliver. 2008. COPI complex is a regulator of lipid homeostasis. *PLoS biology*. 6:e292.

Ben-Tekaya, H., R.A. Kahn, and H.P. Hauri. 2010. ADP ribosylation factors 1 and 4 and group VIA phospholipase A regulate morphology and intraorganellar traffic in the endoplasmic reticulum-Golgi intermediate compartment. *Molecular biology of the cell*. 21:4130-4140.

Ben-Tekaya, H., K. Miura, R. Pepperkok, and H.P. Hauri. 2005. Live imaging of bidirectional traffic from the ERGIC. *J Cell Sci*. 118:357-367.

Beraud-Dufour, S., S. Robineau, P. Chardin, S. Paris, M. Chabre, J. Cherfils, and B. Antonny. 1998. A glutamic finger in the guanine nucleotide exchange factor ARNO displaces Mg2+ and the beta-phosphate to destabilize GDP on ARF1. *EMBO J*. 17:3651-3659.

Berger, J., J. Hauber, R. Hauber, R. Geiger, and B.R. Cullen. 1988. Secreted placental alkaline phosphatase: a powerful new quantitative indicator of gene expression in eukaryotic cells. *Gene*. 66:1-10.

Bethune, J., M. Kol, J. Hoffmann, I. Reckmann, B. Brugger, and F. Wieland. 2006a. Coatomer, the coat protein of COPI transport vesicles, discriminates endoplasmic reticulum residents from p24 proteins. *Mol Cell Biol*. 26:8011-8021.

Bethune, J., F. Wieland, and J. Moelleken. 2006b. COPI-mediated transport. *J Membr Biol*. 211:65-79.

Bhatt, J.M., E.G. Viktorova, T. Busby, P. Wyrozumska, L.E. Newman, H. Lin, E. Lee, J. Wright, G.A. Belov, R.A. Kahn, and E. Sztul. 2016. Oligomerization of the Sec7 domain Arf guanine nucleotide exchange factor GBF1 is dispensable for Golgi localization and function but regulates degradation. *American journal of physiology. Cell physiology*. 310:C456-469.

Bonfanti, L., A.A. Mironov, Jr., J.A. Martinez-Menarguez, O. Martella, A. Fusella, M. Baldassarre, R. Buccione, H.J. Geuze, A.A. Mironov, and A. Luini. 1998. Procollagen traverses the Golgi stack without leaving the lumen of cisternae: evidence for cisternal maturation [see comments]. *Cell*. 95:993-1003.

Bonifacino, J.S., and B.S. Glick. 2004. The mechanisms of vesicle budding and fusion. *Cell*. 116:153-166.

Bonifacino, J.S., and J. Lippincott-Schwartz. 2003. Coat proteins: shaping membrane transport. *Nat Rev Mol Cell Biol*. 4:409-414.

Bouvet, S., M.P. Golinelli-Cohen, V. Contremoulins, and C.L. Jackson. 2013. Targeting of the Arf-GEF GBF1 to lipid droplets and Golgi membranes. *Journal of cell science*. 126:4794-4805.

Bremser, M., W. Nickel, M. Schweikert, M. Ravazzola, M. Amherdt, C.A. Hughes, T.H. Sollner, J.E. Rothman, and F.T. Wieland. 1999. Coupling of coat assembly and vesicle budding to packaging of putative cargo receptors. *Cell*. 96:495-506.

Brown, H.A., S. Gutowsk, C.R. Moomaw, C. Slaughter, and P.C. Sternweis. 1993. ADP-ribosylation factor, a small GTP-dependent regulatory protein, stimulates phospholipase D activity. *Cell*. 75:1137-1144.

Brown, W.J., K. Chambers, and A. Doody. 2003. Phospholipase A2 (PLA2) enzymes in membrane trafficking: mediators of membrane shape and function. *Traffic (Copenhagen, Denmark)*. 4:214-221.

Burke, J.E., and E.A. Dennis. 2009. Phospholipase A2 structure/function, mechanism, and signaling. *Journal of lipid research*. 50 Suppl:S237-242.

Casanova, J.E. 2007. Regulation of Arf activation: the Sec7 family of guanine nucleotide exchange factors. *Traffic*. 8:1476-1485.

Cherfils, J., and P. Melançon. 2005. On the action of Brefeldin A on Sec7-stimulated membrane-recruitment and GDP/GTP exchange of Arf proteins. *Biochem Soc Trans*. 33:635-638.

Cherfils, J., J. Menetrey, M. Mathieu, G. Le Bras, S. Robineau, S. Beraud-Dufour, B. Antonny, and P. Chardin. 1998. Structure of the Sec7 domain of the Arf exchange factor ARNO. *Nature*. 392:101-105.

Chun, J., Z. Shapovalova, S.Y. Dejgaard, J.F. Presley, and P. Melancon. 2008. Characterization of Class I and II ADP-Ribosylation Factors (Arfs) in Live Cells: GDP-bound Class II Arfs Associate with the ER-Golgi Intermediate Compartment Independently of GBF1. *Mol Biol Cell*. 19:3488-3500.

Citterio, C., A. Vichi, G. Pacheco-Rodriguez, A.M. Aponte, J. Moss, and M. Vaughan. 2008. Unfolded protein response and cell death after depletion of brefeldin A-inhibited guanine nucleotide-exchange protein GBF1. *Proc Natl Acad Sci U S A*. 105:2877-2882.

Claude, A., B.P. Zhao, C.E. Kuziemsky, S. Dahan, S.J. Berger, J.P. Yan, A.D. Armold, E.M. Sullivan, and P. Melançon. 1999. GBF1: A novel Golgi-associated BFA-resistant guanine nucleotide exchange factor that displays specificity for ADP-ribosylation factor 5. *J Cell Biol*. 146:71-84.

Claude, A., B.P. Zhao, and P. Melançon. 2003. Characterization of alternatively spliced and truncated forms of the Arf guanine nucleotide exchange factor GBF1 defines regions important for activity. *Biochem Biophys Res Commun*. 303:160-169.

Cohen, L.A., A. Honda, P. Varnai, F.D. Brown, T. Balla, and J.G. Donaldson. 2007. Active Arf6 recruits ARNO/cytohesin GEFs to the PM by binding their PH domains. *Mol Biol Cell*. 18:2244-2253.

Cosson, P., and F. Letourneur. 1994. Coatomer interaction with di-lysine endoplasmic reticulum retention motifs. *Science*. 263:1629-1631.

Cox, R., R.J. Mason-Gamer, C.L. Jackson, and N. Segev. 2004. Phylogenetic analysis of Sec7-domain-containing Arf nucleotide exchangers. *Mol Biol Cell*. 15:1487-1505.

Cukierman, E., I. Huber, M. Rotman, and D. Cassel. 1995. The ARF1 GTPase-activating protein: zinc finger motif and Golgi complex localization. *Science*. 270:1999-2002.

D'Angelo, G., M. Vicinanza, A. Di Campli, and M.A. De Matteis. 2008. The multiple roles of PtdIns(4)P -- not just the precursor of PtdIns(4,5)P2. *J Cell Sci*. 121:1955-1963.

D'Souza-Schorey, C., and P. Chavrier. 2006. ARF proteins: roles in membrane traffic and beyond. *Nat Rev Mol Cell Biol*. 7:347-358.

Dancourt, J., H. Zheng, F. Bottanelli, E.S. Allgeyer, J. Bewersdorf, M. Graham, X. Liu, J.E. Rothman, and G. Lavieu. 2016. Small cargoes pass through synthetically glued Golgi stacks. *FEBS Lett*. 590:1675-1686.

Dascher, C., and W.E. Balch. 1994. Dominant inhibitory mutants of ARF1 block endoplasmic reticulum to Golgi transport and trigger disassembly of the Golgi apparatus. *J Biol Chem*. 269:1437-1448.

De Matteis, M.A., A. Di Campli, and A. Godi. 2005. The role of the phosphoinositides at the Golgi complex. *Biochim Biophys Acta*. 1744:396-405.

De Matteis, M.A., and A. Godi. 2004. Protein-lipid interactions in membrane trafficking at the Golgi complex. *Biochim Biophys Acta*. 1666:264-274.

De Matteis, M.A., and A. Luini. 2008. Exiting the Golgi complex. *Nat Rev Mol Cell Biol*. 9:273-284.

Dejgaard, S.Y., A. Murshid, K.M. Dee, and J.F. Presley. 2007. Confocal microscopy-based linescan methodologies for intra-Golgi localization of proteins. *J Histochem Cytochem*. 55:709-719.

Dominguez, M., A. Fazel, S. Dahan, J. Lovell, L. Hermo, A. Claude, P. Melançon, and J.J. Bergeron. 1999. Fusogenic domains of golgi membranes are sequestered into specialized regions of the stack that can be released by mechanical fragmentation. *J Cell Biol*. 145:673-688.

Doms, R.W., G. Russ, and J.W. Yewdell. 1989. Brefeldin A redistributes resident and itinerant Golgi proteins to the endoplasmic reticulum. *J Cell Biol*. 109:61-72.

Donaldson, J.G., D. Finazzi, and R.D. Klausner. 1992. Brefeldin A inhibits Golgi membrane-catalysed exchange of guanine nucleotide onto ARF protein. *Nature*. 360:350-352.

Donaldson, J.G., A. Honda, and R. Weigert. 2005. Multiple activities for Arf1 at the Golgi complex. *Biochim Biophys Acta*. 1744:364-373.

Donaldson, J.G., and C.L. Jackson. 2011. ARF family G proteins and their regulators: roles in membrane transport, development and disease. *Nature reviews. Molecular cell biology*. 12:362-375.

Donohoe, B.S., S. Mogelsvang, and L.A. Staehelin. 2006. Electron tomography of ER, Golgi and related membrane systems. *Methods*. 39:154-162.

Duden, R. 2003. ER-to-Golgi transport: COP I and COP II function (Review). *Mol Membr Biol*. 20:197-207.

Dumaresq-Doiron, K., M.F. Savard, S. Akam, S. Costantino, and S. Lefrancois. 2010. The phosphatidylinositol 4-kinase PI4KIIIalpha is required for the recruitment of GBF1 to Golgi membranes. *J Cell Sci*. 123:2273-2280.

East, M.P., and R.A. Kahn. 2011. Models for the functions of Arf GAPs. *Seminars in cell & developmental biology*. 22:3-9.

Ellong, E.N., K.G. Soni, Q.T. Bui, R. Sougrat, M.P. Golinelli-Cohen, and C.L. Jackson. 2011. Interaction between the triglyceride lipase ATGL and the Arf1 activator GBF1. *PloS one*. 6:e21889.

Elsner, M., H. Hashimoto, J.C. Simpson, D. Cassel, T. Nilsson, and M. Weiss. 2003. Spatiotemporal dynamics of the COPI vesicle machinery. *EMBO Rep*. 4:1000-1004.

Emr, S., B.S. Glick, A.D. Linstedt, J. Lippincott-Schwartz, A. Luini, V. Malhotra, B.J. Marsh, A. Nakano, S.R. Pfeffer, C. Rabouille, J.E. Rothman, G. Warren, and F.T. Wieland. 2009. Journeys through the Golgi--taking stock in a new era. *J Cell Biol*. 187:449-453.

Eugster, A., G. Frigerio, M. Dale, and R. Duden. 2000. COP I domains required for coatomer integrity, and novel interactions with ARF and ARF-GAP. *EMBO J*. 19:3905-3917.

Fan, J.Y., J. Roth, and C. Zuber. 2003. Ultrastructural analysis of transitional endoplasmic reticulum and pre-Golgi intermediates: a highway for cars and trucks. *Histochem Cell Biol*. 120:455-463.

Farquhar, M.G., and G.E. Palade. 1998. The Golgi apparatus: 100 years of progress and controversy. *Trends Cell Biol*. 8:2-10.

Feng, Y., S. Yu, T.K. Lasell, A.P. Jadhav, E. Macia, P. Chardin, P. Melançon, M. Roth, T. Mitchison, and T. Kirchhausen. 2003. Exo1: a new chemical inhibitor of the exocytic pathway. *Proc Natl Acad Sci U S A*. 100:6469-6474.

Franco, M., P. Chardin, M. Chabre, and S. Paris. 1993. Myristoylation is not required for GTP-dependent binding of ADP-ribosylation factor ARF1 to phospholipids. *Journal of Biological Chemistry*. 268:24531-24534.

Franco, M., P. Chardin, M. Chabre, and S. Paris. 1996. Myristoylation-facilitated binding of the G protein ARF1GDP to membrane phospholipids is required for its activation by a soluble nucleotide exchange factor. *J Biol Chem*. 271:1573-1578.

Frigerio, G., N. Grimsey, M. Dale, I. Majoul, and R. Duden. 2007. Two human ARFGAPs associated with COP-I-coated vesicles. *Traffic*. 8:1644-1655.

Fujiwara, T., K. Oda, S. Yokota, A. Takatsuki, and Y. Ikehara. 1988. Brefeldin A causes disassembly of the Golgi complex and accumulation of secretory proteins in the endoplasmic reticulum. *J Biol Chem*. 263:18545-18552.

Galindo, A., N. Soler, S.H. McLaughlin, M. Yu, R.L. Williams, and S. Munro. 2016. Structural Insights into Arl1-Mediated Targeting of the Arf-GEF BIG1 to the trans-Golgi. *Cell Rep*. 16:839-850.

Gallop, J.L., C.C. Jao, H.M. Kent, P.J. Butler, P.R. Evans, R. Langen, and H.T. McMahon. 2006. Mechanism of endophilin N-BAR domain-mediated membrane curvature. *EMBO J*. 25:2898-2910.

Gannon, J., J. Fernandez-Rodriguez, H. Alamri, S.B. Feng, F. Kalantari, S. Negi, A.H. Wong, A. Mazur, L. Asp, A. Fazel, A. Salman, A. Lazaris, P. Metrakos, J.J. Bergeron, and T. Nilsson. 2014. ARFGAP1 is dynamically associated with lipid droplets in hepatocytes. *PloS one*. 9:e111309.

Garcia-Mata, R., and E. Sztul. 2003. The membrane-tethering protein p115 interacts with GBF1, an ARF guanine-nucleotide-exchange factor. *EMBO Rep*. 4:320-325.

Garcia-Mata, R., T. Szul, C. Alvarez, and E. Sztul. 2003. ADP-ribosylation factor/COPI-dependent events at the endoplasmic reticulum-Golgi interface are regulated by the guanine nucleotide exchange factor GBF1. *Mol Biol Cell*. 14:2250-2261.

Gilchrist, A., C.E. Au, J. Hiding, A.W. Bell, J. Fernandez-Rodriguez, S. Lesimple, H. Nagaya, L. Roy, S.J. Gosline, M. Hallett, J. Paiement, R.E. Kearney, T. Nilsson, and J.J. Bergeron. 2006. Quantitative proteomics analysis of the secretory pathway. *Cell*. 127:1265-1281.

Gillingham, A.K., and S. Munro. 2007. The small G proteins of the Arf family and their regulators. *Annual review of cell and developmental biology*. 23:579-611.

Glick, B.S., T. Elston, and G. Oster. 1997. A cisternal maturation mechanism can explain the asymmetry of the Golgi stack. *FEBS Lett*. 414:177-181.

Glick, B.S., and A. Nakano. 2009. Membrane Traffic within the Golgi Stack. *Annu Rev Cell Dev Biol*. 25:113-132.

Godi, A., A. Di Campli, A. Konstantakopoulos, G. Di Tullio, D.R. Alessi, G.S. Kular, T. Daniele, P. Marra, J.M. Lucocq, and M.A. De Matteis. 2004. FAPPs control Golgi-to-cell-surface membrane traffic by binding to ARF and PtdIns(4)P. *Nat Cell Biol*. 6:393-404.

Goldberg, J. 1998. Structural basis for activation of ARF GTPase: mechanisms of guanine nucleotide exchange and GTP-myristoyl switching. *Cell*. 95:237-248.

Goldberg, J. 2000. Decoding of sorting signals by coatomer through a GTPase switch in the COPI coat complex. *Cell*. 100:671-679.

Gommel, D.U., A.R. Memon, A. Heiss, F. Lottspeich, J. Pfannstiel, J. Lechner, C. Reinhard, J.B. Helms, W. Nickel, and F.T. Wieland. 2001. Recruitment to Golgi membranes of ADP-ribosylation factor 1 is mediated by the cytoplasmic domain of p23. *EMBO J*. 20:6751-6760.

Grebe, M., J. Gadea, T. Steinmann, M. Kientz, J.U. Rahfeld, K. Salchert, C. Koncz, and G. Jurgens. 2000. A conserved domain of the arabidopsis GNOM protein mediates subunit interaction and cyclophilin 5 binding. *Plant Cell*. 12:343-356.

Gregory, A., S.K. Westaway, I.E. Holm, P.T. Kotzbauer, P. Hogarth, S. Sonek, J.C. Coryell, T.M. Nguyen, N. Nardocci, G. Zorzi, D. Rodriguez, I. Desguerre, E. Bertini, A. Simonati, B. Levinson, C. Dias, C. Barbot, I. Carrilho, M. Santos, I. Malik, J. Gitschier, and S.J. Hayflick. 2008. Neurodegeneration associated with genetic defects in phospholipase A(2). *Neurology*. 71:1402-1409.

Guo, Y., T.C. Walther, M. Rao, N. Stuurman, G. Goshima, K. Terayama, J.S. Wong, R.D. Vale, P. Walter, and R.V. Farese. 2008. Functional genomic screen reveals genes involved in lipid-droplet formation and utilization. *Nature*. 453:657-661.

Gupta, G.D., M.G. Swetha, S. Kumari, R. Lakshminarayan, G. Dey, and S. Mayor. 2009. Analysis of endocytic pathways in Drosophila cells reveals a conserved role for GBF1 in internalization via GEECs. *PloS one*. 4:e6768.

Hara-Kuge, S., O. Kuge, L. Orci, M. Amherdt, M. Ravazzola, F.T. Wieland, and J.E. Rothman. 1994. En bloc incorporation of coatomer subunits during the assembly of COP-coated vesicles. *J Cell Biol*. 124:883-892.

Haun, R.S., S.C. Tsai, R. Adamik, J. Moss, and M. Vaughan. 1993. Effect of myristoylation on GTP-dependent binding of ADP-ribosylation factor to Golgi. *Journal of Biological Chemistry*. 268:7064-7068.

Hauri, H.P., and A. Schweizer. 1992. The endoplasmic reticulum-Golgi intermediate compartment. *Curr Opin Cell Biol*. 4:600-608.

Helms, J.B., and J.E. Rothman. 1992. Inhibition by brefeldin A of a Golgi membrane enzyme that catalyses exchange of guanine nucleotide bound to ARF. *Nature*. 360:352-354.

Hofmann, I., A. Thompson, C.M. Sanderson, and S. Munro. 2007. The Arl4 family of small G proteins can recruit the cytohesin Arf6 exchange factors to the plasma membrane. *Curr Biol*. 17:711-716.

Honda, A., O.S. Al-Awar, J.C. Hay, and J.G. Donaldson. 2005. Targeting of Arf-1 to the early Golgi by membrin, an ER-Golgi SNARE. *J Cell Biol*. 168:1039-1051.

Hong, J.X., F. Lee, W.A. Patton, C.Y. Lin, J. Moss, and M. Vaughan. 1998. Phospholipid- and GTP-dependent activation of cholera toxin and phospholipase D by human ADP-ribosylation factor-like protein 1 (HARL1) [In Process Citation]. *J Biol Chem*. 273:15872-15876.

Hsu, V.W., S.Y. Lee, and J.S. Yang. 2009. The evolving understanding of COPI vesicle formation. *Nature reviews. Molecular cell biology*. 10:360-364.

Huber, I., E. Cukierman, M. Rotman, T. Aoe, V.W. Hsu, and D. Cassel. 1998. Requirement for both the amino-terminal catalytic domain and a noncatalytic domain for in vivo activity of ADP-ribosylation factor GTPase-activating protein. *The Journal of biological chemistry*. 273:24786-24791.

Ishii, M., Y. Suda, K. Kurokawa, and A. Nakano. 2016. COPI is essential for Golgi cisternal maturation and dynamics. *Journal of cell science*. 129:3251-3261.

Ismail, S.A., I.R. Vetter, B. Sot, and A. Wittinghofer. 2010. The structure of an Arf-ArfGAP complex reveals a Ca2+ regulatory mechanism. *Cell*. 141:812-821.

Jackson, C.L., and J.E. Casanova. 2000. Turning on ARF: the Sec7 family of guanine-nucleotide-exchange factors. *Trends Cell Biol*. 10:60-67.

Jackson, L.P. 2014. Structure and mechanism of COPI vesicle biogenesis. *Current opinion in cell biology*. 29:67-73.

Jackson, L.P., M. Lewis, H.M. Kent, M.A. Edeling, P.R. Evans, R. Duden, and D.J. Owen. 2012. Molecular basis for recognition of dilysine trafficking motifs by COPI. *Developmental cell*. 23:1255-1262.

Jackson, S.K., W. Abate, and A.J. Tonks. 2008. Lysophospholipid acyltransferases: novel potential regulators of the inflammatory response and target for new drug discovery. *Pharmacology & therapeutics*. 119:104-114.

Judson, B.L., and W.J. Brown. 2009. Assembly of an intact Golgi complex requires phospholipase A2 (PLA2) activity, membrane tubules, and dynein-mediated microtubule transport. *Biochemical and biophysical research communications*. 389:473-477.

Jurgens, G. 1995. Axis formation in plant embryogenesis: cues and clues. *Cell*. 81:467-470.

Kahn, R.A., E. Bruford, H. Inoue, J.M. Logsdon, Jr., Z. Nie, R.T. Premont, P.A. Randazzo, M. Satake, A.B. Theibert, M.L. Zapp, and D. Cassel. 2008. Consensus

nomenclature for the human ArfGAP domain-containing proteins. *J Cell Biol*. 182:1039-1044.

Kahn, R.A., J. Clark, C. Rulka, T. Stearns, C.J. Zhang, P.A. Randazzo, T. Terui, and M. Cavenagh. 1995. Mutational analysis of Saccharomyces cerevisiae ARF1. *J Biol Chem*. 270:143-150.

Kahn, R.A., and A.G. Gilman. 1986. The protein cofactor necessary for ADP-ribosylation of Gs by cholera toxin is itself a GTP binding protein. *J Biol Chem*. 261:7906-7911.

Kahn, R.A., C. Goddard, and M. Newkirk. 1988. Chemical and immunological characterization of the 21-kDa ADP- ribosylation factor of adenylate cyclase. *J Biol Chem*. 263:8282-8287.

Kahn, R.A., F.G. Kern, J. Clark, E.P. Gelmann, and C. Rulka. 1991. Human ADP-ribosylation factors. A functionally conserved family of GTP-binding proteins. *J Biol Chem*. 266:2606-2614.

Kahn, R.A., P. Randazzo, T. Serafini, O. Weiss, C. Rulka, J. Clark, M. Amherdt, P. Roller, L. Orci, and J.E. Rothman. 1992. The amino terminus of ADP-ribosylation factor (ARF) is a critical determinant of ARF activities and is a potent and specific inhibitor of protein transport. *J Biol Chem*. 267:13039-13046.

Kartberg, F., L. Asp, S.Y. Dejgaard, M. Smedh, J. Fernandez-Rodriguez, T. Nilsson, and J.F. Presley. 2010. ARFGAP2 and ARFGAP3 are essential for COPI coat assembly on the Golgi membrane of living cells. *The Journal of biological chemistry*. 285:36709-36720.

Kawamoto, K., Y. Yoshida, H. Tamaki, S. Torii, C. Shinotsuka, S. Yamashina, and K. Nakayama. 2002. GBF1, a Guanine Nucleotide Exchange Factor for ADP-Ribosylation Factors, is Localized to the cis-Golgi and Involved in Membrane Association of the COPI Coat. *Traffic*. 3:483-495.

Kim, D.I., and K.J. Roux. 2016. Filling the Void: Proximity-Based Labeling of Proteins in Living Cells. *Trends Cell Biol*. 26:804-817.

Kliouchnikov, L., J. Bigay, B. Mesmin, A. Parnis, M. Rawet, N. Goldfeder, B. Antonny, and D. Cassel. 2009. Discrete determinants in ArfGAP2/3 conferring Golgi localization and regulation by the COPI coat. *Mol Biol Cell*. 20:859-869.

Klumperman, J., A. Schweizer, H. Clausen, B.L. Tang, W. Hong, V. Oorschot, and H.P. Hauri. 1998. The recycling pathway of protein ERGIC-53 and dynamics of the ER-Golgi intermediate compartment. *J Cell Sci*. 111:3411-3425.

Kumari, S., and S. Mayor. 2008. ARF1 is directly involved in dynamin-independent endocytosis. *Nature cell biology*. 10:30-41.

Lanoix, J., J. Ouwendijk, A. Stark, E. Szafer, D. Cassel, K. Dejgaard, M. Weiss, and T. Nilsson. 2001. Sorting of Golgi resident proteins into different subpopulations of COPI vesicles: a role for ArfGAP1. *J Cell Biol*. 155:1199-1212.

Lavieu, G., M.H. Dunlop, A. Lerich, H. Zheng, F. Bottanelli, and J.E. Rothman. 2014. The Golgi ribbon structure facilitates anterograde transport of large cargoes. *Molecular biology of the cell*. 25:3028-3036.

Lavieu, G., H. Zheng, and J.E. Rothman. 2013. Stapled Golgi cisternae remain in place as cargo passes through the stack. *eLife*. 2:e00558.

Lee, S.Y., J.S. Yang, W. Hong, R.T. Premont, and V.W. Hsu. 2005. ARFGAP1 plays a central role in coupling COPI cargo sorting with vesicle formation. *J Cell Biol*. 168:281-290.

Lefrancois, S., and P.J. McCormick. 2007. The Arf GEF GBF1 is required for GGA recruitment to Golgi membranes. *Traffic*. 8:1440-1451.

Leslie, C.C., T.A. Gangelhoff, and M.H. Gelb. 2010. Localization and function of cytosolic phospholipase A2alpha at the Golgi. *Biochimie*. 92:620-626.

Letourneur, F., E.C. Gaynor, S. Hennecke, C. Demolliere, R. Duden, S.D. Emr, H. Riezman, and P. Cosson. 1994. Coatomer is essential for retrival of dilysine-tagged proteins to the endoplasmic reticulum. *Cell*. 79:1199-1207.

Linstedt, A.D., S.A. Jesch, A. Mehta, T.H. Lee, R. Garcia-Mata, D.S. Nelson, and E. Sztul. 2000. Binding relationships of membrane tethering components. The giantin N terminus and the GM130 N terminus compete for binding to the p115 C terminus. *The Journal of biological chemistry*. 275:10196-10201.

Lippincott-Schwartz, J. 2011. An evolving paradigm for the secretory pathway? *Mol Biol Cell*. 22:3929-3932.

Lippincott-Schwartz, J., J.G. Donaldson, A. Schweizer, E.G. Berger, H.P. Hauri, L.C. Yuan, and R.D. Klausner. 1990. Microtubule-dependent retrograde transport of proteins into the ER in the presence of brefeldin A suggests an ER recycling pathway. *Cell*. 60:821-836.

Lippincott-Schwartz, J., L.C. Yuan, J.S. Bonifacino, and R.D. Klausner. 1989. Rapid redistribution of Golgi proteins into the ER in cells treated with brefeldin A: evidence for membrane cycling from Golgi to ER. *Cell*. 56:801-813.

Liu, W., R. Duden, R.D. Phair, and J. Lippincott-Schwartz. 2005. ArfGAP1 dynamics and its role in COPI coat assembly on Golgi membranes of living cells. *J Cell Biol*. 168:1053-1063.

Lowe, M., and T.E. Kreis. 1998. Regulation of membrane traffic in animal cells by COPI. *Biochim Biophys Acta*. 1404:53-66.

Lowery, J., T. Szul, M. Styers, Z. Holloway, V. Oorschot, J. Klumperman, and E. Sztul. 2013. The Sec7 guanine nucleotide exchange factor GBF1 regulates membrane recruitment of BIG1 and BIG2 guanine nucleotide exchange factors to the trans-Golgi network (TGN). *J Biol Chem*. 288:11532-11545.

Luo, R., B. Ahvazi, D. Amariei, D. Shroder, B. Burrola, W. Losert, and P.A. Randazzo. 2007. Kinetic analysis of GTP hydrolysis catalysed by the Arf1-GTP-ASAP1 complex. *Biochem J*. 402:439-447.

Luo, R., and P.A. Randazzo. 2008. Kinetic analysis of Arf GAP1 indicates a regulatory role for coatomer. *J Biol Chem*. 283:21965-21977.

Ma, W., and J. Goldberg. 2013. Rules for the recognition of dilysine retrieval motifs by coatomer. *The EMBO journal*. 32:926-937.

Manolea, F., J. Chun, D.W. Chen, I. Clarke, N. Summerfeldt, J.B. Dacks, and P. Melancon. 2010. Arf3 Is Activated Selectively by BIGs at the trans-Golgi Network. *Mol Biol Cell*.

Manolea, F., A. Claude, J. Chun, J. Rosas, and P. Melançon. 2008. Distinct Functions for Arf Guanine Nucleotide Exchange Factors at the Golgi Complex: GBF1 and BIGs Are Required for Assembly and Maintenance of the Golgi Stack and trans-Golgi Network, Respectively. *Mol Biol Cell*. 19:523-535.

Mansour, S.J., J. Skaug, X.H. Zhao, J. Giordano, S.W. Scherer, and P. Melançon. 1999. p200 ARF-GEP1: a Golgi-localized guanine nucleotide exchange protein whose Sec7 domain is targeted by the drug brefeldin A. *Proc Natl Acad Sci U S A*. 96:7968-7973.

Marsh, B.J., D.N. Mastronarde, K.F. Buttle, K.E. Howell, and J.R. McIntosh. 2001. Organellar relationships in the Golgi region of the pancreatic beta cell line, HIT-T15, visualized by high resolution electron tomography. *Proc Natl Acad Sci U S A*. 98:2399-2406.

Martinez-Menarguez, J.A., H.J. Geuze, J.W. Slot, and J. Klumperman. 1999. Vesicular tubular clusters between the ER and Golgi mediate concentration of soluble secretory proteins by exclusion from COPI-coated vesicles. *Cell*. 98:81-90.

McNew, J.A., F. Parlati, R. Fukuda, R.J. Johnston, K. Paz, F. Paumet, T.H. Sollner, and J.E. Rothman. 2000. Compartmental specificity of cellular membrane fusion encoded in SNARE proteins. *Nature*. 407:153-159.

Melançon, P., X. Zhao, and T.K. Lasell. 2003. Large Arf-GEFs of the Golgi complex: In search of mechanisms for the cellular effects of BFA. *In* ARF Family GTPases. R.A. Kahn, editor. Kluwer Academic Publishers, Dordrecht. 101-119.

Mellman, I., and K. Simons. 1992. The Golgi complex: in vitro veritas? *Cell*. 68:829-840.

Mironov, A.A., A.A. Mironov, Jr., G.V. Beznoussenko, A. Trucco, P. Lupetti, J.D. Smith, W.J. Geerts, A.J. Koster, K.N. Burger, M.E. Martone, T.J. Deerinck, M.H. Ellisman, and A. Luini. 2003. ER-to-Golgi carriers arise through direct en bloc protrusion and multistage maturation of specialized ER exit domains. *Dev Cell*. 5:583-594.

Mitrovic, S., H. Ben-Tekaya, E. Koegler, J. Gruenberg, and H.P. Hauri. 2008. The Cargo Receptors Surf4, Endoplasmic Reticulum-Golgi Intermediate Compartment (ERGIC)-53, and p25 Are Required to Maintain the Architecture of ERGIC and Golgi. *Mol Biol Cell*. 19:1976-1990.

Mogelsvang, S., B.J. Marsh, M.S. Ladinsky, and K.E. Howell. 2004. Predicting function from structure: 3D structure studies of the mammalian Golgi complex. *Traffic*. 5:338-345.

Monetta, P., I. Slavin, N. Romero, and C. Alvarez. 2007. Rab1b interacts with GBF1 and modulates both ARF1 dynamics and COPI association. *Mol Biol Cell*. 18:2400-2410.

Morgan, N.V., S.K. Westaway, J.E. Morton, A. Gregory, P. Gissen, S. Sonek, H. Cangul, J. Coryell, N. Canham, N. Nardocci, G. Zorzi, S. Pasha, D. Rodriguez, I. Desguerre, A. Mubaidin, E. Bertini, R.C. Trembath, A. Simonati, C. Schanen, C.A. Johnson, B. Levinson, C.G. Woods, B. Wilmot, P. Kramer, J. Gitschier, E.R. Maher, and S.J. Hayflick. 2006. PLA2G6, encoding a phospholipase A2, is mutated in neurodegenerative disorders with high brain iron. *Nature genetics*. 38:752-754.

Mossessova, E., R.A. Corpina, and J. Goldberg. 2003. Crystal structure of ARF1*Sec7 complexed with Brefeldin A and its implications for the guanine nucleotide exchange mechanism. *Mol Cell*. 12:1403-1411.

Mouratou, B., V. Biou, A. Joubert, J. Cohen, D.J. Shields, N. Geldner, G. Jurgens, P. Melançon, and J. Cherfils. 2005. The domain architecture of large guanine

nucleotide exchange factors for the small GTP-binding protein Arf. *BMC Genomics*. 6:20.

Moyer, B.D., B.B. Allan, and W.E. Balch. 2001. Rab1 interaction with a GM130 effector complex regulates COPII vesicle cis--Golgi tethering. *Traffic*. 2:268-276.

Murakami, M., and I. Kudo. 2002. Phospholipase A2. *Journal of biochemistry*. 131:285-292.

Nelson, D.S., C. Alvarez, Y.S. Gao, R. Garcia-Mata, E. Fialkowski, and E. Sztul. 1998. The membrane transport factor TAP/p115 cycles between the Golgi and earlier secretory compartments and contains distinct domains required for its localization and function. *J Cell Biol*. 143:319-331.

Nickel, W., J. Malsam, K. Gorgas, M. Ravazzola, N. Jenne, J.B. Helms, and F.T. Wieland. 1998. Uptake by COPI-coated vesicles of both anterograde and retrograde cargo is inhibited by GTPgammaS in vitro. *J Cell Sci*. 111:3081-3090.

Niu, T.K., A.C. Pfeifer, J. Lippincott-Schwartz, and C.L. Jackson. 2005. Dynamics of GBF1, a Brefeldin A-sensitive Arf1 exchange factor at the Golgi. *Mol Biol Cell*. 16:1213-1222.

Odorizzi, G., M. Babst, and S.D. Emr. 2000. Phosphoinositide signaling and the regulation of membrane trafficking in yeast. *Trends Biochem Sci*. 25:229-235.

Orci, L., A. Perrelet, and J.E. Rothman. 1998. Vesicles on strings: morphological evidence for processive transport within the Golgi stack. *Proc Natl Acad Sci U S A*. 95:2279-2283.

Orci, L., M. Ravazzola, A. Volchuk, T. Engel, M. Gmachl, M. Amherdt, A. Perrelet, T.H. Sollner, and J.E. Rothman. 2000. Anterograde flow of cargo across the golgi stack potentially mediated via bidirectional "percolating" COPI vesicles. *Proc Natl Acad Sci U S A*. 97:10400-10405.

Paris, S., S. Beraud-Dufour, S. Robineau, J. Bigay, B. Antonny, M. Chabre, and P. Chardin. 1997. Role of protein-phospholipid interactions in the activation of ARF1 by the guanine nucleotide exchange factor arno [In Process Citation]. *J Biol Chem*. 272:22221-22226.

Park, S.Y., J.S. Yang, A.B. Schmider, R.J. Soberman, and V.W. Hsu. 2015. Coordinated regulation of bidirectional COPI transport at the Golgi by CDC42. *Nature*. 521:529-532.

Parnis, A., M. Rawet, L. Regev, B. Barkan, M. Rotman, M. Gaitner, and D. Cassel. 2006. Golgi localization determinants in ArfGAP1 and in new tissue-specific ArfGAP1 isoforms. *J Biol Chem*. 281:3785-3792.

Pasqualato, S., L. Renault, and J. Cherfils. 2002. Arf, Arl, Arp and Sar proteins: a family of GTP-binding proteins with a structural device for 'front-back' communication. *EMBO Rep*. 3:1035-1041.

Patterson, G.H., K. Hirschberg, R.S. Polishchuk, D. Gerlich, R.D. Phair, and J. Lippincott-Schwartz. 2008. Transport through the Golgi apparatus by rapid partitioning within a two-phase membrane system. *Cell*. 133:1055-1067.

Pelham, H.R., and J.E. Rothman. 2000. The debate about transport in the Golgi--two sides of the same coin? *Cell*. 102:713-719.

Pellett, P.A., F. Dietrich, J. Bewersdorf, J.E. Rothman, and G. Lavieu. 2013. Inter-Golgi transport mediated by COPI-containing vesicles carrying small cargoes. *eLife*. 2:e01296.

Pepperkok, R., J.A. Whitney, M. Gomez, and T.E. Kreis. 2000. COPI vesicles accumulating in the presence of a GTP restricted arf1 mutant are depleted of anterograde and retrograde cargo. *J Cell Sci*. 113:135-144.

Peters, P.J., V.W. Hsu, C.E. Ooi, D. Finazzi, S.B. Teal, V. Oorschot, J.G. Donaldson, and R.D. Klausner. 1995. Overexpression of wild-type and mutant ARF1 and ARF6: distinct perturbations of nonoverlapping membrane compartments. *J Cell Biol*. 128:1003-1017.

Pevzner, I., J. Strating, L. Lifshitz, A. Parnis, F. Glaser, A. Herrmann, B. Brugger, F. Wieland, and D. Cassel. 2012. Distinct role of subcomplexes of the COPI coat in the regulation of ArfGAP2 activity. *Traffic*. 13:849-856.

Peyroche, A., B. Antonny, S. Robineau, J. Acker, J. Cherfils, and C.L. Jackson. 1999. Brefeldin A acts to stabilize an abortive ARF-GDP-Sec7 domain protein complex: involvement of specific residues of the Sec7 domain. *Mol Cell*. 3:275-285.

Peyroche, A., S. Paris, and C.L. Jackson. 1996. Nucleotide exchange on ARF mediated by yeast Gea1 protein. *Nature*. 384:479-481.

Pfeffer, S. 2003. Membrane domains in the secretory and endocytic pathways. *Cell*. 112:507-517.

Pfeffer, S.R. 2010. How the Golgi works: a cisternal progenitor model. *Proc Natl Acad Sci U S A*. 107:19614-19618.

Pfeffer, S.R. 2012. Rab GTPase localization and Rab cascades in Golgi transport. *Biochem Soc Trans*. 40:1373-1377.

Pfeffer, S.R. 2013. Hopping rim to rim through the Golgi. *eLife*. 2:e00903.

Presley, J.F., N.B. Cole, T.A. Schroer, K. Hirschberg, K.J. Zaal, and J. Lippincott-Schwartz. 1997. ER-to-Golgi transport visualized in living cells. *Nature*. 389:81-85.

Quilty, D., F. Gray, N. Summerfeldt, D. Cassel, and P. Melancon. 2014. Arf activation at the Golgi is modulated by feed-forward stimulation of the exchange factor GBF1. *Journal of cell science*. 127:354-364.

Ramaen, O., A. Joubert, P. Simister, N. Belgareh-Touze, M.C. Olivares-Sanchez, J.C. Zeeh, S. Chantalat, M.P. Golinelli-Cohen, C.L. Jackson, V. Biou, and J. Cherfils. 2007. Interactions between conserved domains within homodimers in the big1, big2 and GBF1 ARF guanine nucleotide exchange factors. *J Biol Chem*.

Ramanadham, S., F.F. Hsu, A. Bohrer, Z. Ma, and J. Turk. 1999. Studies of the role of group VI phospholipase A2 in fatty acid incorporation, phospholipid remodeling, lysophosphatidylcholine generation, and secretagogue-induced arachidonic acid release in pancreatic islets and insulinoma cells. *The Journal of biological chemistry*. 274:13915-13927.

Randazzo, P.A., and R.A. Kahn. 1995. Myristoylation and ADP-ribosylation factor function. *Methods Enzymol*. 250:394-405.

Ren, X., G.G. Farias, B.J. Canagarajah, J.S. Bonifacino, and J.H. Hurley. 2013. Structural basis for recruitment and activation of the AP-1 clathrin adaptor complex by Arf1. *Cell*. 152:755-767.

Renault, L., B. Guibert, and J. Cherfils. 2003. Structural snapshots of the mechanism and inhibition of a guanine nucleotide exchange factor. *Nature*. 426:525-530.

Richardson, B.C., and J.C. Fromme. 2012. Autoregulation of Sec7 Arf-GEF activity and localization by positive feedback. *Small GTPases*. 3:240-243.

Richardson, B.C., C.M. McDonold, and J.C. Fromme. 2012. The Sec7 Arf-GEF is recruited to the trans-Golgi network by positive feedback. *Dev Cell*. 22:799-810.

Robineau, S., M. Chabre, and B. Antonny. 2000. Binding site of brefeldin A at the interface between the small G protein ADP-ribosylation factor 1 (ARF1) and the nucleotide-exchange factor Sec7 domain. *Proc Natl Acad Sci U S A*. 97:9913-9918.

Rojo, M., R. Pepperkok, G. Emery, R. Kellner, E. Stang, R.G. Parton, and J. Gruenberg. 1997. Involvement of the transmembrane protein p23 in biosynthetic protein transport. *J Cell Biol*. 139:1119-1135.

Roux, K.J., D.I. Kim, M. Raida, and B. Burke. 2012. A promiscuous biotin ligase fusion protein identifies proximal and interacting proteins in mammalian cells. *J Cell Biol*. 196:801-810.

Saenz, J.B., W.J. Sun, J.W. Chang, J. Li, B. Bursulaya, N.S. Gray, and D.B. Haslam. 2009. Golgicide A reveals essential roles for GBF1 in Golgi assembly and function. *Nat Chem Biol*.

Saitoh, A., H.W. Shin, A. Yamada, S. Waguri, and K. Nakayama. 2009. Three homologous ArfGAPs participate in coat protein I-mediated transport. *The Journal of biological chemistry*. 284:13948-13957.

San Pietro, E., M. Capestrano, E.V. Polishchuk, A. DiPentima, A. Trucco, P. Zizza, S. Mariggio, T. Pulvirenti, M. Sallese, S. Tete, A.A. Mironov, C.C. Leslie, D. Corda, A. Luini, and R.S. Polishchuk. 2009. Group IV phospholipase A(2)alpha controls the formation of inter-cisternal continuities involved in intra-Golgi transport. *PLoS biology*. 7:e1000194.

Saraste, J., and E. Kuismanen. 1992. Pathways of protein sorting and membrane traffic between the rough endoplasmic reticulum and the Golgi complex. *Semin Cell Biol*. 3:343-355.

Sata, M., J.G. Donaldson, J. Moss, and M. Vaughan. 1998. Brefeldin A-inhibited guanine nucleotide-exchange activity of Sec7 domain from yeast Sec7 with yeast and mammalian ADP ribosylation factors. *Proc Natl Acad Sci U S A*. 95:4204-4208.

Scales, S.J., R. Pepperkok, and T.E. Kreis. 1997. Visualization of ER-to-Golgi transport in living cells reveals a sequential mode of action for COPII and COPI. *Cell*. 90:1137-1148.

Schindler, R., C. Itin, M. Zerial, F. Lottspeich, and H.P. Hauri. 1993. ERGIC-53, a membrane protein of the ER-Golgi intermediate compartment, carries an ER retention motif. *Eur J Cell Biol*. 61:1-9.

Schlacht, A., K. Mowbrey, M. Elias, R.A. Kahn, and J.B. Dacks. 2013. Ancient complexity, opisthokont plasticity, and discovery of the 11th subfamily of Arf GAP proteins. *Traffic*. 14:636-649.

Schmidt, J.A., and W.J. Brown. 2009. Lysophosphatidic acid acyltransferase 3 regulates Golgi complex structure and function. *The Journal of cell biology*. 186:211-218.

Schmidt, J.A., G.M. Yvone, and W.J. Brown. 2010. Membrane topology of human AGPAT3 (LPAAT3). *Biochemical and biophysical research communications*. 397:661-667.

Schweizer, A., J.A. Fransen, T. Bachi, L. Ginsel, and H.P. Hauri. 1988. Identification, by a monoclonal antibody, of a 53-kD protein associated with a tubulo-vesicular compartment at the cis-side of the Golgi apparatus. *J Cell Biol*. 107:1643-1653.

Schweizer, A., J.A. Fransen, K. Matter, T.E. Kreis, L. Ginsel, and H.P. Hauri. 1990. Identification of an intermediate compartment involved in protein transport from endoplasmic reticulum to Golgi apparatus. *Eur J Cell Biol*. 53:185-196.

Sciaky, N., J. Presley, C. Smith, K.J. Zaal, N. Cole, J.E. Moreira, M. Terasaki, E. Siggia, and J. Lippincott-Schwartz. 1997. Golgi tubule traffic and the effects of brefeldin A visualized in living cells. *J Cell Biol*. 139:1137-1155.

Serafini, T., L. Orci, M. Amherdt, M. Brunner, R.A. Kahn, and J.E. Rothman. 1991. ADP-ribosylation factor is a subunit of the coat of Golgi-derived COP- coated vesicles: a novel role for a GTP-binding protein. *Cell*. 67:239-253.

Shevell, D.E., W.M. Leu, C.S. Gillmor, G. Xia, K.A. Feldmann, and N.H. Chua. 1994. EMB30 is essential for normal cell division, cell expansion, and cell adhesion in Arabidopsis and encodes a protein that has similarity to Sec7. *Cell*. 77:1051-1062.

Shiba, Y., S. Kametaka, S. Waguri, J.F. Presley, and P.A. Randazzo. 2013. ArfGAP3 regulates the transport of cation-independent mannose 6-phosphate receptor in the post-Golgi compartment. *Current biology : CB*. 23:1945-1951.

Shiba, Y., R. Luo, J.E. Hinshaw, T. Szul, R. Hayashi, E. Sztul, K. Nagashima, U. Baxa, and P.A. Randazzo. 2011. ArfGAP1 promotes COPI vesicle formation by facilitating coatomer polymerization. *Cellular logistics*. 1:139-154.

Shinotsuka, C., S. Waguri, M. Wakasugi, Y. Uchiyama, and K. Nakayama. 2002a. Dominant-negative mutant of BIG2, an ARF-guanine nucleotide exchange factor, specifically affects membrane trafficking from the trans-Golgi network through inhibiting membrane association of AP-1 and GGA coat proteins. *Biochem Biophys Res Commun*. 294:254-260.

Shinotsuka, C., Y. Yoshida, K. Kawamoto, H. Takatsu, and K. Nakayama. 2002b. Overexpression of an ADP-ribosylation factor-guanine nucleotide exchange factor, BIG2, uncouples brefeldin A-induced adaptor protein-1 coat dissociation and membrane tubulation. *J Biol Chem*. 277:9468-9473.

Shorter, J., M.B. Beard, J. Seemann, A.B. Dirac-Svejstrup, and G. Warren. 2002. Sequential tethering of Golgins and catalysis of SNAREpin assembly by the vesicle-tethering protein p115. *The Journal of cell biology*. 157:45-62.

Sitia, R., and J. Meldolesi. 1992. Endoplasmic reticulum: a dynamic patchwork of specialized subregions. *Molecular biology of the cell*. 3:1067-1072.

Soni, K.G., G.A. Mardones, R. Sougrat, E. Smirnova, C.L. Jackson, and J.S. Bonifacino. 2009. Coatomer-dependent protein delivery to lipid droplets. *J Cell Sci*. 122:1834-1841.

Stalder, D., H. Barelli, R. Gautier, E. Macia, C.L. Jackson, and B. Antonny. 2011. Kinetic studies of the Arf activator Arno on model membranes in the presence of Arf effectors suggest control by a positive feedback loop. *The Journal of biological chemistry*. 286:3873-3883.

Stephens, D.J., and R. Pepperkok. 2001. Illuminating the secretory pathway: when do we need vesicles? *Journal of Cell Science*. 114:1053-1059.

Su, X., D.J. Mancuso, P.E. Bickel, C.M. Jenkins, and R.W. Gross. 2004. Small interfering RNA knockdown of calcium-independent phospholipases A2 beta or gamma inhibits the hormone-induced differentiation of 3T3-L1 preadipocytes. *The Journal of biological chemistry*. 279:21740-21748.

Suckling, R.J., P.P. Poon, S.M. Travis, I.V. Majoul, F.M. Hughson, P.R. Evans, R. Duden, and D.J. Owen. 2015. Structural basis for the binding of tryptophan-based motifs by delta-COP. *Proceedings of the National Academy of Sciences of the United States of America*. 112:14242-14247.

Sutterlin, C., P. Hsu, A. Mallabiabarrena, and V. Malhotra. 2002. Fragmentation and dispersal of the pericentriolar Golgi complex is required for entry into mitosis in mammalian cells. *Cell*. 109:359-369.

Suzuki, M., T. Murakami, J. Cheng, H. Kano, M. Fukata, and T. Fujimoto. 2015. ELMOD2 is anchored to lipid droplets by palmitoylation and regulates adipocyte triglyceride lipase recruitment. *Molecular biology of the cell*. 26:2333-2342.

Szafer, E., E. Pick, M. Rotman, S. Zuck, I. Huber, and D. Cassel. 2000. Role of coatomer and phospholipids in GTPase-activating protein-dependent hydrolysis of GTP by ADP-ribosylation factor-1. *J Biol Chem*. 275:23615-23619.

Szafer, E., M. Rotman, and D. Cassel. 2001. Regulation of GTP hydrolysis on ADP-ribosylation factor-1 at the Golgi membrane. *J Biol Chem*. 276:47834-47839.

Szul, T., R. Garcia-Mata, E. Brandon, S. Shestopal, C. Alvarez, and E. Sztul. 2005. Dissection of membrane dynamics of the ARF-guanine nucleotide exchange factor GBF1. *Traffic*. 6:374-385.

Szul, T., R. Grabski, S. Lyons, Y. Morohashi, S. Shestopal, M. Lowe, and E. Sztul. 2007. Dissecting the role of the ARF guanine nucleotide exchange factor GBF1 in Golgi biogenesis and protein trafficking. *J Cell Sci*. 120:3929-3940.

Takashima, K., A. Saitoh, S. Hirose, W. Nakai, Y. Kondo, Y. Takasu, H. Kakeya, H.W. Shin, and K. Nakayama. 2011. GBF1-Arf-COPI-ArfGAP-mediated Golgi-to-ER transport involved in regulation of lipid homeostasis. *Cell structure and function*. 36:223-235.

Taylor, T.C., R.A. Kahn, and P. Melançon. 1992. Two distinct members of the ADP-ribosylation factor family of GTP- binding proteins regulate cell-free intra-Golgi transport. *Cell*. 70:69-79.

Thiam, A.R., B. Antonny, J. Wang, J. Delacotte, F. Wilfling, T.C. Walther, R. Beck, J.E. Rothman, and F. Pincet. 2013. COPI buds 60-nm lipid droplets from reconstituted water-phospholipid-triacylglyceride interfaces, suggesting a tension clamp function. *Proceedings of the National Academy of Sciences of the United States of America*. 110:13244-13249.

Traut, T.W. 1994. Physiological concentrations of purines and pyrimidines. *Mol Cell Biochem*. 140:1-22.

Trucco, A., R.S. Polishchuk, O. Martella, A. Di Pentima, A. Fusella, D. Di Giandomenico, E. San Pietro, G.V. Beznoussenko, E.V. Polishchuk, M. Baldassarre, R. Buccione, W.J. Geerts, A.J. Koster, K.N. Burger, A.A. Mironov, and A. Luini. 2004.

Secretory traffic triggers the formation of tubular continuities across Golgi sub-compartments. *Nat Cell Biol*. 6:1071-1081.

Tsai, S.C., R. Adamik, J. Moss, and M. Vaughan. 1996. Purification and characterization of a guanine nucleotide-exchange protein for ADP-ribosylation factor from spleen cytosol. *Proc Natl Acad Sci U S A*. 93:305-309.

Uchiyama, K., G. Totsukawa, M. Puhka, Y. Kaneko, E. Jokitalo, I. Dreveny, F. Beuron, X. Zhang, P. Freemont, and H. Kondo. 2006. p37 is a p97 adaptor required for Golgi and ER biogenesis in interphase and at the end of mitosis. *Developmental cell*. 11:803-816.

Velasco, A., L. Hendricks, K.W. Moremen, D.R. Tulsiani, O. Touster, and M.G. Farquhar. 1993. Cell type-dependent variations in the subcellular distribution of alpha-mannosidase I and II. *The Journal of cell biology*. 122:39-51.

Volchuk, A., M. Amherdt, M. Ravazzola, B. Brugger, V.M. Rivera, T. Clackson, A. Perrelet, T.H. Sollner, J.E. Rothman, and L. Orci. 2000. Megavesicles implicated in the rapid transport of intracisternal aggregates across the Golgi stack. *Cell*. 102:335-348.

Volpicelli-Daley, L.A., Y. Li, C.J. Zhang, and R.A. Kahn. 2005. Isoform-selective Effects of the Depletion of Arfs1-5 on Membrane Traffic. *Mol Biol Cell*. 16:4495-4508.

Watson, P.J., G. Frigerio, B.M. Collins, R. Duden, and D.J. Owen. 2004. Gamma-COP appendage domain - structure and function. *Traffic*. 5:79-88.

Weimer, C., R. Beck, P. Eckert, I. Reckmann, J. Moelleken, B. Brugger, and F. Wieland. 2008. Differential roles of ArfGAP1, ArfGAP2, and ArfGAP3 in COPI trafficking. *J Cell Biol*. 183:725-735.

Wilfling, F., A.R. Thiam, M.J. Olarte, J. Wang, R. Beck, T.J. Gould, E.S. Allgeyer, F. Pincet, J. Bewersdorf, R.V. Farese, Jr., and T.C. Walther. 2014. Arf1/COPI machinery acts directly on lipid droplets and enables their connection to the ER for protein targeting. *eLife*. 3:e01607.

Wright, J., R.A. Kahn, and E. Sztul. 2014. Regulating the large Sec7 ARF guanine nucleotide exchange factors: the when, where and how of activation. *Cell Mol Life Sci*. 71:3419-3438.

Yan, J.P., and P. Melancon. 1994. Characterization of a soluble BFA-resistance factor which regulates association of coatomer to Golgi membranes. *Faseb J.* 8:1458.

Yang, J.S., S.Y. Lee, M. Gao, S. Bourgoin, P.A. Randazzo, R.T. Premont, and V.W. Hsu. 2002. ARFGAP1 promotes the formation of COPI vesicles, suggesting function as a component of the coat. *J Cell Biol*. 159:69-78.

Yang, J.S., C. Valente, R.S. Polishchuk, G. Turacchio, E. Layre, D.B. Moody, C.C. Leslie, M.H. Gelb, W.J. Brown, D. Corda, A. Luini, and V.W. Hsu. 2011a. COPI acts in both vesicular and tubular transport. *Nature cell biology*. 13:996-1003.

Yang, J.S., C. Valente, R.S. Polishchuk, G. Turacchio, E. Layre, D.B. Moody, C.C. Leslie, M.H. Gelb, W.J. Brown, D. Corda, A. Luini, and V.W. Hsu. 2011b. COPI acts in both vesicular and tubular transport. *Nature cell biology*. 13:996-1003.

Yu, X., M. Breitman, and J. Goldberg. 2012. A structure-based mechanism for Arf1-dependent recruitment of coatomer to membranes. *Cell*. 148:530-542.

Zhang, C.J., J.B. Bowzard, A. Anido, and R.A. Kahn. 2003. Four ARF GAPs in Saccharomyces cerevisiae have both overlapping and distinct functions. *Yeast*. 20:315-330.

Zhao, X., A. Claude, J. Chun, D.J. Shields, J.F. Presley, and P. Melançon. 2006. GBF1, a cis-Golgi and VTCs-localized ARF-GEF, is implicated in ER-to-Golgi protein traffic. *J Cell Sci*. 119:3743-3753.

Zhao, X., T.K. Lasell, and P. Melançon. 2002. Localization of large ADP-ribosylation factor-guanine nucleotide exchange factors to different Golgi compartments: evidence for distinct functions in protein traffic. *Mol Biol Cell*. 13:119-133.

Zimmerberg, J., and M.M. Kozlov. 2006. How proteins produce cellular membrane curvature. *Nature reviews. Molecular cell biology*. 7:9-19.